

Manith Randula Attanapola

Power-to-Gas Methanation of Carbon Dioxide

Master's thesis in Mechanical Engineering

Supervisor: Bjørn Austbø

June 2023

Manith Randula Attanapola

Power-to-Gas Methanation of Carbon Dioxide

Master's thesis in Mechanical Engineering
Supervisor: Bjørn Austbø
June 2023

Norwegian University of Science and Technology
Faculty of Engineering
Department of Energy and Process Engineering



Preface

This thesis was written as the final work for the Master's degree Program in Mechanical Engineering at the Norwegian University of Science and Technology during the spring of 2023.

I want to thank my supervisor, Bjørn Austbø and Sayed Ebrahim Hashemi, for allowing me to continue working on his Ph.D. thesis, which has an exciting future in the process industry. I am also grateful to my supervisor for the valuable guidance during my Master's project. Further, I would like to thank my fellow students for the engaging conversations, support, and not to mention fun we had during our studies.

Manith Randula Attanapola

Trondheim, 11.06.2023

Abstract

This thesis aims to optimize and analyze the Power-to-gas methanation of carbon dioxide for a direct methanation process model that could be operated at lower H_2/CO_2 ratios. The sensitivity analysis and optimization were split into the methanation and polishing units and conducted on four cases with H_2/CO_2 ratios 3.0, 3.2, 3.5, and 3.8. The process model was designed and evaluated in Aspen HYSYS V10.1, and the Hyprotech SQP optimizer tool was used for optimization.

The sensitivity analysis and optimization results for the methanation unit indicated that the process favored higher pressures, coolant temperatures, and the number of tubes in the reactors to ensure good conditions for the Sabatier reaction. The optimization objective was to maximize CH_4 content, resulting in the optimal pressure, coolant temperature, and the number of tubes between 15-20 bar 240°C and 2000-3000 for the different cases. This gave a H_2 conversions of 99.97%, 99.95%, 99.95%, and 99.92% for case ratios 3.0, 3.2, 3.5, and 3.8, respectively.

The sensitivity analysis results for the polishing unit indicated the process favored a high pressure into the absorption column. The MDEA amine molar flow rate to the absorber was dependent on the CO_2 fraction in the stream, with higher CO_2 fraction requiring higher MDEA amine molar flow rates. From the case studies, the amine concentration favored a concentration between 40-45%. The optimization objective was to minimize the CO_2 fraction in the product stream to meet the product restriction of 50 PPM, with cases 3.0, 3.2, and 3.5 satisfying the product restrictions. For case 3.8, independent variables were fixed to satisfy the product restriction.

The results obtained from optimization indicated that the direct methanation process could operate at lower H_2/CO_2 ratios. The cost evaluation for the different H_2/CO_2 cases indicated that the production cost per Sm^3 was high and made the processes not profitable yet, with the cost of H_2 and knock-vessels being the primary cost driver factor. The cost estimation was based on literature by Sinnott & Towler and Turton et al. and makes the cost uncertain.

Sammendrag

Denne masteroppgaven analyserte om Power-to-gas metanisering av en direkte metanisering prosess modell kan operere med lavere H_2/CO_2 . Sensitivitet analysen og optimaliseringen ble delt i to deler, en for metaniserings enheten og en for polishing enheten og ble gjennomført på disse casestudiene med 3.0, 3.2, 3.5 og 3.8 H_2/CO_2 rater. Prosess modellen er modellert og evaluert i Aspen HYSYS V.10, og Hyprotech SQP optimizer verktøyet ble brukt for optimalisering.

Sensitivitet analysen og optimaliserings resultatene for metaniserings enheten indikerte at høyere trykk, kjøle temperatur, og antall tuber i reaktorene ga gode forhold for Sabatier reaksjonen. Målet for optimaliseringen var å maksimere CH_4 innholdet for de ulike casene. Resultatet fra optimaliseringen på casestudiene viste best mulige trykk, kjøle temperatur, og antall tuber i reaktorene til å være mellom 15-20 bar, $240^\circ C$ og 2000-3000 for de ulike casestudiene. Dette ga en H_2 omdannelse på 99.97%, 99.95%, 99.95%, og 99.92% for casestudiene 3.0, 3.2, 3.5 og 3.8.

Sensitivitet analysen og optimaliserings resultatene polishing enheten indikerte at prosessen favoriserte høyt trykk inn til absorbering kolonnen. Mengde MDEA amine som var injisert inn i absorbering kolonnen var avhengig av CO_2 mengden i strømmen. Høyere CO_2 mengde i strømmen trengte en høyere MDEA amine molar rate. Casestudiene viste at en amine konsentrasjon mellom 40-45% ga best absorbering evne av CO_2 i kolonnen. Målet for optimaliseringen var å minimere mengden CO_2 i produktet slik at det møter produkt restriksjonen med en maksimum CO_2 mengde på 50 PPM, hvor optimalisering av 3.0, 3.2, og 3.5 oppnådde produkt spesifikasjonene. Optimalisering for H_2/CO_2 rate 3.8 ble det valgt verdier som oppnår produkt spesifikasjonene da optimaliseringen ble sluttet på grunn av Step Convergering.

Resultatene fra sensitivitet analysene og optimaliseringen indikerte at den direkte metanisering prosess modellen kunne operere med lavere H_2/CO_2 verdier. En kostnads analyse ble gjennomført. Analysen viste de at ulike H_2/CO_2 casestudiene ga høye produksjonen kostnader per Sm^3 , og indikerte at prosessen ikke var økonomisk lønnsomt sammenlignet med snitt prisen for LNG i 2022 and andre metan produksjon prosesser fra biogass. Kostnaden på H_2 og separasjons kolonnen for vann utgjorde store deler av kostnadene, med en lavere markeds kostnad for H_2 kan gjøre direkte metanisering lønnsomt.

Table of Contents

Preface	i
Abstract	ii
Sammendrag	iii
List of Figures	viii
List of Tables	ix
Nomenclature	xii
1 Introduction	1
1.1 Previous Work	4
1.2 Project Objective	5
1.3 Thesis Structure	5
2 Theoretical Background	6
2.1 Power-to-Gas	6
2.1.1 Methanation	7
2.2 Biogas Upgrading	17
2.2.1 Physical absorption with a Water Scrubbing System	18
2.2.2 Chemical Absorption with Amine Solutions	18
2.2.3 Adsorption with Pressure Swing Adsorption	20
2.2.4 Membrane Separation	21
2.2.5 Cryogenic Separation	21
3 Process Description	23

3.1	Power-to-Methane Process Model	23
3.2	Methanation Process	23
3.3	Polishing Process	24
3.4	Liquefaction Process	25
4	Design Basis	27
4.1	Feed Specifications and Product Specifications	27
4.2	Design Variables	29
4.2.1	Design Variables for the Methanation Unit	29
4.2.2	Design Variables for the Polishing Unit	31
5	Process Modeling	33
5.1	Simulation Tool	33
5.1.1	Process Assumptions	33
5.2	Modelling of Methanation Reactor	34
5.3	Modeling of the Polishing Unit	38
6	Sensitivity Analysis and Optimization Results	40
6.1	Methanation Optimization	40
6.1.1	Sensitivity Analysis on Methane Molar Flow Rate	40
6.1.2	Sensitivity Analysis on Hydrogen Conversion	42
6.1.3	Sensitivity Analysis on Heat Flow	44
6.1.4	Sensitivity Analysis on Number of Tubes in Reactor 1	47
6.1.5	Hyprotech SQP Optimization of the Methanation Process	50
6.2	Polishing Optimization	54
6.2.1	Sensitivity Analysis on Case: 3.0	54

6.2.2	Sensitivity Analysis on Case: 3.2	55
6.2.3	Sensitivity Analysis on Case: 3.5	58
6.2.4	Sensitivity Analysis on Case: 3.8	59
6.2.5	Hyprotech SQP Optimizer Polishing Unit	61
7	Cost Analysis	65
7.1	Capital Expenditures CAPEX	65
7.1.1	Estimating Purchased Equipment Costs	66
7.1.2	Installation Cost	68
7.1.3	Total Fixed Capital Cost	69
7.2	OPEX - Operational Expenditures	70
7.2.1	Variable Costs of Production	70
7.2.2	Fixed cost of Production	72
7.3	Total Annualized Investment Cost	73
8	Discussion	76
8.1	Methanation Process	76
8.2	Polishing Process	77
8.3	Cost Analysis	79
9	Conclusion	82
10	Further Work	84
Appendix		I
A	Conventional Biogas Upgrading	I
B	Direct Methanation Process Model	IV

C	Liquefaction Process Model	VI
D	Modelling of the Methanation Reactors	VIII
D.1	Continuity Equation	VIII
D.2	Energy Balance	IX
D.3	Mass Balance Equation	XII
D.4	Momentum Balance: Pressure Distribution	XIII
D.5	Boundary Conditions	XIV
D.6	Reaction Rate	XV
D.7	Intraparticle Mass Transport Limitations	XVI
E	Cost Analysis: Calculations and Sizing	XVIII
E.1	Heat Exchangers	XVIII
E.2	Compressors and Pump	XXI
E.3	Knock-Out Vessel	XXII
E.4	Absorber and Stripper	XXIV
E.5	Expander and Expansion Valves	XXV
E.6	Variable Cost of Production	XXV
F	Cost analysis calculation Excel sheet	XXIX
G	HYSYS Workbooks	XXXVIII
G.1	Case 3.0	XXXVIII
G.2	Case 3.2	XLIII
G.3	Case 3.5	XLVIII
G.4	Case 3.8	LIII

List of Figures

1	World total energy supply by source 2019 [2]	2
2	Process route for a Power-to-gas facility for conversion of renewable energy.	3
3	Examples of a PtG chain from Götz et al. paper[5]	7
4	Calculated equilibrium constants K of the eight reactions involved in methanation process [12]	10
5	Reactor concepts for methanation process.	11
6	Adiabatic fixed bed reactor (Left), Polytropic fixed bed reactor (Right).	13
7	Monolith Reactor	14
8	Micro structure reactor	14
9	Sorption Enhanced methanation reactor	15
10	Process flow diagram for In situ BM and Separate reactor BM	16
11	Process flow diagram of BM in a separate reactor.	17
12	Pressure water scrubbing system from [20].	18
13	Amine absorption system example from [20]	19
14	Example of a Pressure Swing Adsorption system [20]	20
15	Example of a membrane separation system [20]	21
16	Example of a cryogenic process from [20]	22
17	Simplified Process Model for Direct Biogas Methanation	23
18	Simplified model of the methanation unit in the process model.	24
19	Simplified model of the polishing process	24
20	Simplified model of an N ₂ Liquefaction process	26
21	Illustration of a cooled walled fixed-bed reactor [4]	35
22	Methane flow rate out of methanation unit	41

23	Methane flow rate out of 1st reactor.	42
24	Hydrogen molar flow rate out of methanation unit	43
25	Hydrogen conversion in out of methanation unit	44
26	Heat flow first methanation reactor	45
27	Heat flow from the second reactor	46
28	Change on heat flow in reactor 1 from variation in the number of tubes	48
29	Change on methane molar flow in reactor 1 from variation in the number of tubes	49
30	Hyprotech optimizer case 3.0 solution: Step convergence	50
31	Sensitivity analysis from pressure, MDEA flow rate, and concentration on case 3.0	56
32	Sensitivity analysis from pressure, MDEA flow rate, and concentration on case 3.2	57
33	Sensitivity analysis from pressure, MDEA flow rate, and concentration on case 3.5	58
34	Sensitivity analysis from pressure, MDEA flow rate, and concentration on case 3.8	60
35	Optimizer results on the polishing process for case 3.0	61
36	Optimizer results on the polishing process for case 3.2	62
37	Optimizer results on the polishing process for case 3.5	63
38	Optimizer results on the polishing process for case 3.8	64
39	Conventional amine upgrading unit	II

List of Tables

1	Mechanism that causes catalyst deactivation[16]	12
---	---	----

2	Boiling point temperatures [°C] for different components in Biogas	22
3	Inlet raw biogas specifications	27
4	Inlet biogas and Hydrogen specifications for H ₂ /CO ₂ ratio.	28
5	Product specifications [22]	28
6	Independent Variables used in the case studies for the methanation process	29
7	Process variables and constraints used in Hyprotech SQP optimizer for methanation unit.	30
8	Independent Variables used in the case studies for the polishing unit	31
9	Process variables and constraints used in Hyprotech SQP optimizer for pol- ishing unit	32
10	Parameters and characteristics of the methanation reactors	38
11	Specified independent variables for case 3.0	51
12	Specified independent variables for case 3.2	52
13	Specified independent variables for case 3.5	53
14	Specified independent variables for case 3.8	53
15	CEPCI values for Sinnott & Towler (2009), Turton (1996) and Current day (Jan 2023) [28] [30]	67
16	Cost estimation for the equipment	67
17	Factor for estimation of fluid type process projects [28].	68
18	Installation Cost for the equipment	69
19	Total Fixed capital cost of the PtM plant for the cases.	70
20	Utility specific price parameters	71
21	Variable cost for utility	71
22	Fixed cost of production	73
23	Total revenue of LBM for the different cases	74

24	Summary of total cost estimate for each case	75
25	Production cost for each case	75
26	Conventional Inlet Biogas specifications	I
27	Diffusion Volumes of simple molecules [45]	XVII
28	Heat exchanger cost factors and characteristics	XIX
29	Cost estimate and Installation cost for the heat exchangers in MUSD	XX
30	Compressors and Pump cost factors, characteristics, and calculated cost . .	XXI
31	Knock-out vessel cost factors and characteristics	XXIII
32	Absorber and Stripper cost factors and characteristics [9]	XXIV
33	Expander and expansion valve cost factors and characteristics [9]	XXV
34	Variable cost of production for case 3.0	XXVI
35	Variable cost of production for case 3.2	XXVII
36	Variable cost of production for case 3.5	XXVII
37	Variable cost of production for case 3.8	XXVIII

Nomenclature

Abbreviations

ACCR	Annual capital charge ratio
BM	Biological methanation
CAPEX	Capital expenditures
CNG	Compressed natural gas
CS	Carbon Steel
D&E	Design and Engineering
GHSV	Gas hourly space velocity
HX	Heat Exchanger
ISBL	Inside battery limit
LBG	Liquid Biogas
LBM	Liquid Biomethane
LNG	Liquid Natural Gas
MFR	Methane formation rate
NG	Natural Gas
OPEX	Operating expenditures
OSBL	Outside battery limit
PPM	Parts per million
PSA	Pressure swing adsorption
PtG	Power-to-Gas
PtM	Power-to-Methane
R&D	Research & Development
SNG	Substitute natural gas
SS	Stainless Steel
TAC	Total annualized cost
X	Contingency factor

Symbols

A	Tube area	$[m^2]$
Bi	Biot number	$[-]$
C	Installation Cost	$[\text{USD}]$
C_{FC}	Fixed capital cost	$[\text{USD}]$
C_e	Cost estimate	$[\text{USD}]$
C_P	Heat capacity	$[\text{J/K}]$
D	Tube diameter	$[\text{m}]$
D_i^j	Effective diffusivity	$[m^2/s]$
D_P	Particle diameter	$[\text{mm}]$
D_{Pore}	Pore diameter	$[\text{nm}]$
D_r	Effective dispersion coefficient	$[-]$
D_v	Vessel Diameter	$[\text{m}]$
ΔG	Gibbs free energy	$[kJ/mol^{-1}]$
ΔH_r	Heat of reaction	$[kJ/mol]$
ΔT_{LM}	Log mean temperature difference	$[\text{K}]$
f	friction factor	$[-]$
$H_{i,L}$	Henry's law coefficient	$[-]$
H_v	Vessel Height	$[\text{m}]$
j_α	Flux Fick's Law	$[-]$
k_{La}	Mass transfer coefficient	$[\text{m/s}]$
k_w	Heat transfer coefficient	$[\frac{W}{m^2K}]$
λ	Radial thermal conductivity	$[\frac{W}{m \cdot K}]$
λ_g	Gas mixture conductivity	$[\text{W/mK}]$
$L_{Y,OP}$	Shift handled by operator	$[-]$
m_s	Shell mass	$[\text{kg}]$
M_α	Molar mass	$[\text{kg/mol}]$
N_t	Number of tubes	$[-]$
ν_α	Stoichiometry coefficient	$[-]$
P	Pressure	$[\text{bar}]$
Pr	Prandtl number	$[-]$
Q	Reaction quotient	$[-]$
r	Reaction rate	$[-]$
$r_{i,eff}$	Effective reaction rate	$[\text{M/s}]$
Re	Reynolds number	$[-]$
R	Gas constant	$[\frac{J}{mol \cdot K}]$
R_r	Number of reactions	$[-]$
ρ	Mass density	$[\text{kg}/m^3]$
T	Temperature	$[\text{°C}]$
T_C	Coolant temperature	$[\text{°C}]$
t_w	Vessel Thickness	$[\text{m}]$
U	Overall heat transfer coefficient	$[\frac{W}{m^2K}]$
u	Velocity	$[\text{m/s}]$
u_z	Superficial velocity	$[\text{m/s}]$
\dot{Q}	Heat flow	$[\text{W}]$
\dot{V}	Gas volumetric flow rate	$[m^3/h]$
q	Heat flux	$[\frac{W}{m^2}]$

Symbols

Sub- and superscripts

τ_p	Particle porosity	$[-]$	α	Component
θ	Specific diffusion volume	$[-]$	eq	Equilibrium
ΔT_{LM}	Log mean temp diff	$[K]$		
ε	Catalyst void fraction	$[-]$		
ε_p	Particle tortuosity	$[-]$		
ω_α	Mass fraction	$[-]$		
η	Effectiveness factor	$[-]$		
λ	Radial thermal conductivity	$[\frac{W}{m \cdot K}]$		
ϕ	Thiele modulus	$[-]$		
ρ	Mass density	$[kg/m^3]$		
ε	Catalyst void fraction	$[-]$		
λ	Radial thermal conductivity	$[\frac{W}{m \cdot K}]$		
ϕ	Thiele modulus	$[-]$		
τ_p	Particle porosity	$[-]$		
ε_p	Particle tortuosity	$[-]$		
λ_g	Gas mixture conductivity	$[W/mK]$		
K_i	Adsorption constant	$[-]$		
θ	Specific diffusion volume	$[-]$		

1 Introduction

With the ongoing war in Ukraine, the EU Commission, in response to the hardships and global energy market disruption, has devised the REPowerEU plan. The plan will accelerate Europe's clean energy transition and increase energy independence from unreliable suppliers and volatile fossil fuels. Ending the EU's reliance on Russian fossil fuels will require a massive scale-up of renewable as well as faster electrification and replacements for fossil-based heat and fuel in the industry and transport sector, and with a high demand for Natural Gas (NG), an alternative to fuel also in high demand. One of the core acts for renewable in the plan is to increase the production of renewable gases such as Hydrogen and Biomethane, with an action plan to boost biomethane production to 35 bcm (billion cubic meters of natural gas) by 2030 [1].

With the increasing demand for alternative renewable energy sources, sustainable alternative fuels are being researched continuously. Especially in the transport industry, fossil fuels dominate as the energy source; However, electric cars are on the rise for small personal vehicles, and an alternate fuel source in the heavy-duty vehicle sector is lacking. The most significant barrier is the lack of infrastructure, one of the significant barriers to developing renewable energy in the heavy-duty transportation sector. Also, since fossil fuels account for 80.9% of the world's energy supply by source, an alternate solution must be researched. With a strong demand to increase the share of renewable energy sources in the energy mix, the transition from fossil fuels to renewable energy sources will make electricity production more dependent on the available wind and solar power production sites. Due to the intermittent nature of wind and solar energy sources, the electricity network will have to endure large fluctuations over short and extensive periods. An option to support wind and solar power while balancing supply and demand is to store the surplus electricity. Storing the electricity in alternate ways supports the electricity network by minimizing energy loss and using the stored electricity in periods with high demand. By the statistics from the IEA (International Energy Agency), the world's energy supply from renewable sources accounts for less than 10% (counting Nuclear, Hydro, and others) of the world's supply in 2019 [2].

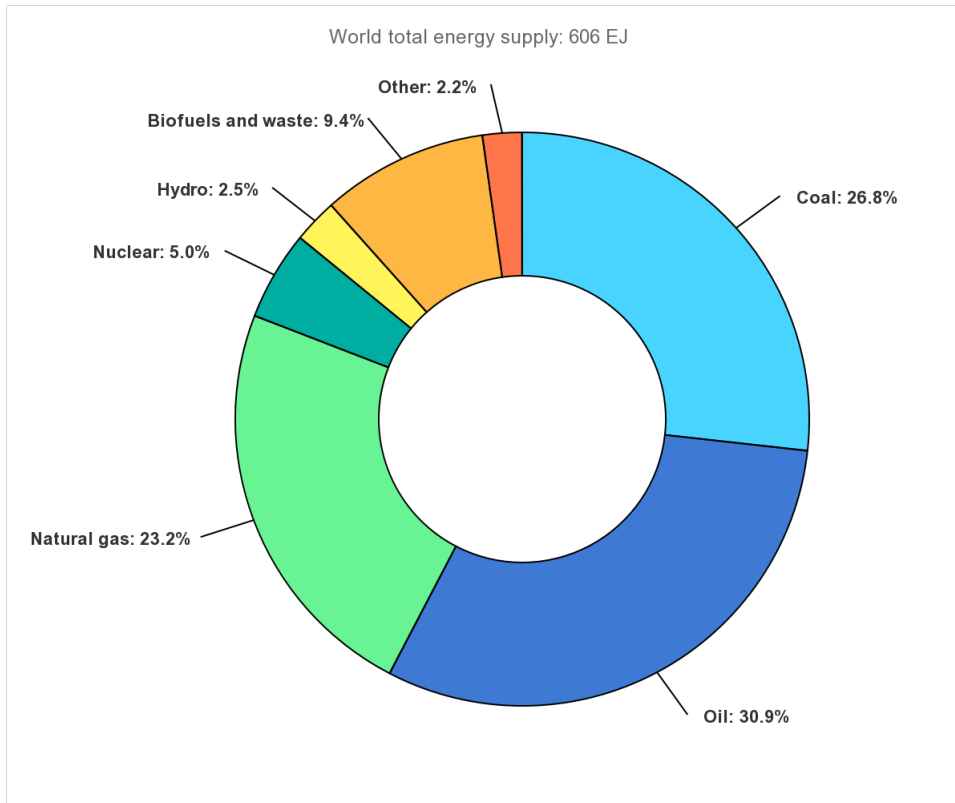


Figure 1: World total energy supply by source 2019 [2]

There are several different technologies to store excess electricity that is classified according to their working principle: electrical (superconducting magnetic energy storage), mechanical (pumped storage, compressed air, and flywheels), thermal (latent heat, sensible heat, and thermochemical) and chemical (supercapacitors, batteries, power-to-gas, power-to-liquid). Besides the working principle, the different technologies have different characteristics to cover various fields of application. The significant differences between the technologies are in energy capacity, response time, efficiency, and operating constraints [3].

An up-and-coming method for energy storage technologies is the Power-to-Gas from chemical processes. Mainly Power-to-Methane, alternative can be applied to regions where a natural gas infrastructure already exists and is a promising option to absorb and exploit surplus energy. Power-to-Methane is a method that converts electrical energy into chemical energy using CO_2 and H_2O . A Power-to-Methane plant usually consists of a water electrolyzer, a CO_2 separation unit or a source of CO_2 in pure gas or suitable gas mixture, and a methanation module shown in the Figure below 2. To utilize the surplus energy in power-to-gas applications in methane production comes from H_2 produced by water splitting in an electrolyzer. The generated H_2 and CO_2 converts through the Sabatier

reaction in the methanation unit to a gas mixture mainly consisting of CH_4 and H_2O [3] [4]. The resulting CH_4 is also known as substitute natural gas (SNG) and can be injected into an existing gas grid, used as CNG (compressed natural gas) motor fuel, or utilized in all other established natural gas facilities. This interest in Power-to-gas technology has grown mainly in Europe recently, with Switzerland, Denmark, France, Germany, and Japan, where pilot plants are under construction or in operation [5].

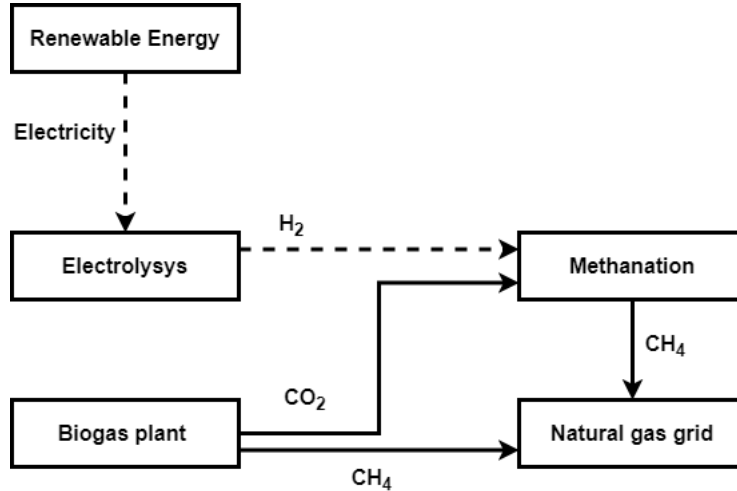


Figure 2: Process route for a Power-to-gas facility for conversion of renewable energy.

Liquid Natural Gas (LNG) is the preferred fuel in the transportation sector. There are many alternatives to alternative fuels, such as biofuels, hydrogen, and biomethane blended with conventional fuels or electrification of the transport sector using batteries and fuel cells. This concept suggests the alternate fuel biomethane from purified biogas for the transport sector. The biomethane must be liquid as Liquid Biomethane (LBM) for fuel use. Biomethane is a favorable alternative to LNG because it has some of the same characteristics as LNG, with methane content, heating value, and volumetric energy density, and similar to LNG, it can be transported in compressed gaseous form or the liquid form as LBM. The LBM is feasible as a fuel for long distances thanks to its volumetric energy density and available infrastructure for transportation and distribution [6]. One commercial plant producing liquefied biomethane is Biokraft, located in Skogn, Trøndelag. This plant is the world's largest production site for LBM. It uses biomass sources such as fish and paper waste to convert biomass into biogas by an anaerobic digestion process[7]. In a typical biomethane production facility, the biogas has to be processed through an upgrading process, typically by absorption, adsorption, or cryogenic methods, to clean the biogas into pure methane. Then a liquefaction process is to convert the pure methane in

gas form into Liquid Biomethane that can be utilized[8]. Non purified Biogas is mainly consist of CH_4 (50-70%), CO_2 (30-50%) and minor components as H_2O , N_2 , H_2S , H_2 and siloxanes [9]. The CO_2 captured from the biogas upgrading process is emitted directly to the atmosphere or transported by pipelines in liquid form for sequestration. Combining Power-to-gas technology with a biomethane production facility, one can convert the CO_2 in the biogas into CH_4 to produce more LBM, increasing productivity, reducing the greenhouse gas emission of the plant and balance the electricity network.

In this master thesis project, we will look at an alternate way to produce liquid biomethane using the direct methanation approach applying the Power-to-methane principle to reduce the carbon emissions in the existing designs. The process models are designed in Aspen HYSYS version 10. In the project thesis, we will dive into different technologies used in biogas upgrading and what's been chosen for the design given. Look into the Power-to-methane concept using the Sabatier reaction by adding hydrogen produced from renewable energy, with direct and indirect methods for methanation.

1.1 Previous Work

The master thesis continues the specialization project worked on during the autumn semester 2022. The theory described in the specialization project is used as a basis for the master's thesis and further expanded upon. In the specialization project, a sensitivity analysis from variation in pressure, temperature, and H_2/CO_2 was covered for the direct methanation process. The pressure, temperature, and the H_2/CO_2 ratio were varied while keeping the reactor design constant. The results concluded that the pressure and the H_2/CO_2 ratio impacted the Sabatier reaction in the methanation reactors, but temperature gave little to no change. Only a small variation H_2/CO_2 ratio between 3.9-4.0 was covered due to problems with convergence in the model. The HYSYS models studied were from Sayed Ebrahim Hashemi's Ph.D. on the topic "Development and Optimization of Processes for Liquefied Biomethane Production" is a continuation study on Article VI [9]. The process model developed from the Ph.D. is used and will be optimized further for different H_2/CO_2 ratios in this master thesis.

1.2 Project Objective

The objective of the master thesis is to simulate and optimize for a direct methanation process operating at lower H_2/CO_2 ratios of [3.0, 3.2, 3.5, 3.8], and if it can produce product liquid biomethane satisfying the product specifications for the biogas plant in Skogn. The process model is a direct methanation design for utilizing Power-to-gas technology. The optimization will be based on sensitivity analysis of different independent variables, expand from the sensitivity analysis and use the Hyprotech SQP optimization tool in Aspen HYSYS to maximize the LBM production of the plant to find the best plant specifications for each case. Then an economic evaluation of the equipment and operational costs will be evaluated to indicate if a direct methanation model with lower H_2/CO_2 ratios is economically feasible.

1.3 Thesis Structure

Chapter 2 presents the theoretical background on Power-to-gas technology, Power-to-Methane, methanation technology, and different biogas upgrading technology. Chapter 3 describes the Power-to-Methane processes modeled, with the methanation step, polishing step, and liquefaction. Chapter 4 clarifies the plant, design, case study, and optimizer specifications. Chapter 5 describes the simulation tool, process assumptions, and modeling of the main components in the process model. Chapter 6 illustrates and presents the results obtained from the case studies and optimization. Chapter 7 presents the cost estimation for the equipment and operational cost for the cases. Chapter 8 discusses the results of the sensitivity analysis, optimization, and cost analysis. Chapter 9 covers the conclusion of this thesis, and finally, chapter 10 covers further work that was not covered in this thesis and should be looked into. The master thesis contains a bibliography and several appendix chapters supporting modeling, sensitivity analysis, and cost analysis calculations.

2 Theoretical Background

Biogas is playing a key role in the emerging energy market for renewable energy. It can be produced from nearly all kinds of biological feedstock types, primarily from agricultural sectors and from various organic waste streams from overall society. The largest source is animal manure, slurries from cattle and pig production units, and poultry and fish production. Anaerobic digestion of animal manure aims to convert organic residues into two categories of valuable products. On the other hand, digested substrate is used for fertilizer in agriculture. Biogas can be used as a renewable fuel to produce green electricity and heat or vehicle fuel and substitute for Liquid Natural gas from fossil fuels.

In the theoretical background, the chapter will give an overview of which technologies are available for biogas upgrading and how they can be characterized and utilized. An overview of the technologies in the Power-to-Methane process, from chemical methanation to biological methanation, will be explained in more detail, and a highlight of the Power-to-gas technologies and their fundamentals will be covered. Parts of the theory chapter are taken from the project work from December 2022 [10].

2.1 Power-to-Gas

This subsection will highlight the fundamentals and technologies for Power-to-gas (PtG) and Power-to-methane (PtM). PtG process links the power grid with the gas grid by converting surplus energy into a grid-compatible gas via a two-step process from H_2 . The two step process includes H_2 production by water electrolysis, H_2 conversion with an external CO or CO_2 source and CH_4 production via methanation [5]. The CH_4 can be further used for different purposes such as storage of electricity, heat production, raw materials for the chemical industry, and transportation services. The sub-chapters will include state-of-the-art research on different methanation processes. The topic of water electrolysis will not be covered in this project thesis.

The PtG option represents a suitable solution for the long-term storage of the electricity produced by renewable energy source-based plants (wind, solar, water) and utilization of surplus energy. PtG can add more flexibility to the electrical system and allow it to be coupled to other energy systems, such as heating districts and transportation systems, and methane production via methanation. Methanation becomes a promising option to

absorb and exploit surplus energy where existing natural gas infrastructure exists. In the paper from Götzt et al., Götzt showed that the PtG process chain could be broken down, seen in Figure 1, with an Electrolysis process for the production of H₂ and methanation from a Carbon Capture method (CC).

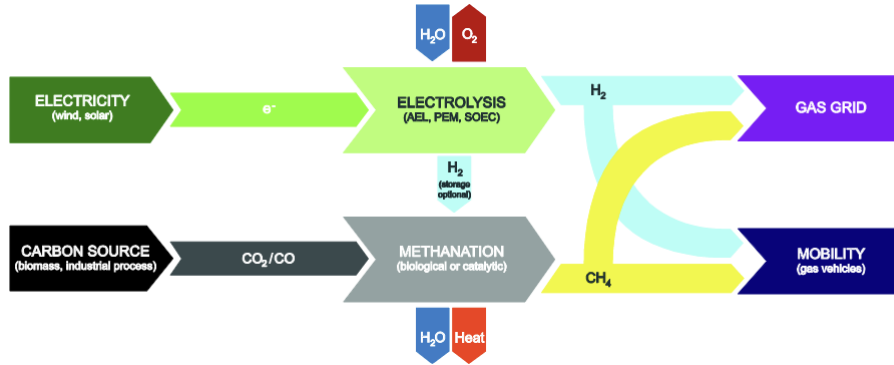


Figure 3: Examples of a PtG chain from Götzt et al. paper[5]

From Mazza et al. they described a typical PtG plant consisting of four components [11]. All the components can be shown in Figure 3

- An electrolyzer that allows H₂ to be produced.
- A methanation process device;
- A source of CO₂, which is necessary for the methanation step.
- Storage facilities, to allow H₂, CH₄ and CO₂ to be stored safely and buffered.

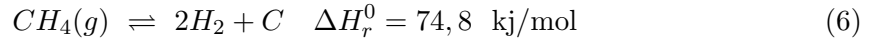
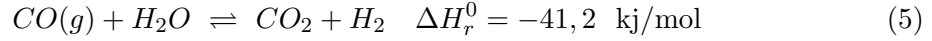
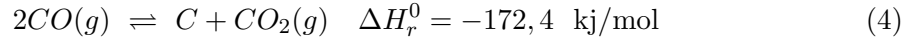
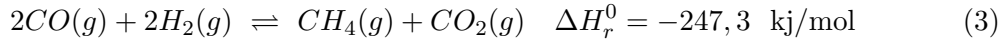
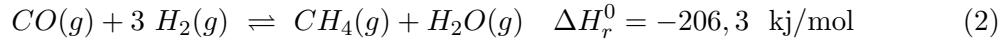
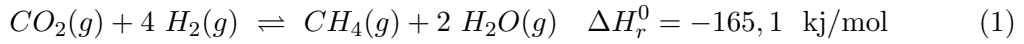
Further, the Power of Methane processes and different technologies will be covered.

2.1.1 Methanation

Power-to-Methane is a concept that converts electrical energy into chemical energy using CO₂, and H₂O and is a concept that brings the possibility of connecting the gas grid with the electrical grid with the exploitation of surplus energy. From extra power, H₂ is produced by water electrolysis and converted with CO₂ in the methanation unit to a gas mixture with mainly CH₄ and H₂O seen in Figure 3. The CH₄ gas mixture can then be treated to a methane-rich gas or so-called Synthetic Natural Gas (SNG) and can be used as fuel for transport, residential sector, or for power generation [3]. If SNG produced will be used in the gas grid, it must have similar properties to natural gas distributed. Usually, natural gas contains more than 80% CH₄ and has higher values for hydrocarbons [5].

Thermodynamics

Several thermodynamic reactions play a role in methanation processes. The chemical reactions from equation 1 to 8 list the main possible reactions involved in the methanation process. Equation 1 for CO_2 is called the Sabatier Reaction or hydrogenation, and equation 2 using CO are the most normal reactions for methanation. Reaction 3 is a carbon monoxide methanation reaction that can also occur at a lower H_2/CO ratio [12]. The carbon monoxide disproportionation reaction 4, also known as the Boudouard reaction. This reaction is important since the carbon on the catalyst surface is considered a necessary intermediate during the methanation reaction. The water gas shift reaction 5 is also important because water plays an important role, which would modify the surface and catalytic chemistry of methanation catalysts. Reactions 3, 4, and 6 are three independent reactions. The other reactions can be described as a linear combination of these three reactions.



Both reactions 3 and 4 are highly exothermic reactions assuming a Gas Hourly Space Velocity (GHSV) of 5000 h^{-1} the consequence of high temperatures limits the CO and CO_2 conversions. The study by [5] found that a temperature below $225 \text{ }^\circ\text{C}$ at 1 bar and $300 \text{ }^\circ\text{C}$ at 300 bar is required to have a CO_2 conversion of at least 98% and that elevated pressure gave positive effects on methanation process. The Sabatier reaction is highly favorable according to Le Chateliers's principles with high pressure and lower temperature. The H_2/CO_2 ratio will increase or decrease depending on the limiting component selected [13], and by manipulation of the H_2/CO_2 ratio concentration of the limiting component

can be controlled. With a H_2/CO_2 ratio at the inlet lower than stoichiometric 4.0, carbon is expected to be present in the gas mixture. An increase in the ratio will reduce carbon in the gas mixture but will leave a highly valuable hydrogen product in the stream [13].

The Gibbs free energy for the methanation reaction can be calculated as

$$\Delta G = \Delta G^\circ + RT \ln(Q) \quad (9)$$

where ΔG is the Gibbs free energy ΔG° is the standard Gibbs free energy, R is the gas constant, T is the temperature, and Q is the reaction quotient. As the reaction reaches equilibrium, ΔG becomes Zero and Q can be exchanged for the equilibrium constant K_{eq} [14].

$$\ln(K_{eq}) = \frac{-\Delta G^\circ}{RT} \quad (10)$$

Gao et al. modeled the calculated equilibrium constants for the eight reactions at different temperatures represented in Figure 4 involved in methanation with CO_2 is modeled as R2 in the figure. The reaction can be seen as suppressed with higher temperatures and has high equilibrium constants in the temperature range from 200-500°C. Elevating the temperature above 450°C increases the CO byproduct due to the reverse water gas shift reaction. 3



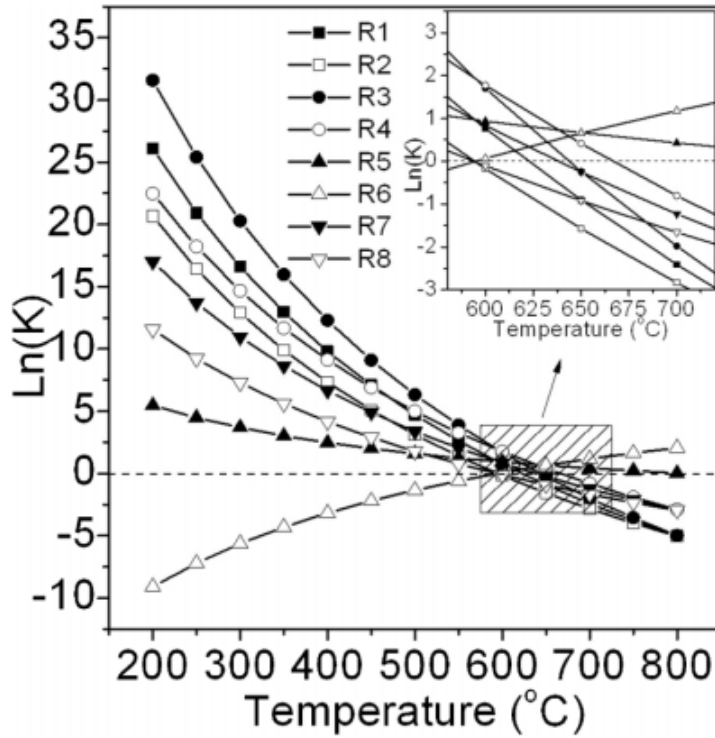


Figure 4: Calculated equilibrium constants K of the eight reactions involved in methanation process [12]

Catalyst in Methanation

Methanation can be done both biologically and chemically via catalytic reactors. The biological route is known in biogas production, which can be distinguished into two main reaction paths: acetoclastic, methanogenesis, and hydrogenotrophic methanogenesis. The chemical route results in production of CH_4 from CO_2 and H_2 [3] by catalytic methanation. While CO_2 methanation is highly exothermic, a catalyst is favorable to overcome the low kinetics with reduction of CO_2 to CH_4 [3]. CO_2 methanation is an eight electron exchange reaction from fully oxidized carbon (-4) to methane (+4) [15]. With this, an efficient and effective catalyst is important to improve the reaction. Figure 5 gives a visual illustration of the different methanation processes.

Typical catalytic methanation reactors are operated at high temperatures ranging from 200 °C to 500 °C and pressures ranging from 1 to 100 bar. A suitable catalyst must consider activity, selectivity towards the CH_4 , and be economically viable for large-scale operations. Mills and Steffen, in their paper, suggested an order for the available metal catalyst for the methanation in terms of activity and selectivity:

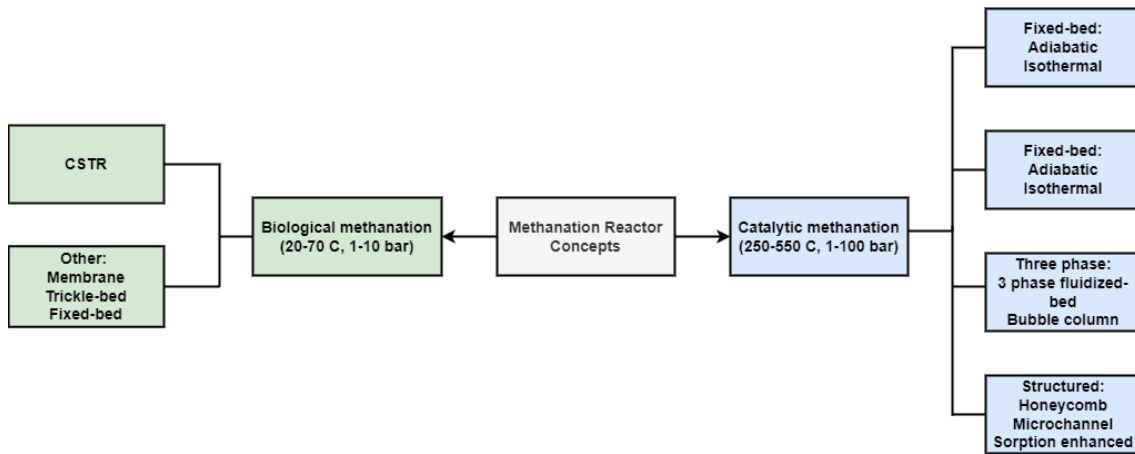


Figure 5: Reactor concepts for methanation process.

Activity: Ru > Fe > Ni > Co > Mo

Selectivity: Ni > Co > Fe > Ru

Ni, Ru, Rh, and Co are the most popular metals used as a catalyst for methanation reactions. Ni is the most used in the industry due to its high activity and good CH₄ selectivity and cheap raw material price. The main drawbacks for nickel-based catalysts are the requirement of high-purity feed gas and a high tendency to oxidize in oxidizing atmospheres.

It is often required to have supporting materials to increase the surface area of the active metals. Increasing the surface area will increase the active sites available to selectively convert CO₂ by methanation. Most used support metals commercially are Al₂O₃, SiO₂ or TiO₂ in that order [16]. The main disadvantage of using Al₂O₃ as a support metal is problems with sintering in the presence of water at high temperatures [12].

With high exothermic reactions, a consequence of heat removal needs to be implemented, and a significant issue is to realize good temperature control in the reactor. This is to prevent thermodynamic limitation and catalyst sintering. The catalyst must withstand high temperature ranges to avoid deactivation of the catalyst [5]. A Higher temperature change in the catalyst leads to more catalyst deactivation [17]. The deactivation temperature range depends on the chosen catalyst, but a temperature higher than 550°C should be avoided. Some methanation catalysts operate in the 600 °C range but are not widely used [16]. The choice of catalyst and its active material depends most on the system's operational conditions, the presence of contamination required selectivity/activity, and the price of the catalyst. Table 1 summarizes the most relevant mechanism for catalyst

deactivation var and is listed by Rönsch et al. [16].

Table 1: Mechanism that causes catalyst deactivation[16]

Mechanism	Description	Deactivation problem
Poisoning (Chemical)	Chemisorption of species on catalytic sites	Chemisorption of sulfur (H_2S , thiophenes)
Vapor-solid reactions (chemical)	Reaction of fluid, support or promoter with catalytic phase	Formation of nickel carbonyls at temperatures below $230\text{ }^\circ\text{C}$ in the presence of CO
Thermal Degradation (thermal)	Thermally induced loss of active surface area	Thermal sintering of active nickel, especially in quasi-adiabatic fixed-bed reactors.
Fouling (mechanical)	Physical deposition of species from fluid phase onto the catalytic surface and into catalyst pores	Carbon or coke deposition on nickel surface caused by the Boudouard reaction or decomposition of higher hydrocarbons.
Attrition (mechanical)	Loss of catalytic material due to abrasion	Attrition of active material in fluidized-bed reactors
Crushing (mechanical)	Breakup of catalyst particles due to thermal or mechanical stress.	Thermal stress caused by reactor startup/shutdown: mechanical stress caused by pressure fluctuations.

Reactors

In this thesis, the steady-state reactor concepts for a fixed-bed, fluidized-bed, three-phase, and structured reactor are covered.

Fixed bed reactors are the most used reactors for methanation. They are characterized by their extended contact of catalyst particles by the gas tend to be uniform, the possibilities for long contacting times, and relatively simple and cost-effective systems [3]. They are usually designed as adiabatic or polytropic. If necessary, the adiabatic fixed bed reactors rely on various reactors with intercooling and gas re-circulation to achieve high conversion rates. The adiabatic catalyst must withstand a broad temperature range and gives the main concerns as possible cracking, sintering, hot spots, and poor flexibility concerning the load [5][3]. In the polytropic fixed bed reactors, its design is a cooled tube bundle system where many tubes with relatively small diameters are placed in parallel. The reactors give lower temperature gradients that lead to an increased life span of the system, but

the polytropic reactors are more expensive and relatively complex [3]. Figure 6 shows an example of a simple adiabatic and polytropic fixed bed reactor.

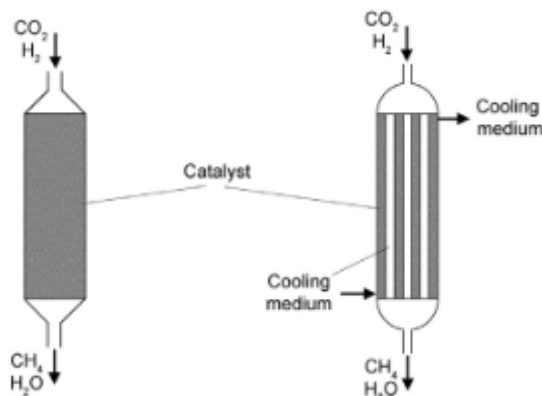


Figure 6: Adiabatic fixed bed reactor (Left), Polytropic fixed bed reactor (Right).

Fluidized bed reactors mix fluidized solids, leading to isothermal conditions in the reactor. This facilitates the control of the operation under methanation, which gives more effective heat removal as a significant advantage. The effect of heat removal can allow the methanation process to have a single reactor. From [5], one of the drawbacks comes from high mechanical load due to fluidization. Effects cause attrition processes to occur about the catalyst and the reactor's wall, which eventually will deactivate the catalyst. Incomplete CO_2 conversion caused by bubbling and superficial gas velocities within the reactor are other disadvantages associated with fluidized bed reactors.

The Three-phase reactor for methanation is generally a slurry reactor with a liquid phase. The fine catalyst particles are suspended in the liquid phase due to the gas flow. Using a liquid with high heating capacity allows for effective and accurate temperature control. This contributes to complete heat removal and isothermal operations in the reactor, which leads to simpler process designs. Most of the three-phase reactor challenges come from resistances in the liquid's mass transfer, decomposition, and evaporation.

There are several types of structured reactors. Those covered are monolith reactors, microstructured reactors, and sorption-enhanced reactors. The monolith reactor is the most common of these three reactors and is mostly used in exhaust gas cleaning [3]. It was developed to tackle the drawback of temperature hot spots and high-pressure drops in the adiabatic fixed bed reactor. It has the advantages of high specific catalyst surface area, small pressure drops, and short response time. With an internal metallic structure, the reactor enhances radial heat transport by heat conduction with an order of 2-3 in

magnitude[5].

Microstructured reactors are very compact reactors with a high surface-to-volume ratio which gives them good attributes for high heat transfer and low-pressure drops and the advantages of improved hydrodynamics that suppress the formation of hot spots. The big drawbacks of this concept are the complicated structures which is a single-use system, which means that deactivation of the catalyst is irreversible and the whole reactor needs to be replaced.

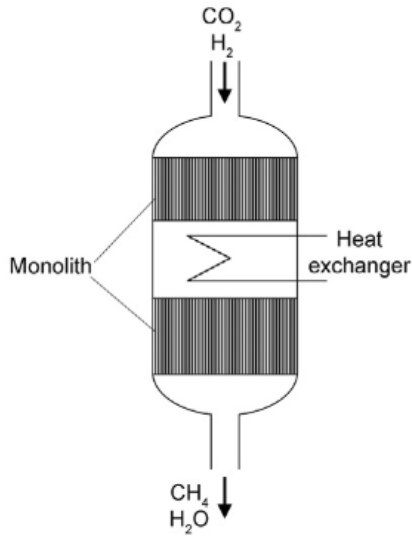


Figure 7: Monolith Reactor

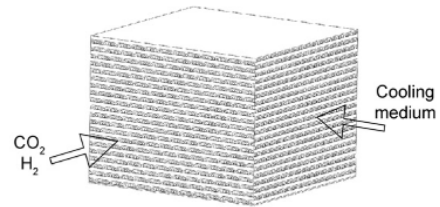


Figure 8: Micro structure reactor

The sorption-enhanced reactor concept is applied to reverse water gas shift and steam reforming processes. In reverse water gas shift, a catalyst carrier removes the water produced by the methanation reaction from the gas phase. The conversion rate for CO_2 to CH_4 can be increased up to 100% by using a mix of adsorbent and a catalyst [3].

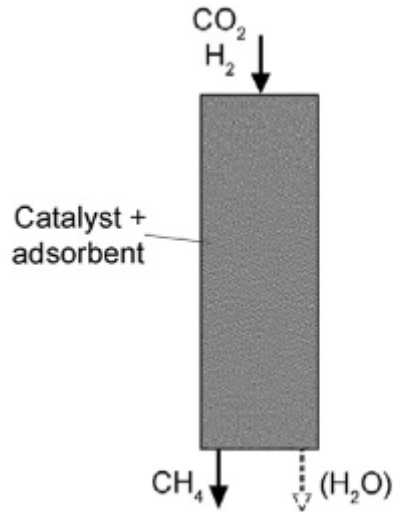


Figure 9: Sorption Enhanced methanation reactor

Biological Methanation

Another option from the Power to gas process chain is Biological methanation. In biological methanation (BM), methanogenic microorganisms serve as bio-catalysts. The first step in a typical biogas plant using biological methanation is biomass hydrolysis to simple monomers. Next, the monomers are converted into acetate, carbon dioxide, and hydrogen. Last step, the methane is produced by syntrophic methanogenesis; CO_2 reduction with H_2 [18]. The biological production of methane from CO_2 and H_2 is carried out by microorganisms, which obtain energy for growth through the anaerobic metabolism of hydrogen and carbon dioxide. Methane is produced via hydrogenotrophic methanogenesis from CO_2 and H_2 for most biological methanation.

There are two main process concepts possible for biological methanation: methanation in situ digester and methanation in a separate reactor, and proceeds under anaerobic conditions at temperatures between 20 and 70°C, and for most cases, at ambient pressure. While operating at relatively low temperatures and pressure, there is still an issue with technical implementation for a reactor in BM. The methane formation rate (MFR), the GHSV (gas hourly space velocity), and the methane content are important parameters to consider when evaluating the reactor efficiency. The efficiency depends on the type of microorganisms used, cell concentration, reactor concept, pressure, pH value, and temper-

ature. The MFR equation is given below:

$$MFR = \frac{F_{V,CH_4,out} - F_{V,CH_4,in}}{V_R} \quad (12)$$

Here, $F_{V,CO_4,out,in}$ is the volumetric flow rate of the CH_4 , without inert gases in and out of the reactor, and V_R is the reactor volume. With the microorganisms present in a fermentation broth, the methanation reaction takes place within the aqueous solution. There is additional gas-liquid mass transfer resistance compared to 2-phase catalytic methanation reactors, and can be described by [5]:

$$r_{i,eff} = \frac{F_{(n,I,G|L)}}{V_R} = (k_La)_i \cdot (c_{i,L}^* - c_{i,L}) = (k_La)_i \cdot \left(\frac{p_i \dot{\rho}_L}{h_{i,L}} - c_{i,L} \right) \quad (13)$$

Here, $r_{i,eff}$ is the effective reaction rate, k_La is the mass transfer coefficient, $c_{i,L}^*$ is the solubility from increasing pressure p_i , and $H_{i,L}$ is the Henry's law coefficient for H_2 and CO_2 in water.

For the two process concepts, the in situ biological methanation uses hydrogen directly fed into the biogas digester instead of having a separate reactor for methanation. A process flow diagram for in situ BM and BM in a separate reactor is shown in Figure 10. For in situ method, the solid lines show biogas goes straight to the gas cleaning step from the digester. The hydrogen is introduced into the digester step. The dashed line represents the utilization of the thermal energy in the system.

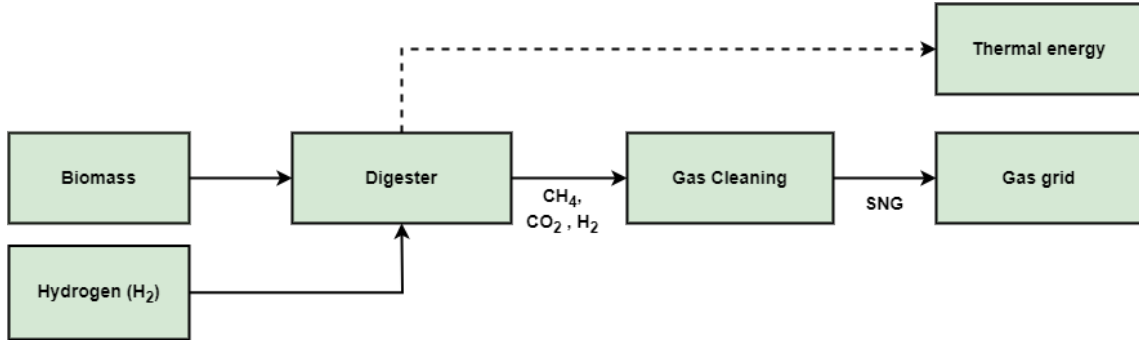


Figure 10: Process flow diagram for In situ BM and Separate reactor BM

The CO_2 produced by the biogas plant is in situ converted to CH_4 giving biogas with high methane content and calorific value. The MFR for in situ production is small with only MFRs of 0.1 h^{-1} to make it possible. The reaction rate is limited by the CO_2 production of the plant. Further, in a in situ plant, the process conditions cannot be adapted to optimal conditions for the hydrogenotrophic methanogens. Achieving high CO_2 conversion is very

difficult with in situ BM. Using energy crops as feedstock resulted in an increase in methane from 52 to 75% in an in situ biogas plant in Germany [5].

In biological methanation using a separate reactor, pure gases are converted by methanogen cultures into CH_4 . Using a separate reactor offers the possibility to increase the calorific value of biogas but is not limited to biogas as a carbon source. Unlike in situ concept using a separate reactor, the process conditions and reactor design can be adjusted for the optimal conditions. Several reactor concepts can be used for BM, with CSTR, fixed-bed, trickle-bed, and membrane reactors being heavily researched. In Götz et al. study for biological methanation in a separate reactor, the CSTR reactor concepts achieved a CH_4 content ranging from 13.4-85%, fixed-bed achieved 34%, and the Trickle-bed concept had the highest CH_4 content with 98%. They concluded that for all reactor design concepts, hydrogen supply to the microorganisms is the rate-limiting factor. To conclude, the biggest challenge for BM is the delivery of the gaseous hydrogen to the microorganisms and adequate and energy-efficient mixing on large-scale biological reactors concerning hydrogen supply.

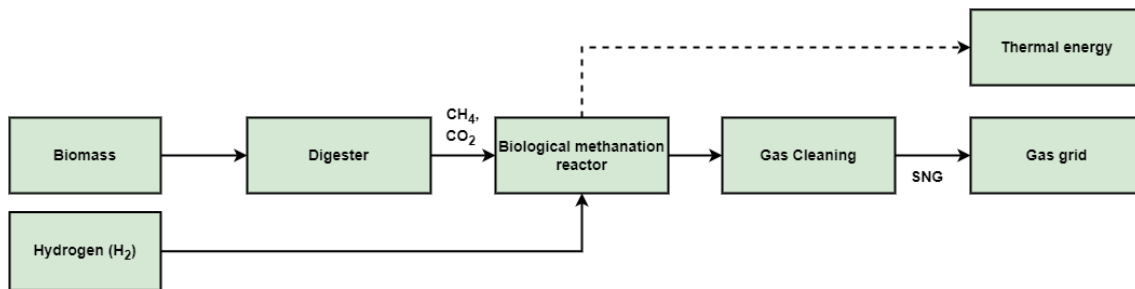


Figure 11: Process flow diagram of BM in a separate reactor.

2.2 Biogas Upgrading

In this subsection, the fundamentals and different technologies for biogas upgrading will be highlighted. The topic will include the four major technologies in absorption, adsorption, membrane, and cryogenic. Non purified Biogas consist mainly of CH_4 (50-70%), CO_2 (30-50%) and minor components of H_2O , N_2 , H_2S , H_2 and siloxanes and to separate CO_2 out the CH_4 upgrading has to be applied. The biogas upgrading technologies are applied for the polishing unit in the process model.

2.2.1 Physical absorption with a Water Scrubbing System

Pressurized water scrubbing is the most commonly used for biogas upgrading methods. It takes advantage of the high solubility of CO_2 and H_2S in water compared to CH_4 , thereby separating CO_2 and H_2S from the biogas stream [19]. The biogas is compressed from 6-12 bar to enhance the absorption in a scrubber via the bottom side of the tank, and water is sprayed from the top of the scrubber. Inside biogas and water flows, counter-current and absorption occur on the surface of a packing media [20]. The cleaned biogas can have a concentration of 96% or higher methane after the dehydration process and leaves from the top of the scrubber. The CO_2 and H_2S solvent is circulated into a flash column, where the pressure decreases, and some traces of CH_4 recovered from the solvent, and the methane and water are redirected to a regeneration stripper. The biggest advantage of using pressure water scrubber absorption is using water instead of chemicals to remove CO_2 , H_2S , and other impurities. Still, the other challenge is the high water demand [20]. The typical water required that is needed to upgrade $1000 \text{ Nm}^3/\text{h}$ of raw biogas ranges between 180 to 200 $\text{ m}^3/\text{h}$ of water flow, depending on pressure and temperatures [19].

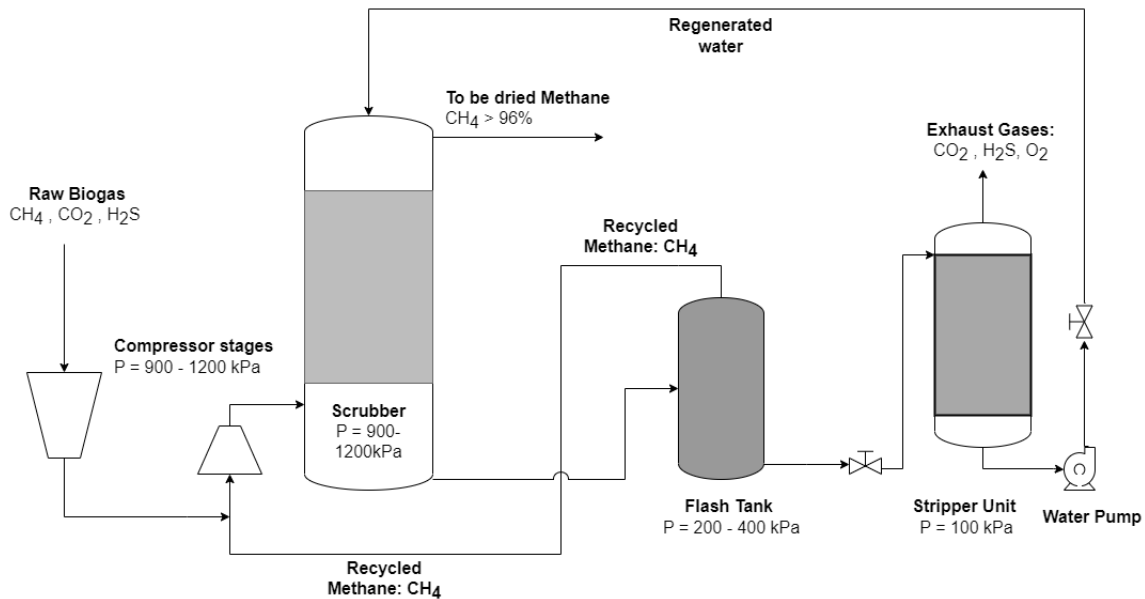
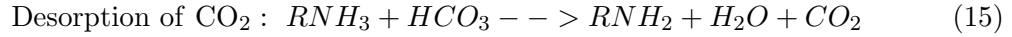
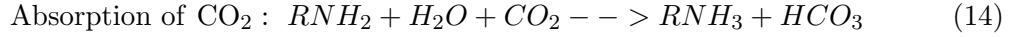


Figure 12: Pressure water scrubbing system from [20].

2.2.2 Chemical Absorption with Amine Solutions

Amine solvent has been used to separate CO_2 from coal-fired power plant flue gas for years and was adopted later in the 1980s for biogas cleaning technology. The amine solvent has a high absorption selectivity of CO_2 from the gas stream, and commonly used solvents are

alkanolamines, such as monoethanolamine (MEA), which is the most common one used for low-pressure absorption [20]. Biogas is usually compressed at 2-7 Bar before being fed into an absorption reactor. There CO_2 and H_2S gas dissolve into the amine solvent, and high purity CH_4 leaves the amine reactor. The CO_2 and H_2S rich amine solution is routed to a desorption process in a stripping unit for regeneration. The chemical reactions for the absorption and desorption process are shown below.



Because of the high temperature in the regeneration reactor (stripper) and the lower temperature in the absorption reactor, a heat exchanger is placed to increase the temperature of the CO_2 solvent before the regeneration stripper. A cooler is often set to reduce the temperature of the CO_2 lean product leaving the stripper. A big reason to choose an amine solution for biogas cleaning is that the clean biogas has high purity of CH_4 and CH_4 losses can be as low as 0.1% [19]. Amine absorption is therefore preferred for processes where strict environmental regulation for CH_4 content and emissions are applied [20]. One of the main disadvantages of this method is the intensive energy demand and the high price of the amine solvents. The price for MEA is about \$ 1-1.5 per kg, and to capture 1 ton of CO_2 , the amount of MEA solvent that will be needed theoretically is 1.39 tons. Another disadvantage of amine absorption is that the solvents are highly toxic to humans and the environment, and their losses are due to evaporation[19]. A figure of a general absorption model is given below, with absorption and desorption columns [20].

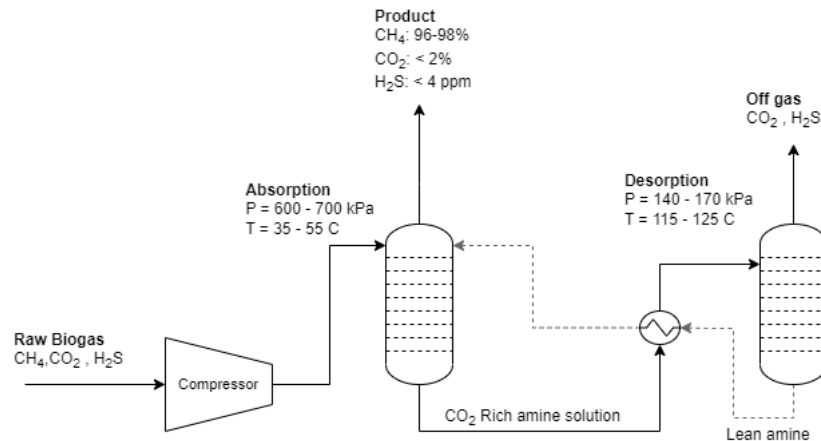


Figure 13: Amine absorption system example from [20]

2.2.3 Adsorption with Pressure Swing Adsorption

This method of biogas upgrading uses adsorbent differences in gas adsorption rates to capture preferred gases at high pressure. Then it releases the adsorbents at a low pressure to regenerate the adsorption process. The adsorption is based on their molecular characteristics and the affinity of the adsorbent material. The adsorbent is designed to have specific pore sizes which enable selective adsorption of CO_2 , O_2 and N_2 molecules than the designed pore size. Pressure swing adsorption follows four steps, adsorption, blow-down, purge, and pressurization [19]. Pressurized biogas enters the adsorption column at high pressure 4-10 bar where CO_2 and other minor gases are adsorbed, and rich CH_4 leaves the top and decreasing of pressure happens. There is usually a need for four or more vessels to ensure continuous operation. When the adsorbents are saturated, the biogas flows to another vessel. There it will be regenerated by a desorption process, in which pressure is decreased to atmospheric conditions, and the trapped gasses are released. The trapped gas contains a significant amount of CH_4 , so it needs to be recycled into the PSA inlet (step 2). In step 3, the pressure is then further decreased, which desorption captures impurities with regenerating of the adsorbents CO_2 , N_2 and O_2 leaves the vessel. In step 4, the pressure is built up for the subsequent cleaning cycle [19][20]. One of the significant problems with PSA is its toxicity and overloading of adsorbents. H_2S is usually a sticky gas, and adsorption is irreversible. Therefore, it must be removed before biogas is injected into the adsorption column, shown in the figure below. The effectiveness of PSA is that it can upgrade raw biogas to 96-98% methane concentration, but up to 4% of the methane can be lost within the off-gas stream[19].

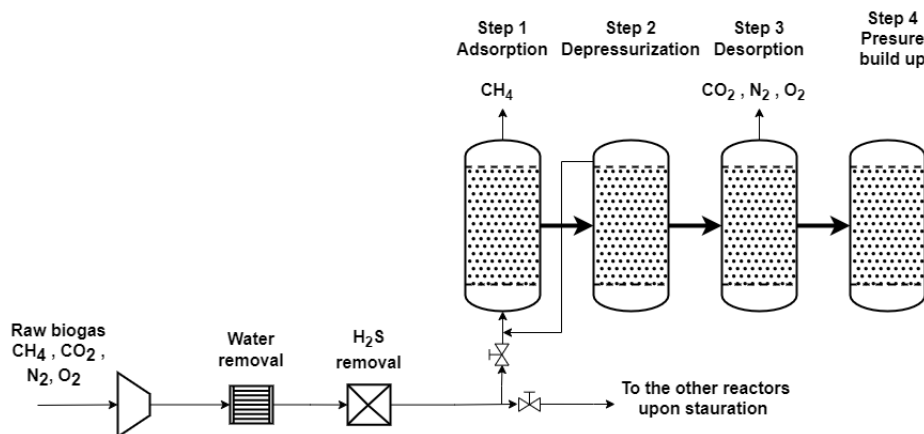


Figure 14: Example of a Pressure Swing Adsorption system [20]

2.2.4 Membrane Separation

Membrane separation uses the principle of selective permeability properties to separate biogas components. The different components in biogas have different permeation rates. Gases with high permeability, such as CO_2 , H_2O and O_2 can be transported through the membrane, while gases with low permeability CH_4 are retained and collected at the end of the column. An ideal membrane should have a significant permeability difference between CH_4 and CO_2 to reduce the methane losses and get the high efficiency for biogas purification[19]. There are four main manufacturing configurations for gas-gas membrane cascade with the three stages with three biogas streams having the highest CH_4 content with 95-98% [19].

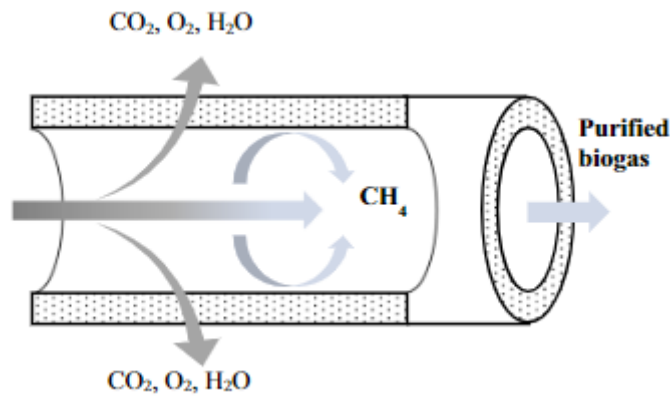


Figure 15: Example of a membrane separation system [20]

2.2.5 Cryogenic Separation

The cryogenic separation technology uses the different condensation temperatures of gases to purify the biogas. The temperature is gradually decreased until -78.5°C when CO_2 is condensed and one can separate CH_4 and CO_2 . The different boiling points for the feed gas components are given below. The cryogenic process is usually done in four steps. Moisture removal, usually water and other organic impurities. H_2S and siloxanes removal. CO_2 removal via condensation, and lastly CH_4 condensation into Liquid Biogas (LBG). The produced LBG usually has a methane content of 99% [20]. The cryogenic separation method gives promising results but is still under development, and few facilities use it. The high investment cost, operating cost, and the CH_4 losses are one of the major drawbacks of this technology. Hashemi et al. studied energy analysis using cryogenic vs. amine-based biogas upgrading to produce LBM. They found that the cryogenic upgrading required the

specific work of 2.07 kWh/kg LBM, while amine-based upgrading needed the specific work of 1.54 kWh/kg LBM. Further optimization of the purity by removing other components would not be recommended as reaching the lower temperatures requires high amounts of energy [21].

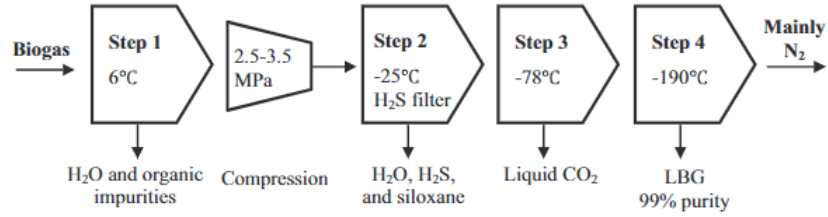


Figure 16: Example of a cryogenic process from [20]

Table 2: Boiling point temperatures [°C] for different components in Biogas

Components in biogas	Boiling Point at 1.013 bar	Unit
H ₂	-252.8	°C
N ₂	-195	°C
CO ₂	-78.5	°C
CO	-191.5	°C
CH ₄	161.5	°C

3 Process Description

This chapter describes the Power-to-methane process that is modeled in the master thesis. The description covers the methanation, polishing, and liquefaction units separately.

3.1 Power-to-Methane Process Model

Figure 17 is a simplified direct biogas processing model. The methanation unit is represented in blue, the polishing unit is represented in red, and the liquefaction unit is represented in green.

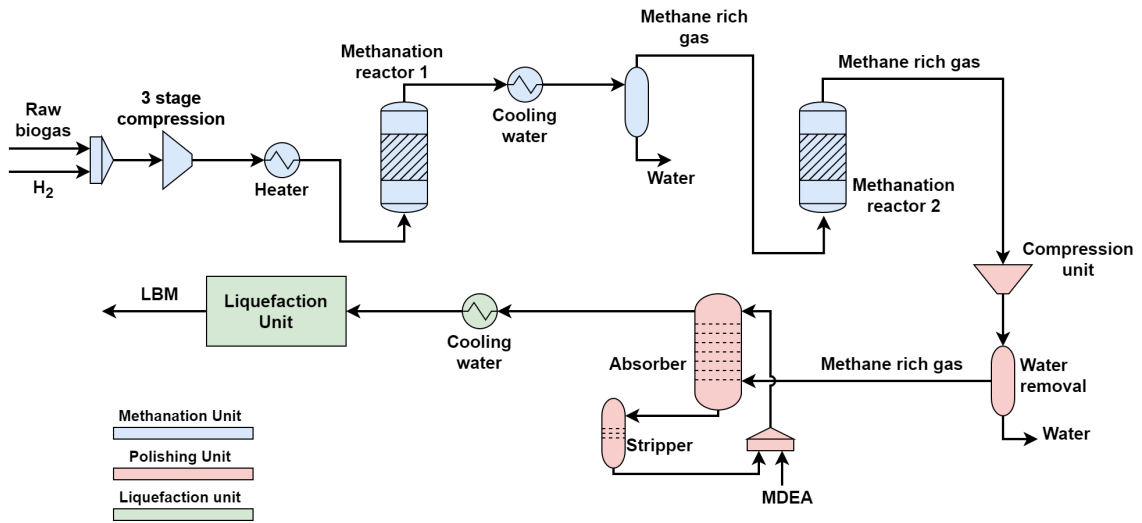


Figure 17: Simplified Process Model for Direct Biogas Methanation

3.2 Methanation Process

The methanation unit has been modeled by implementing the inlet specifications of raw biogas from the biogas plant in Skogn with an appropriate flow rate of H₂ to achieve the different H₂/CO₂ ratios in the case studies. The model uses the Direct methanation process model studied in the project thesis. A Simplified model of the methanation unit is shown in Figure 18.

In the methanation unit, green H₂ from an alkaline electrolyzer is injected into the raw biogas stream before entering the compression stage. The inlet stream goes through a three-stage compression cycle with intermediate cooling to achieve the desired pressure. A heater is placed to ensure the right temperature before the first methanation reactor.

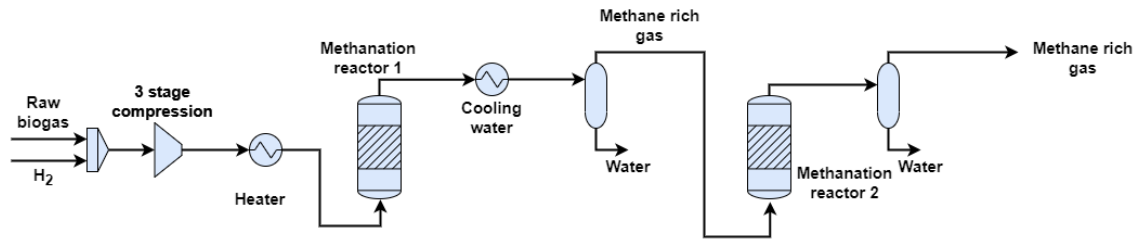


Figure 18: Simplified model of the methanation unit in the process model.

In the first reactor, CO_2 and the H_2 react together through the Sabatier reaction to create methane and increase the methane content in the stream. H_2O is a by-product from the reaction, which a component-splitter removes after the cooling heat exchanger. The water needs to be removed before the second reactor to ensure a clean Sabatier reaction. After the first water splitter, the methane-rich stream with leftover CO_2 and H_2 goes through the second methanation reactor to further increase the CH_4 content in the stream. For the different H_2/CO_2 ratios, there will be some contents of CO_2 in the stream. The stream is then sent to a polishing unit after a water-removal unit.

3.3 Polishing Process

The polishing unit is modeled after a conventional biogas upgrading process. A conventional biogas upgrading process model can be seen in Appendix A. Figure 19 is a simplified figure used in the polishing process.

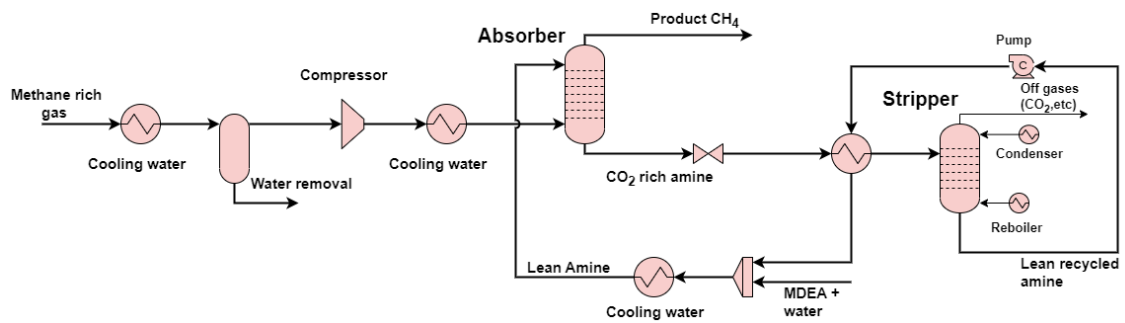


Figure 19: Simplified model of the polishing process

Here, the methane-rich stream from the methanation unit goes through a cooling and water removal unit. This is to ensure all the water is removed before entering a compressor. The compressor is placed there to increase the pressure of the stream to have an optimal setup before the amine absorber. Since amine absorption columns for CO_2 favor higher pressure values. In the absorber, methane-rich biogas product from the methanation process and

lean MDEA amine are injected with identical pressure, and CO₂ left in the stream is absorbed by the amine. From the top of the absorber, product CH₄ with ≤ 50 PPM CO₂ is sent to the liquefaction process to produce LBM. CO₂ rich amine leaves the bottom, leading to an amine regeneration stripper.

Before the stripper, the CO₂ rich amine solvent is depressurized. Because of the high temperature in the regeneration stripper, a heat exchanger is placed before the stripper to increase the temperature of the CO₂. A cooler is usually also set to reduce the temperature of the regenerated CO₂ solvent. Here, an integrated shell and tube heat exchanger is used to utilize the high temperature CO₂ regenerated solvent to heat the CO₂ rich amine before the stripper while also cooling the high temperature regenerated solvent. The regenerated solvent is then sent to a stream combiner to add more MDEA amine and water before the absorption column. A cooler using cooling water is also placed to further decrease the temperature of the Lean amine before the absorber.

3.4 Liquefaction Process

The liquefaction process consists of a single nitrogen expander refrigeration cycle and an expander to produce LBM at -162°C and atmospheric pressure. A single nitrogen expander refrigeration cycle was chosen for its simple design. More efficient options are available, such as a dual nitrogen expander cycle[9]. An example of the single nitrogen expander refrigeration cycle used in the model is shown in figure 20. In the single expander refrigeration process, Nitrogen is compressed in the N₂ compression cycle with precooling before the multi-stream heat exchangers. The nitrogen pressure is then reduced in the expander. This is to supply adequate cooling duty for both Nitrogen streams and the product methane. The N₂ liquefaction unit provides a cooling duty to the sub-cooled Nitrogen, product methane with small parts of CO₂ and the cooler is used to sub-cool the product biomethane to -162 °. After the Biomethane is sub-cooled to liquefaction values, the pressure is reduced through the valve/expander to atmospheric values and sent to a separation column. The product LBM is produced from the bottom, and the boil-off gases (unliquefied parts of product methane) are split from the top of the column.

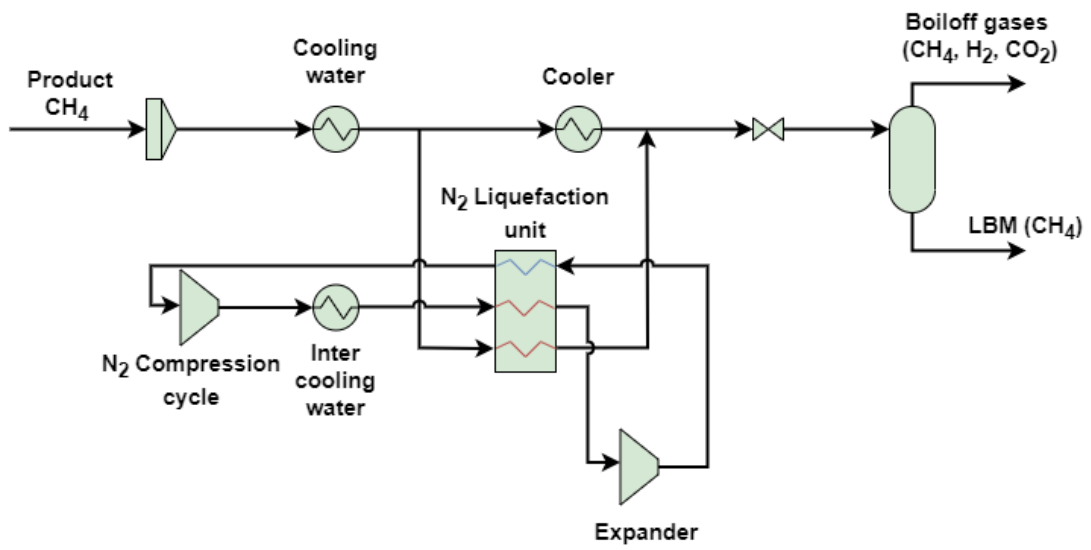


Figure 20: Simplified model of an N₂ Liquefaction process

4 Design Basis

In this chapter, the different design aspects and specifications will be clarified and consist of feed and product specifications, design variables used in the case studies, and the optimizer variables and constraints are clarified.

4.1 Feed Specifications and Product Specifications

The biogas used in the process is assumed from the biogas plant in Skogn, Trøndelag. The biogas composition is shown in Table 3. To simplify the process, we assumed that the minor components, namely H₂O, N₂, H₂S, H₂, and H₂, were not present in the biogas stream.

Table 3: Inlet raw biogas specifications

Parameter	Biogas	Pressure
CO ₂	40 mol%	1 atm
CH ₄	60 mol%	1 atm

The inlet biogas specifications are adapted to and simplified to fit a large biogas plant located in Skogn, Norway, with a capacity to produce 25 million Nm³/year biogas. The inlet biogas has a molar flow of 200 kgmole/h of raw biogas. The H₂ used in the methanation process is assumed to come from an alkaline-type electrolyzer (Green Hydrogen) with the same temperature and pressure as the raw biogas. The molar flow rate of hydrogen was varied to achieve the ratios between 3.0-4.0 in the master thesis, and the specifications are given in Table 4 for each case.

Table 4: Inlet biogas and Hydrogen specifications for H₂/CO₂ ratio.

H ₂ /CO ₂ ratio	Parameter	Flowrate	Total Flowrate
3.0	CH ₄	120 [kgmole/h]	450 [kgmole/h]
	CO ₂	80 kgmole/h	
	H ₂	240 kgmole/h	
3.2	CH ₄	120 kgmole/h	456 [kgmole/h]
	CO ₂	80 kgmole/h	
	H ₂	256 kgmole/h	
3.5	CH ₄	120 kgmole/h	480 [kgmole/h]
	CO ₂	80 kgmole/h	
	H ₂	280 kgmole/h	
3.8	CH ₄	120 kgmole/h	504 [kgmole/h]
	CO ₂	80 kgmole/h	
	H ₂	304 kgmole/h	

The product specifications from the plant in the form of Liquid biomethane with CH₄, CO₂, and other impurity contents are given in Table 5 [22].

Table 5: Product specifications [22]

Parameter	Biomethane	Unit
CH ₄	99.9	mol%
CO ₂	≤ 50	ppm mol
H ₂ S	≤ 1 – 4	ppm mol
H ₂ O	≤ 0.1 – 1	ppm mol
Pressure	1.013	bar
Temperature	≤ 40	°C

As seen from Table 5, the product stream needs to be purified of almost all contamination present. The main reason for the high purity content or LBM is the liquefaction step in the methanation process that takes place in cryogenic temperatures that causes the solidification of the impurities.

4.2 Design Variables

In this section, the independent and dependent variables are stated for this Power-to-Methane model made. These selected variables are used for the case studies in Aspen HYSYS V10.1, and the results of the case studies will be presented and discussed in Chapter 6. First, the independent and dependent variables for the methanation process are presented, and then the independent and dependent variables for the polishing unit. The case studies were divided into four parts for different H_2/CO_2 ratios. The ratios chosen for the case study and the optimization were a ratio of $H_2/CO_2 = [3.0, 3.2, 3.5, \text{ and } 3.8]$. To optimize the results from the case studies, the processes were optimized sequentially (i.e., optimizing the methanation unit and polishing unit separately) using the Hyprotech SQP optimizer in Aspen HYSYS V10.1.

4.2.1 Design Variables for the Methanation Unit

Case Studies:

In the methanation process, the selected independent variables to be varied in the different case studies were the methanation temperature, methanation pressure, the coolant temperature, and the number of tubes in methanation 1 and 2. Table 6 shows the different settings for the methanation case studies.

Table 6: Independent Variables used in the case studies for the methanation process

Independent variables	Low	High	Step size	#Steps	Unit
Methanation inlet temperature	200	320	10	13	°C
Methanation inlet Pressure	10	30	5	5	Bar
Coolant temperature	200	320	10	13	°C
Number of tubes reactor 1	400	4000	200	19	-
Number of tubes reactor 2	400	3000	200	13	-

Hyprotech SQP Optimizer:

The methanation unit was optimized for maximizing the methane content in the stream after the second methanation reactor. The independent variables were the temperature, pressure, coolant temperature, and the number of tubes. The independent variables range and the restrictions used in the optimizer are shown in Table 7.

Table 7: Process variables and constraints used in Hyprotech SQP optimizer for methanation unit.

Methanation Unit		
Variables		
Inlet temperature reactor 1	200 - 330	°C
Inlet temperature reactor 2	200 - 330	°C
Methanation Pressure	10 - 30	Bar
Coolant temperature	200 - 330	°C
Number of tubes reactor 1	100 - 4000	-
Number of tubes reactor 2	400 - 3000	-
Constraints		
Maximum temperature in 1st reactor	≤ 550	°C
Maximum temperature in 2nd reactor	≤ 550	°C
Maximum velocity in 1s reactor	≤ 1	m/s
Maximum velocity in 2nd reactor	≤ 1	m/s
Minimum conversion of H ₂	99.0 - 99.99	%

4.2.2 Design Variables for the Polishing Unit

Case studies:

In the Polishing unit, the selected independent variables to be varied in the different case studies were the pressure into the absorber, the MDEA flow rate into the absorber, and the MDEA concentration in the stream. The different settings for the polishing case studies are given in Table 8.

Table 8: Independent Variables used in the case studies for the polishing unit

Independent variables	Low	High	Step size	#Steps	Unit
Pressure into absorber - 14	30	80	10	6	°C
MDEA flow rate	100	800	100	-	kgmole/h
MDEA concentration	35	60	5	6	%

Hyprotech SQP Optimizer

The polishing unit was optimized for minimizing the CO₂ fraction in the product stream after the absorber unit. The independent variables were absorber pressure, stripper pressure, MDEA amine flow rate, MDEA amine concentration, Lean amine temperature, and rich amine temperature. The different independent variable ranges and constraints used in the Hyprotech SQP optimizer are shown in Table 9.

Table 9: Process variables and constraints used in Hyprotech SQP optimizer for polishing unit

Process unit		
Variables		
Absorber pressure	20 - 80	Bar
Stripper pressure	1 - 6	Bar
MDEA amine flow rate	100 - 3000	kgmole/h
MDEA amine concentration	35 - 60	wt%
Lean amine temperature	40 - 60	°C
Rich amine temperature	70 - 105	°C
Constraints		
CO ₂ Content into Liquifaction	≤ 50	PPM
Reboiler temperature	$\leq 126,7$	°C
CO ₂ rich loading	≤ 0.55	-
Minimum temperature approach in HX ΔT	≥ 10	°C

5 Process Modeling

This chapter describes the simulation tool, process assumptions, and how the main components (methanation reactor, polishing unit) have been modeled.

5.1 Simulation Tool

The Biogas upgrading, methanation, and liquefaction processes were simulated using Aspen HYSYS V10.1. The Soave-Redlich-Kwong (SRK) equation of state was employed for most of the operating units within the processes. For the direct and indirect methanation process unit, the "Refprop" package from Aspen properties is considered for the compressions units, the refrigeration cycle, and the methanation reactors. The "Refprop" package was chosen because of H_2 in the mixture within the liquefaction process. In the Amine based CO_2 capture columns, the "Acid gas- chemical solvent" package is recommended by Aspen HYSYS. The methanation reactor is modeled in MATLAB and imported to the Aspen HYSYS model using MATLAB CAPE-OPEN unit operation. The simulation models and configurations were made under Hashemi's Ph.D. work in "Development and Optimization of Processes for Liquefied Biomethane Production" and are used for this project.

5.1.1 Process Assumptions

The assumptions applied in the process models will be covered in this subchapter. First, the H_2 used for methanation was assumed to be available from an alkaline electrolyzer at the same temperature and pressure as the raw biogas. For a typical alkaline electrolyzer, the temperature and pressure for H_2 are higher than assumed [3]. The following assumptions were applied to the process models:

- The isentropic efficiency of the compressor and expanders is assumed to be 80%, and an isentropic efficiency of 85% for the pumps was made.
- The cooling water used in the condensers and intermediate heat exchangers, a temperature of 20°C and 25°C was utilized.
- Saturated steam at 5 bar was used as a heat source for the reboilers, stripper columns, and heaters.

-
- Saturated steam at 40 bar is considered a heat sink for the methanation reactors.
 - The pressure drops in the heat exchangers and columns are neglected.

The methanation reactors are assumed to be multi-tubular. The velocity field in the reactor is modeled through the plug flow model, and the pressure drop along the reactor length is neglected. Through calculations in Hashemi's Ph.D. work, the pressure drop in the reactor was on a scale of 0.1 kPa [9].

5.2 Modelling of Methanation Reactor

A one-dimensional pseudo-homogenous model was used to represent a fixed-bed methanation reactor in the direct methanation process model. A multi-tubular wall-cooled reactor was assumed for the methanation reactor, detailed in MATLAB, and introduced with the CAPE-OPEN unit operation in Aspen HYSYS. This was to account for the temperature profile and avoid potential thermal runaway in the methanation reactor. The cooled reactor enables better carbon dioxide conversion and heat release controllability than other reactors. This thesis will not cover the implemented MATLAB code and CAPE-OPEN unit operation. The model is similar to Bremer et al. [4] and Fache et al. [17], and a brief description of the governing equations, employed assumptions, and correlations are provided in the sub-chapter. Further explanation of the derivation and symbols used is given in Appendix D.

The multi-tubular methanation reactor was illustrated as a singular tube given by Figure 21. The reactor considers plug flow and describes the velocity field within the methanation reactor. The superficial velocity is usually set constant for simplifications for the axial velocity. The superficial gas velocity is included since the Sabatier reaction mechanism is non-equimolar and can lead to a change in gas velocity. Due to high superficial velocities within the methanation reactor, the convective transport is larger than the axial mass dispersion and heat transport via conduction [4]. Within the pseudo-homogeneous reactor, gas and catalyst phases are considered one pseudo-homogeneous phase neglecting heat and mass transfer resistance between the two phases and within the catalyst pellets. Further, a temperature-dependent effectiveness factor from Kiewidt and Thöming [23] was considered for the intraparticle mass limitations of the pseudo-homogeneous model.

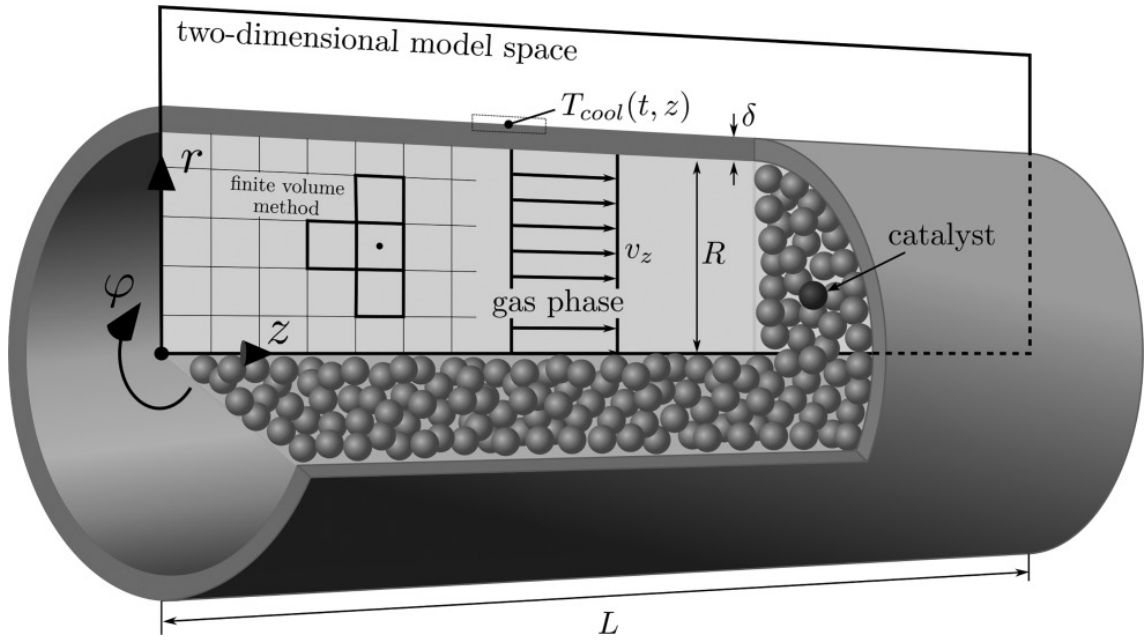


Figure 21: Illustration of a cooled walled fixed-bed reactor [4]

The mass balance equation for a one-dimensional methanation reactor along the direction of z is given by:

$$\frac{d\omega_\alpha}{dz} = \frac{M_\alpha \cdot (1 - \varepsilon) \cdot \eta \cdot \rho_{cat}}{\bar{\rho} \cdot u_z} \sum_{\alpha} \nu_\alpha \cdot r \quad (16)$$

Here, ω_α , M_α , ν_α , ε , ρ_{cat} , and η denote mass fraction, molar mass, stoichiometry coefficient of component $\alpha = [\text{CO}_2, \text{H}_2, \text{CH}_4, \text{and } \text{H}_2\text{O}]$ respectively, catalyst void fraction, catalyst density and effectiveness factor.

From the energy balance, we get the temperature profile along the z -axis of the reactor:

$$\frac{dT}{dz} = -\frac{4}{D} \cdot k_w \cdot (T - T_c) + \frac{(1 - \varepsilon) \cdot \eta \cdot \rho_{cat}}{\bar{\rho} \cdot c_p \cdot u_z} \sum \Delta H_R \cdot r \quad (17)$$

Here, k_w , T , T_c , ΔH_R , and r is the overall heat transfer coefficient, temperature within the reactor, coolant temperature, heat of Sabatier reaction, and reaction rate. Where the superficial velocity u_z for the plug flow is calculated based on the total mass balance:

$$u_z = u_{z,in} \cdot \frac{\bar{\rho}_{in}}{\bar{\rho}} \quad (18)$$

The heat transfer per unit length of the tube bundle for a cooled-wall fixed-bed reactor with coolant temperature T_c , tube diameter D , and the number of tubes N_t can be calculated by:

$$\frac{d\dot{Q}}{dz} = \pi \cdot D \cdot N_t \cdot U \cdot (T(z) - T_c) \quad (19)$$

Heat transfer at the wall of the reactor is described by Dixon and calculated from the overall heat transfer coefficient $k_{w,Dix}$.

$$\frac{1}{k_{w,Dix}} = \frac{1}{\alpha_w} + \frac{D}{6 \cdot \lambda_r^{eff}} \cdot \frac{Bi + 3}{Bi + 4} + \frac{1}{\alpha_{coolant}} \quad (20)$$

It considers resistance at the inner tube wall, the thermal resistance of the catalyst bed, and resistance at the outer tube wall. In the equation, α_w refers to the heat transfer coefficient for the inner tube wall, which considers a reactor cooled by steam, and λ_r^{eff} refers to the effective radial thermal conductivity. Bi is the Biot number defined in Appendix D 57. The effective radial thermal conductivity is calculated based on correlations presented by Tsotsas [24].

$$\lambda_r^{eff} = \lambda_{bed} \frac{Pe}{K_r} \cdot \lambda_G \quad (21)$$

And the heat transfer coefficient for the inner tube wall α_w is calculated using Nusselt's number suggested by Martin and Nilles [25]:

$$Nu_w = \frac{\alpha_w \cdot d}{\lambda_G} = \left(1.3 + \frac{5}{D} \right) \frac{\lambda_{bed}}{\lambda_G} + 0.19 \cdot Re^{0.75} \cdot Pr^{0.33} \quad (22)$$

The boundary conditions used for the pseudo-homogeneous model are:

For Mass Fractions ω_α :

$$\omega_\alpha|_{z=z_0} = \omega_{\alpha,in} \quad \text{for } r_0 \leq r \leq r_1$$

For Temperature T:

$$T|_{z=z_0} = T_{in} \quad \text{for } r_0 \leq r \leq r_1$$

For Heat Flow \dot{Q} :

$$\dot{Q}|_{z=z_0} = 0 \quad \text{for } r_0 \leq r \leq r_1$$

For superficial gas velocity u_z :

$$u_z|_{z=z_0} = u_{z,in} \quad \text{for } r_0 \leq r \leq r_1$$

The effectiveness factor η is calculated based on the Thiele modulus for spherical particles [23]:

$$\eta = \frac{3}{\phi} \cdot \left[\frac{1}{\tanh\phi} - \frac{1}{\phi} \right]. \quad (23)$$

And with assuming CO_2 to be the limiting factor for mass diffusion into the catalyst pellets, Thiele modulus ϕ is defined as:

$$\phi = \frac{D_p}{2} \sqrt{\frac{r \cdot \rho_{cat} \cdot (1 - \varepsilon) \cdot \bar{R} \cdot T}{D_{CO_2}^{eff} \cdot y_{CO_2} \cdot p \cdot 10^5}}, \quad (24)$$

Here, the $D_{CO_2}^{eff}$ is the effective CO_2 diffusivity and considers gas-gas collisions and gas-wall collision through molecular $D_{CO_2}^m$ and Knudson diffusion $D_{CO_2}^{kn}$.

$$\frac{1}{D_{CO_2}^{eff}} = \frac{\tau_p^2}{\varepsilon} \left(\frac{1}{D_{CO_2}^m} \frac{1}{D_{CO_2}^{kn}} \right) \quad (25)$$

$$D_{CO_2}^{kn} = \frac{D_{pore}}{3} \sqrt{\frac{8 \cdot \bar{R} \cdot T}{\pi \cdot M_{CO_2}}} \quad (26)$$

with molecular diffusion of CO_2 proposed by Maxwell-Stefan [26].

$$\frac{1}{D_{CO_2}^m} = \sum_i \frac{y_i}{D_{ij}} + \frac{y_j}{1 - w_j} \sum \frac{w_i}{D_{ij}} \quad (27)$$

Here, D_{ij} from Fuller et al. is a binary coefficient:

$$D_{ij} = \frac{0.00143 \cdot T^{1.75} \cdot \left(\frac{1}{w_i} + \frac{1}{w_j} \right)^{\frac{1}{2}}}{p \cdot \left((\theta_i)^{\frac{1}{3}} + (\theta_j)^{\frac{1}{3}} \right)^2} \quad (28)$$

The reaction rate for CO₂ methanation in the model proposed by Koschany et al. [27] was employed. It is described by the Langmuir-Hinshelwood-Hougen-Watson (LHHW) approach for temperatures between 180-340°C and pressures between 5-15 bar.

$$r = \frac{k \cdot p_{H_2}^{0.5} \cdot p_{CO_2}^{0.5} \left(1 - \frac{p_{CH_4} p_{H_2O}^2}{p_{H_2}^4 p_{CO_2} K_{eq}}\right)}{\left(1 + K_{OH} \cdot \frac{p_{H_2O}}{p_{H_2}^{0.5}} + K_{H_2} \cdot p_{H_2}^{0.5} + K_{mix} \cdot p_{CO_2}^{0.5}\right)^2} \quad (29)$$

Table 10 presents the parameters and characteristics for the CO₂ reactors used in the direct methanation model.

Table 10: Parameters and characteristics of the methanation reactors

Parameter	Symbols	Value	unit
Reactor Length	L	2	m
Tube Diameter	D	0.0254	m
Fixed-bed Void fraction	ε	0.45	m
Catalyst density	ρ_{cat}	2300	kg/m ³
Particle porosity	τ_p	0.6	-
Particle tortuosity	ε_p	2	-
Particle diameter	D _p	3	mm
Average pore diameter	D _{pore}	10	nm
Methanation reactor pressure	p	10-20	bar
Inlet Molar ratio at 1st reactor	H ₂ /CO ₂	4:1	-
Coolant heat transfer coefficient	α_ω	500	W/m ² K
Fixed-bed thermal conductivity	λ_{bed}	3.6	W/mK

5.3 Modeling of the Polishing Unit

MDEA was used as the amine solution in the process model to capture non-converted CO₂ from the methanation unit. An absorber and a stripper column with a 3 m diameter were selected to meet the strict CO₂ PPM fraction requirements set for SNG before it's sent to the liquefaction unit. The number of trays in the absorber was set to 15, and the Stripper was set to 12 trays. The feed stream mixed with MDEA was assumed to have an equal pressure to the stream entering the absorber column. For the absorber, the methanation unit stream enters the bottom stage inlet (tray 1), and the MDEA amine solvent stream enters the top stage inlet (tray 15). For the Stripper, the inlet stream enters the column

at the fifth tray from the top. Further, in the Stripper, a condenser temperature of 30 °C and a CO₂ rich loading of 0.01 mol CO₂/mol MDEA were considered to solve the stripper column.

6 Sensitivity Analysis and Optimization Results

In this chapter, the results of the direct methanation process model with multi-stage compressors, methanation reactors, polishing unit, and liquefaction unit modeled for the different cases will be presented. The chapter is split into two main parts. The case study results and optimization results for the methanation process in the model and the case study and optimization results for the upgrading/polishing unit in the model. The thesis objective is to analyze if the direct methanation model can produce product methane at lower H_2/CO_2 ratios. Further, the case studies and optimization are split into four cases for different H_2/CO_2 has a ratio of 3.0, 3.2, 3.5, and 3.8.

6.1 Methanation Optimization

The main objective of the case studies and optimization was to optimize for the Sabatier reaction in the methanation reactors. From the results of the project thesis, it was established that increased pressure had a significant impact on the conversion ratios for CH_4 and H_2 in the reactors, and variation on the inlet temperature had little to no impact on the H_2 and CO_2 conversion. For the case studies, the variation of pressure, coolant temperature, and the number of tubes in the reactors were varied, and a sensitivity analysis on heat flow in the reactor, H_2 conversion, CH_4 molar flow out of the reactors will be provided. The independent variables are specified in such a way as to look at the impact on the CH_4 molar flow rate and the conversion of Hydrogen in the reactors.

6.1.1 Sensitivity Analysis on Methane Molar Flow Rate

Figure 22 shows the variation of the methane flow rate out of the reactors for the different pressures and varying coolant temperatures. The total molar flow rate after the methanation process is 200.6, 200.7, 200.8, and 202.7 kgmole/h for cases: 3.0, 3.2, 3.5, and 3.8, respectively. It can be seen that with low coolant temperature [$^{\circ}C$], the methane content in the stream is low but has a big increase with just an increase from 200-220 $^{\circ}C$ for all cases and pressures. Especially with low pressure and coolant temperature, the methane content in the outlet stream is low. With a pressure of 10 bar, resulting in a methane molar flow rate below 165 kgmole/h for all cases. The rest of the stream containing different contents of CO_2 , H_2 and H_2O . This leads to the coolant temperature contributing to

methane production and the Sabatier reaction in the methanation reactors. For cases 3.0 and 3.2, the coolant temperature has little impact on an inlet pressure of 25 and 30 Bar, but with increasing H_2 in the inlet stream, the coolant temperature has a larger impact on the methane content in the stream. There is also an increasing methane content after the second methanation reactor with increasing H_2/CO_2 ratio, which correlates to the increase H_2 in the inlet stream before the reactor. With more H_2 in the inlet stream, more of the CO_2 in the biogas can be converted into CH_4 through the Sabatier reaction.

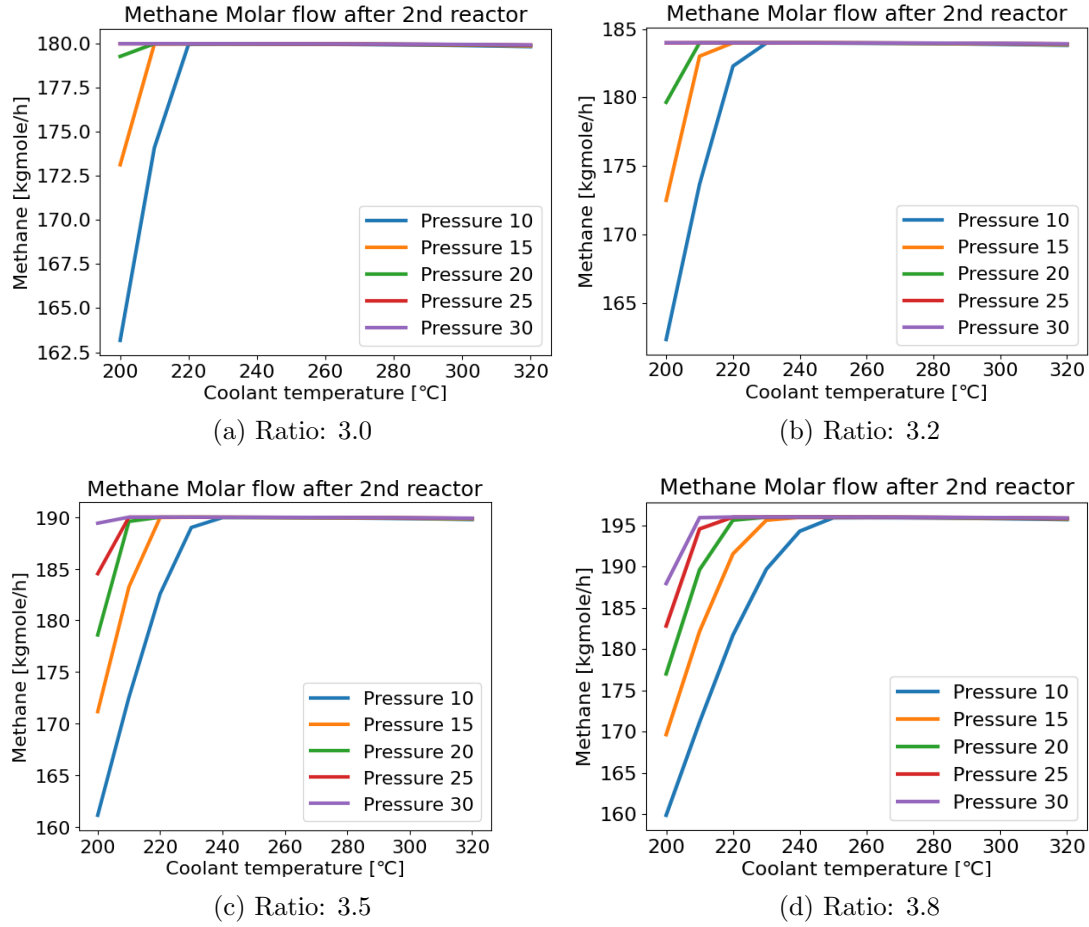


Figure 22: Methane flow rate out of methanation unit

The sensitivity results after the first methanation reactor are shown in Figure 23 and share similar results as Figure 22 out of the whole methanation unit. For all cases, the molar flow rate has almost an identical flow rate after the second reactor. This indicates the majority of the Hydrogen in the stream is converted with CO_2 into CH_4 . The second reactor is then used as a fine-tuning unit to convert leftover hydrogen and CO_2 . For pressures 25 and 30 bar in case ratios 3.0 and 3.2, the coolant temperature has little to no effect on the methane molar flow after the 1st reactor. The pressure is high enough, and

the ΔT between the outlet temperature of reactor 1 and the coolant temperature is small to give good conditions for the Sabatier reaction since the Sabatier reaction favors low temperatures and high-pressure values. For the case ratios 3.5 and 3.8, there is a bigger variation in methane flow rate, with increasing pressure and coolant temperature.

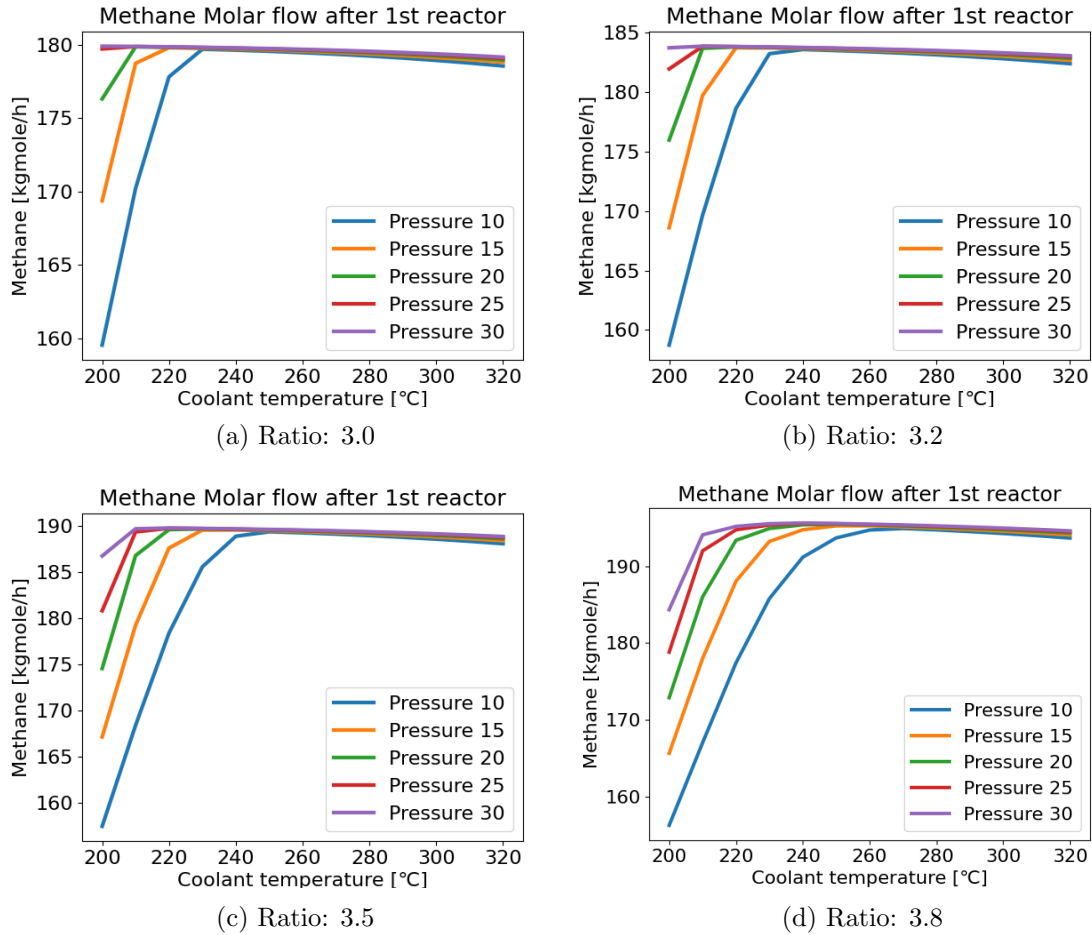


Figure 23: Methane flow rate out of 1st reactor.

6.1.2 Sensitivity Analysis on Hydrogen Conversion

The case study results for the conversion of the hydrogen is presented in Figure 24 and Figure 25. Figure 24 shows the molar flow rate of H_2 in the stream out of the methanation unit (second reactor) and Figure 25 shows the H_2 conversion rate from the methanation reactions. From figure 24, hydrogen decreases with increasing molar flow rate for all cases and reaches a minimum when the coolant temperature is from 220-250°C. This correlates well with the case study on methane molar flow rate, with an increase in methane molar content implying a decrease in Hydrogen molar content caused by the methanation reaction

in the reactors. The reaction favors coolant temperatures between 220-250°C depending on the inlet pressure into the first methanation reactor and the H_2/CO_2 ratio.

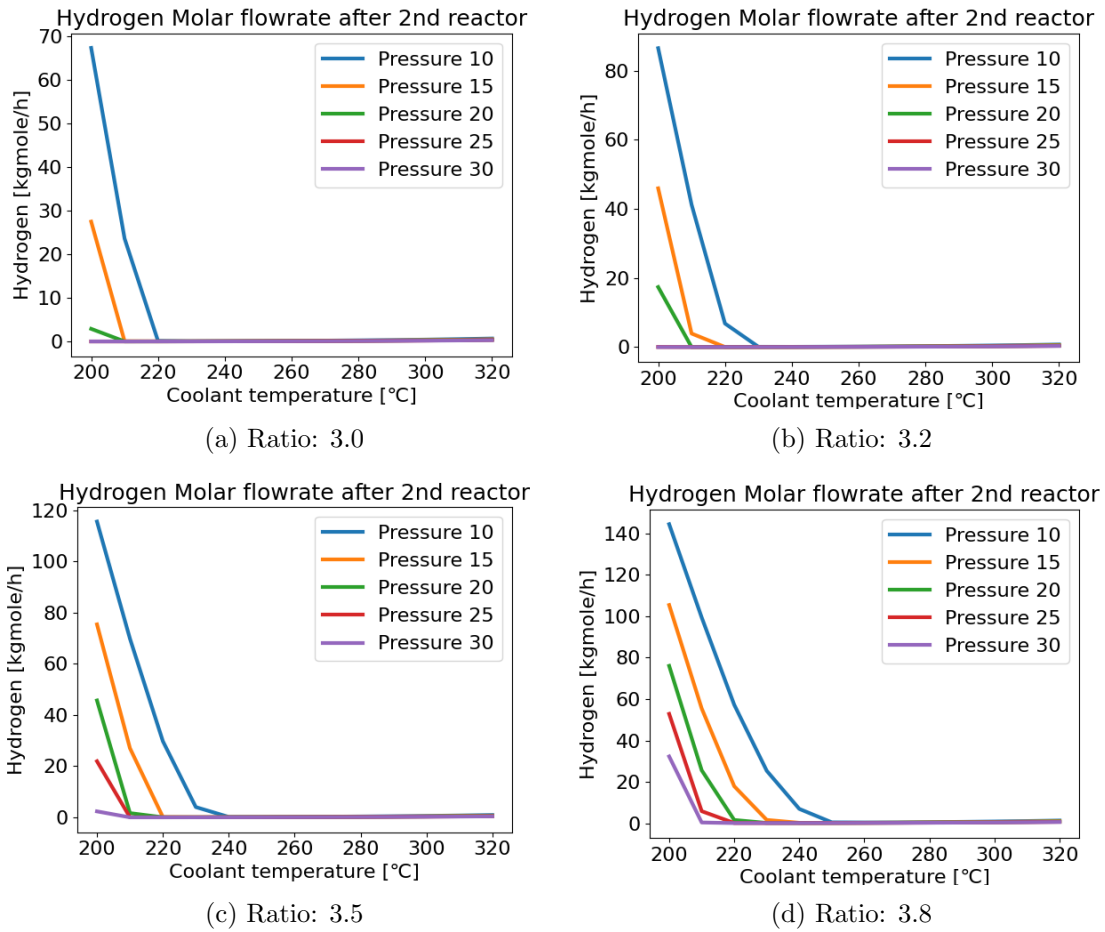


Figure 24: Hydrogen molar flow rate out of methanation unit

Figure 25 indicates that for all cases, the methanation reactor converts almost 100% of the Hydrogen in the biogas stream. For case ratio 3.0, a coolant temperature of 220 can reach almost 99,94% of the H_2O converted into CH_4 . At lower temperatures, a pressure of 10 and 15 Bar reduces the hydrogen conversion percentage. Case 3.2 favors a coolant temperature over 220°C to achieve 99,95 % H_2 conversion, for case ratios of 3.5 and 3.8, a H_2 conversion over 99.9% is achieved when the coolant temperature is above 240°C for all pressure values at the inlet of methanation reactors.

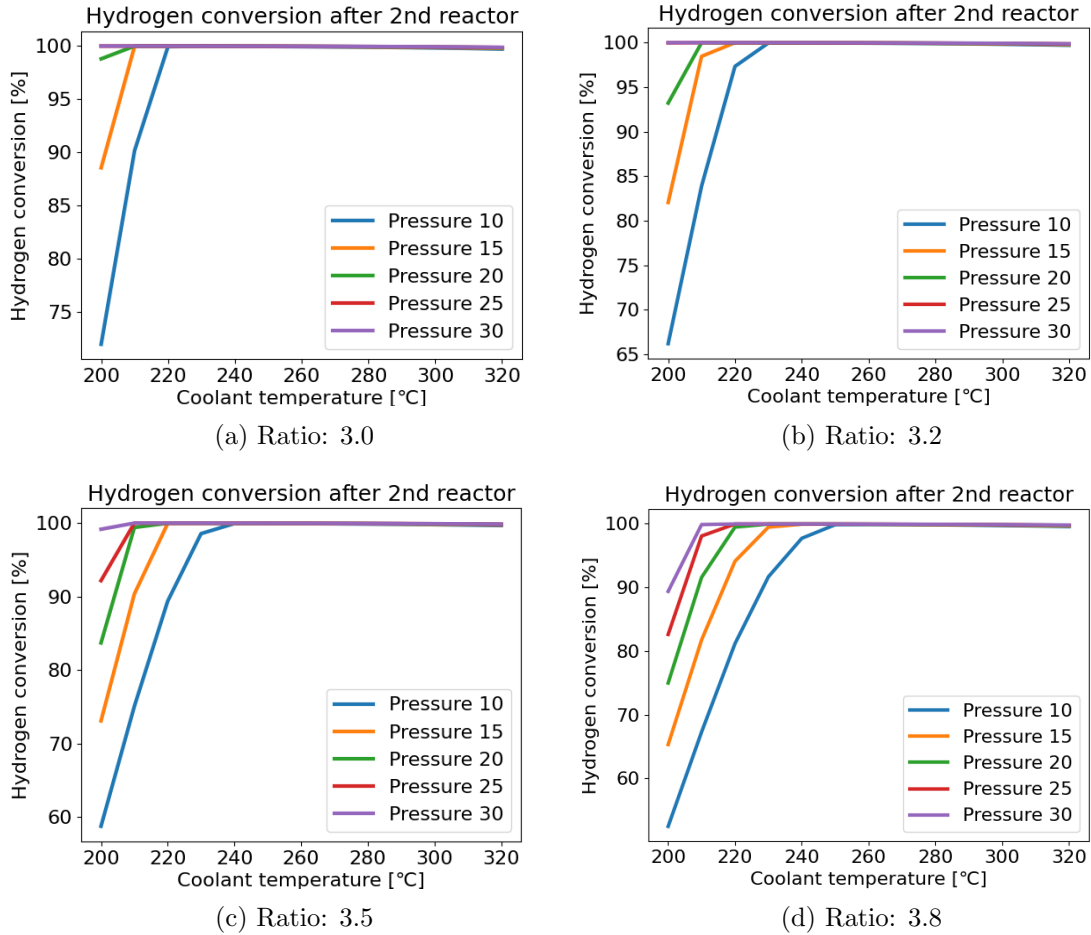


Figure 25: Hydrogen conversion in out of methanation unit

6.1.3 Sensitivity Analysis on Heat Flow

Methanation Reactor 1

The case study results for the heat flow looked at the variation between pressure and coolant temperature and how the two independent variables affected the heat flow inside both methanation reactors. The number of tubes in the reactor was fixed to $N = [3886, 490]$ for methanation reactors 1 and 2, respectively. The number of tubes in the reactor was fixed to simplify the case studies and reduce simulation time. Because the Sabatier reaction is highly exothermic and gives a high-temperature runaway in the reactors. The impact of pressure and coolant temperature are important variables for the heat flow in the reactor and for finding the optimal pressure and cooling needed to operate a methanation reactor.

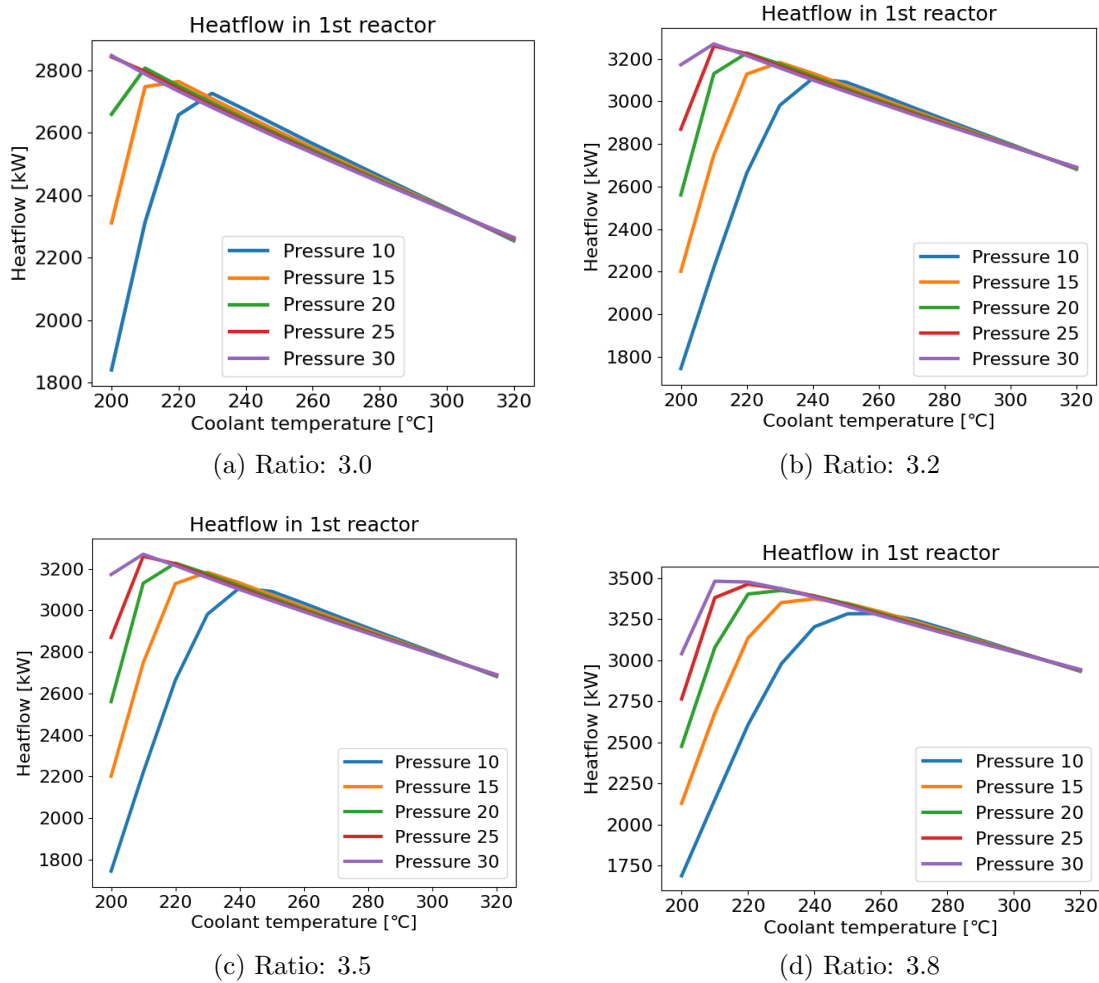


Figure 26: Heat flow first methanation reactor

The impact of the pressure variation and the coolant temperature on the heat flow in the first methanation reactor is shown in Figure 26. The heat flow varied for all the H₂/CO₂ ratios but had the same trends with the increase in heat flow following the increasing coolant temperature, but reached a maximum between 230-260 °C. After around 240-250 °C the heat flow reduces with the increasing temperature for all pressure variations. There is a big jump in heat flow for the different pressure values as the coolant temperature increases from 200-230 °C. A temperature difference between the coolant temperature and the outlet temperature of the reactor causes a big jump. A larger ΔT between the coolant temperature and the outlet temperature gives a larger heat flow inside the required and increases the needed cooling to operate.

Methanation Reactor 2

The impact the pressure and coolant temperature have on the heat flow in the second reactor is shown in Figure 27. All four cases share a similar trend with reduced heat flow in the reactor with increasing coolant temperature for all pressure values. For all cases, the reactor heat flow is below zero when the coolant temperature is increased above 240°C. This means the second reactor needs to be supplied with heating.

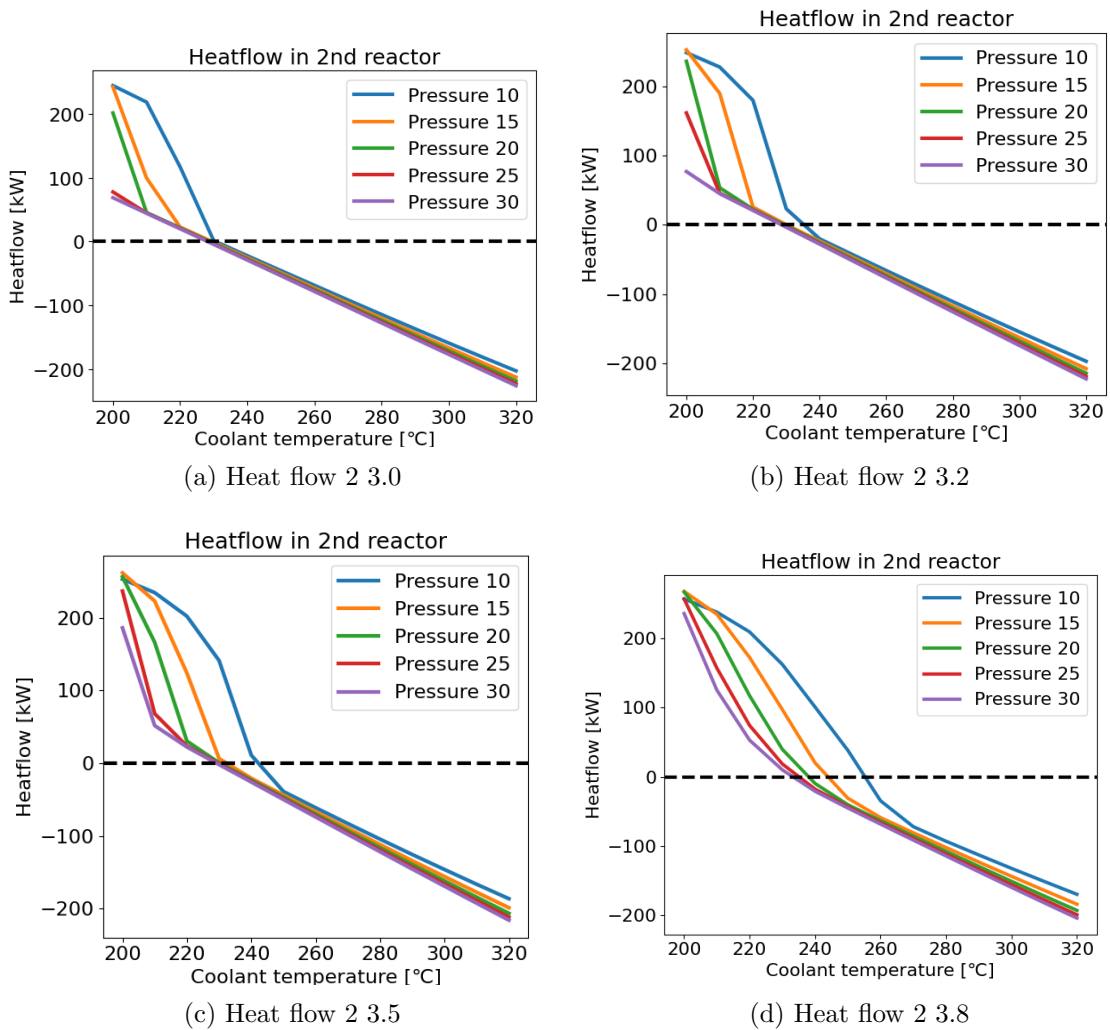
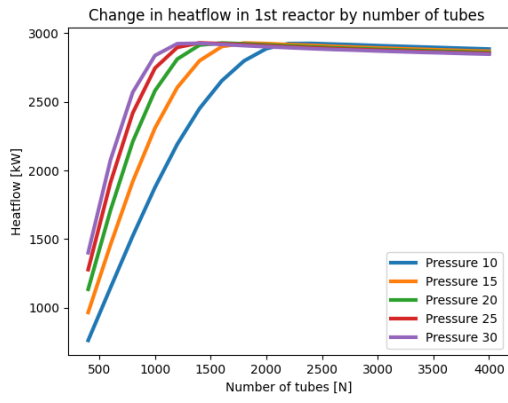


Figure 27: Heat flow from the second reactor

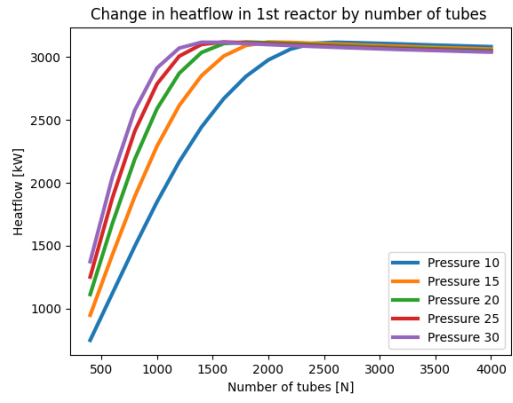
6.1.4 Sensitivity Analysis on Number of Tubes in Reactor 1

For the sensitivity analysis on the number of tubes in the reactor, the temperature at the inlet of the reactors and the coolant temperature was fixed at 200 °C and 240°C, respectively, and the change in the number of tubes from 500-4000. Figure 28 shows how the heat flow in reactor 1 reacts to the change in number of tubes in the reactor. For all case ratios, there is an increase in the heat flow in the methanation reactor with the increasing number of tubes for all cases and all pressure values. In cases 3.0 and 3.2, there is an increase in heat flow from 500-2000 tubes in the reactor for all pressure values and reaches a maximum after 2000 tubes with heat flow of 2700-2900 kW and 3000-3100 kW, respectively. For case ratios of 3.5 and 3.8, the change in heat flow from the increase in tubes reaches a maximum after $N \geq 2500$, and $N \geq 3000$ for all pressure values. The change in heat flow from the increasing number of tubes correlates with how the reactors are designed from equation 19, where an increase in the number of tubes N will increase the heat transfer rate in the reactor linearly.

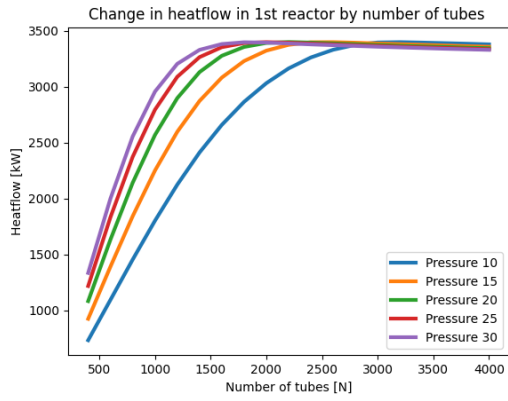
The change in the methane molar flow indicated how the number of tubes affected the methanation reaction in the reactors. In figure 29, the methane content in the stream increases with increasing the number of tubes in the reactor. For cases 3.0 and 3.5, the methane molar flow is unaffected after $N \geq 2000$. For case 3.5, the methane content is unaffected after $N \geq 2750$. The methane content is varied for the different pressure values but follows the same trend with increasing methane molar flow with the increasing number of tubes. The change in methane molar flow rate and the heat flow follows similar trends and can find both optimal values with the number of tubes $N \geq 2000$ for all four case ratios. Lowering the number of tubes under 2000 will result in less favorable conditions for the methanation reaction in the reactor.



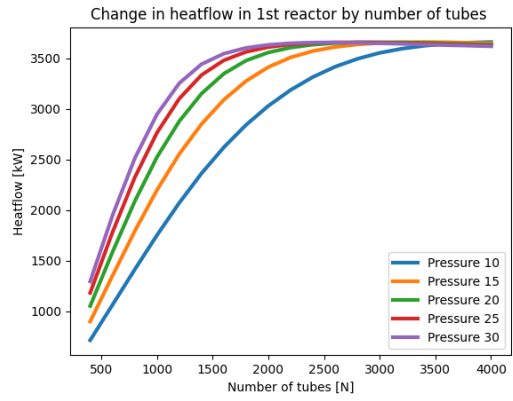
(a) Ratio: 3.0



(b) Ratio: 3.2

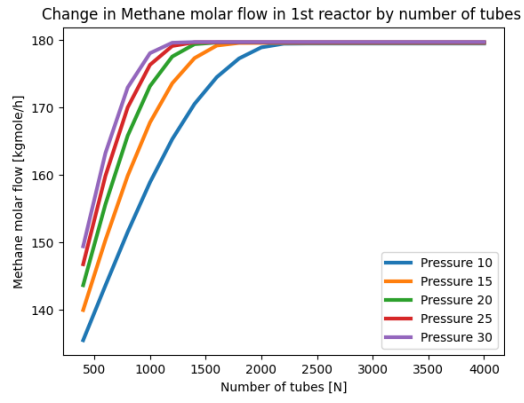


(c) Ratio: 3.5

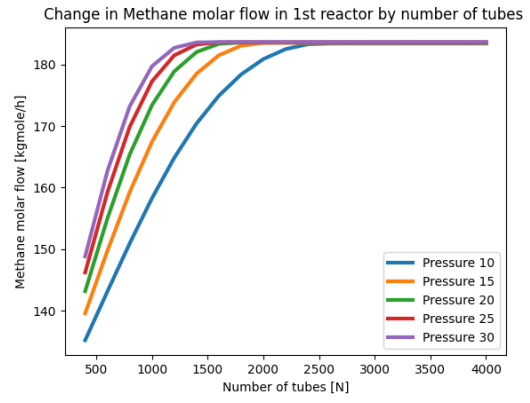


(d) Ratio: 3.8

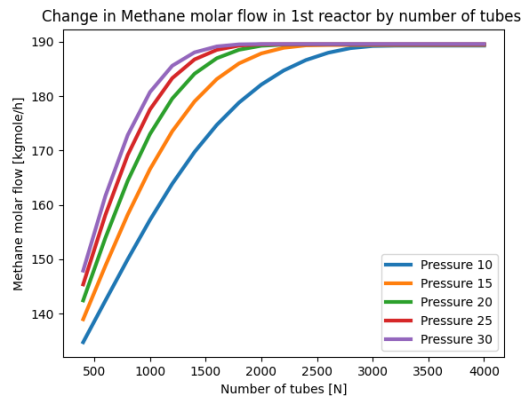
Figure 28: Change on heat flow in reactor 1 from variation in the number of tubes



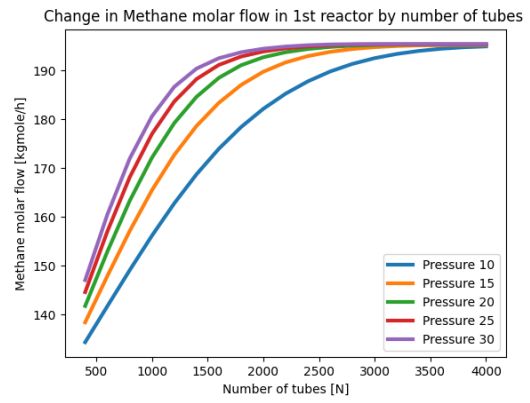
(a) Ratio: 3.0



(b) Ratio: 3.2



(c) Ratio: 3.5



(d) Ratio: 3.8

Figure 29: Change on methane molar flow in reactor 1 from variation in the number of tubes

6.1.5 Hyprotech SQP Optimization of the Methanation Process

After the Case study, each case's process was optimized sequentially using the Hyprotech SQP optimizer in Aspen HYSYS V10.1. For this case, the methanation process is highlighted, and the objective of the methanation process was to maximize the methane molar flow rate in the stream after the methanation reactors.

Unfortunately, the Hyprotech SQP optimizer could not find an optimized solution for the different case ratios. The optimizer was stopped due to step convergence in the process models. This is due to the optimizer reaching a step collapse below the step tolerance during the optimization. The step collapse below the step tolerance can happen when optimizing for small variations in CH₄ molar flow rates. Figure 30 shows the optimizer results for case 3.0 in the methanation unit. Here the optimizer went through 2 iterations before the optimizer stopped due to step convergence troubles. The optimizer for case 3.0 resulted in giving lower CH₄ molar flow rates than what was achieved from the sensitivity analysis. This result was ongoing for all case ratios.

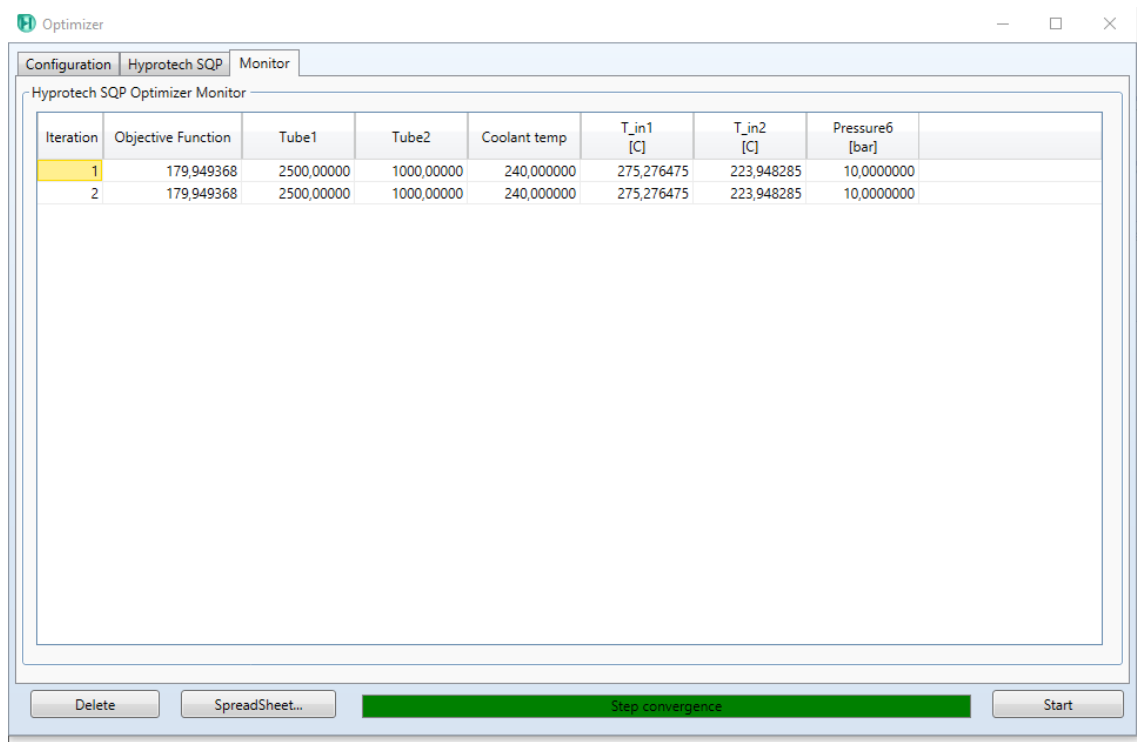


Figure 30: Hyprotech optimizer case 3.0 solution: Step convergence

Since the optimizer for the methanation unit gave unfavorable results, and to do cost estimation of the process and independent variables were set for all case ratios. The independent variables set were pressure at the inlet, Coolant temperature, Number of tubes in reactors 1 and 2, and inlet temperatures for reactors 1 and 2. The values for the variables were chosen from the results of the case studies and set not to break the constraints specified in Table 7 for the methanation unit and to give a Hydrogen conversion of $\geq 99.9\%$ combined from the methanation unit.

For case 3.0, the independent variables specified, the results on Heat flow, methane molar flow rate after both reactors, and the hydrogen conversion percentage are shown in Table 11. Pressure at 20 bar and a coolant temperature of 240 °C was chosen cause of their favorable results for hydrogen conversion in the reactors and the heat flow in the reactors. Decreasing the pressure to 10 bar gave a larger variation in hydrogen conversion and methane content. Increasing the pressure at a coolant temperature of 240°C gave little variation. The number of tubes in the reactors chosen was 2000, and 1000 for reactors 1 and 2, respectively. The independent variables were specified to give a high enough heat flow for a hydrogen conversion percentage of 99.9%.

Table 11: Specified independent variables for case 3.0

Case ratio: 3.0 Independent variables set		
Variable	Value	Unit
Pressure	20	bar
Coolant temperature	240	°C
Number of tubes reactor 1	2000	-
Number of tubes reactor 2	1000	-
Results from specified independent variables		
Heat flow reactor 1	2669	kW
Heat flow reactor 2	24.17	kW
Methane molar flow rate	179,98	kgmole/h
Hydrogen conversion	99.97	%

For case ratio 3.2, the pressure, coolant temperature, and Number of tubes in reactor 1 and 2 was set to 15 bar, 240°C, 2500, and 1000 tubes, respectively. The variables are set to be similar to the case ratio in 3.0, but with an increase in the number of tubes in the first reactor to have leeway for change in heat flow. The variables and results can be seen in Table 12.

Table 12: Specified independent variables for case 3.2

Case ratio: 3.2 Independent variables set		
Variable	Value	Unit
Pressure	15	bar
Coolant temperature	240	°C
Number of tubes reactor 1	2500	-
Number of tubes reactor 2	1000	-
Results from specified independent variables		
Heat flow reactor 1	2830	kW
Heat flow reactor 2	47.49	kW
Methane molar flow rate	183,9676	kgmole/h
Hydrogen conversion	99.95	%

The specified independent variables and the results for case ratio 3.5 can be seen in Table 13. Here pressure, coolant temperature, and the number of tubes in reactors 1 and 2 are set to 20 bar, 240°C, and 2500 and 1000 tubes, respectively. These values were chosen to maximize the methane flow rate, Hydrogen conversion, limit the number of tubes used in the reactors, and ensure non-negative heat flow in reactor 2.

Table 13: Specified independent variables for case 3.5

Case ratio: 3.5 Independent variables set		
Variable	Value	Unit
Pressure	20	bar
Coolant temperature	240	°C
Number of tubes reactor 1	2500	-
Number of tubes reactor 2	1000	-
Results from specified independent variables		
Heat flow reactor 1	3091	kW
Heat flow reactor 2	65.29	kW
Methane molar flow rate	189.9628	kgmole/h
Hydrogen conversion	99.95	%

The independent variables, and the last case ratio of 3.8, are shown in Table 14. The pressure, coolant temperature, and number of tubes in reactors 1 and 2 are set to 20 bar, 240°C, 3000, and 1000 tubes, respectively.

Table 14: Specified independent variables for case 3.8

Case ratio: 3.8 Independent variables set		
Variable	Value	Unit
Pressure	20	bar
Coolant temperature	240	°C
Number of tubes reactor 1	3000	-
Number of tubes reactor 2	1000	-
Results from specified independent variables		
Heat flow reactor 1	3334	kW
Heat flow reactor 2	100.6	kW
Methane molar flow rate	195.9409	kgmole/h
Hydrogen conversion	99.92	%

6.2 Polishing Optimization

The main objective from the case studies and optimization on the polishing unit is to minimize the CO₂ fraction into the liquefaction unit and meet the product specifications of ≤ 50 PPM CO₂. In the case studies for the polishing unit, inlet pressure, MDEA molar flow rate, and the MDEA/water concentration in the absorber were varied. A sensitivity analysis of how the pressure, MDEA molar flow rate, and concentration will be provided. For all case ratios, the pressure was varied between 20-80 bar and the MDEA/water concentration in the recycle stream was varied between 40-60%. The MDEA flow rate varied between 100-800 kgmole/h for the different case ratios. Increasing the pressure higher gave resulted in convergence problems in the amine regeneration stripper, was increased simulation time. Since for cases 3.0 and 3.2, the pressure out of the methanation reactors is set to 15 bar, and for cases 3.5 and 3.8, the pressure is set to 20 bar, lowering the pressures into the absorber was not researched. The results from the case studies will be covered first for each case ratio, then the results for the Hyprotech SQP optimizer will be presented.

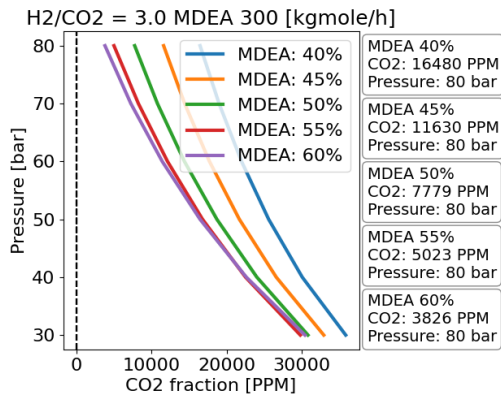
6.2.1 Sensitivity Analysis on Case: 3.0

In the sensitivity analysis for case ratio 3.0, the MDEA flow rate varied from 300 to 800 kgmole/h. This examined the effect pressure and MDEA/water % had on the absorber's chemical absorption process of CO₂. The MDEA flow rate was varied until the CO₂ PPM requirement was met. Figure 31 shows the results of the case studies. The CO₂ PPM was plotted against the pressure for the different MDEA/water% concentrations. The black stippled bar in the plots shows the CO₂ content requirement for the product methane in PPM. The lowest CO₂ PPM value for each concentration is shown for all the different MDEA flow rate variations along with the pressure value achieved. Here, pressure set to 80 bar gave the best results for all flow rates, and increasing the pressure resulted in lower CO₂ content in the product stream out of the absorber. From the MDEA/water concentration, increasing the percentage reduced the CO₂ content for an MDEA flow rate of 300 kgmole/h. Increasing the MDEA flow rate and the concentration in the absorber gave a decrease in CO₂ PPM for concentrations up to 50%, after 50% there is an increase in CO₂ PPM. For Case 3.0, the CO₂ PPM requirement was met with an MDEA flow rate of 600 kgmole/h, with MDEA/water concentration at 40-45% at 80 bar. Increasing the

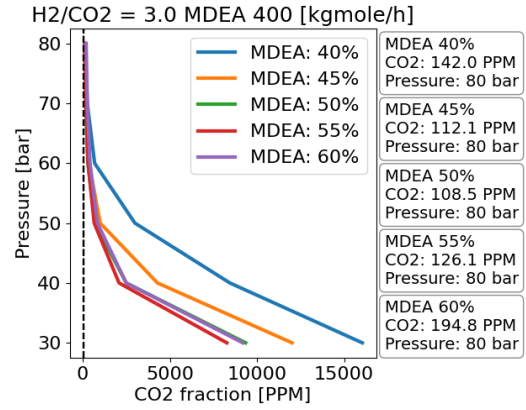
MDEA flow rate to 700 and 800 kgmole/h gave similar results and met the requirement for MDEA/water concentrations at 40-50%.

6.2.2 Sensitivity Analysis on Case: 3.2

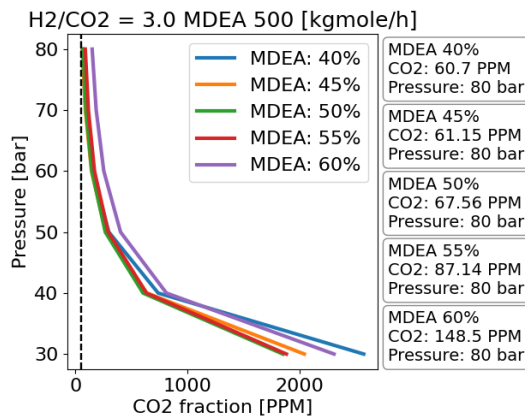
The sensitivity results from pressure, MDEA/water concentration and MDEA molar flow rate is shown in Figure 32 and are similar to case 3.0. Here, Figure 32a to 32c indicated that MDEA molar flow rate from 200-400 gave product methane with CO₂ over the required PPM limit. Increasing the pressure and concentration did result in a decrease of CO₂ content in the product stream out of the absorber. The flow rate of 500-600 kgmole/h gave product methane with CO₂ content under 50 PPM. The lowest CO₂ in the product stream was achieved with an MDEA molar flow of 600 kgmole/h, pressure at 80 bar, and MDEA/water concentration at 40%.



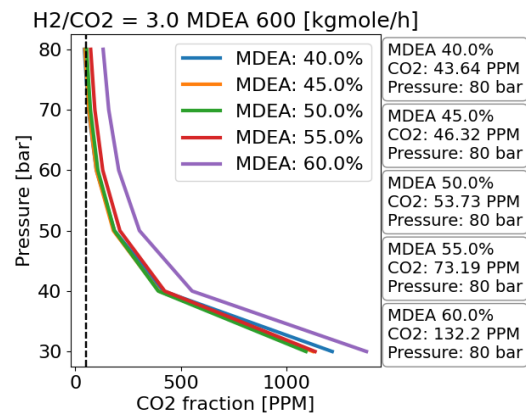
(a) MDEA flow rate 300



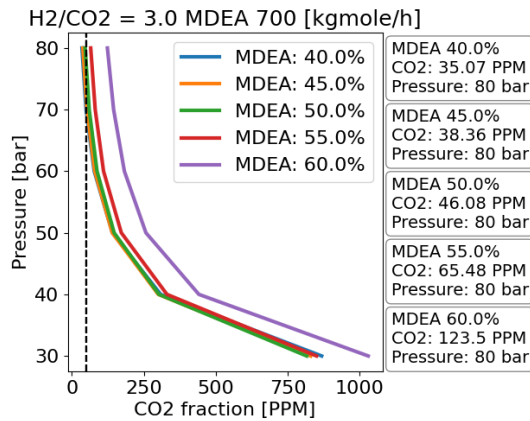
(b) MDEA flow rate 400 kgmole/h



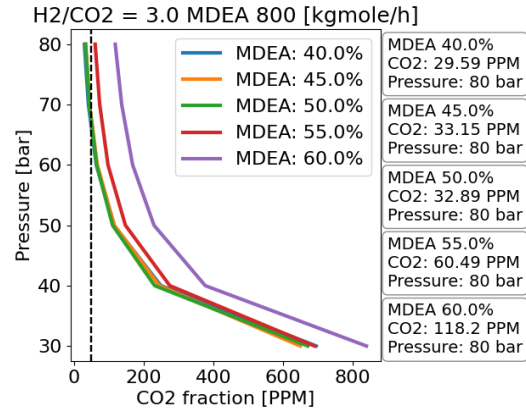
(c) MDEA flow rate 500 kgmole/h



(d) MDEA flow rate 600 kgmole/h

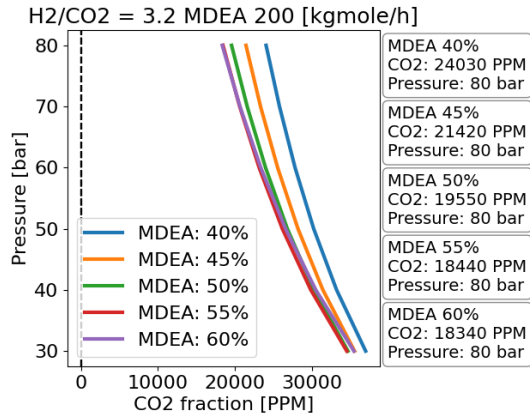


(e) MDEA flow rate 700 kgmole/h

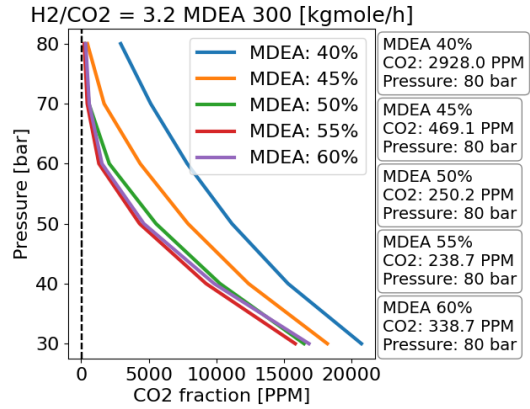


(f) MDEA flow rate 800 kgmole/h

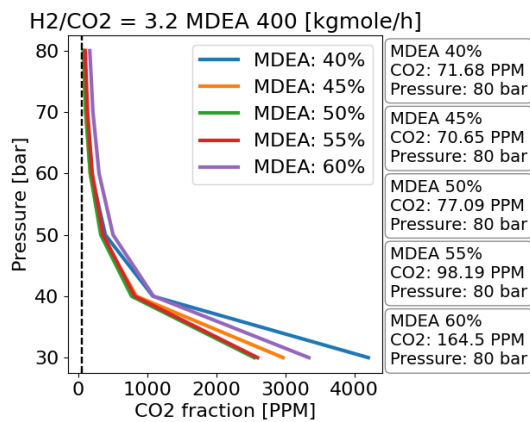
Figure 31: Sensitivity analysis from pressure, MDEA flow rate, and concentration on case 3.0



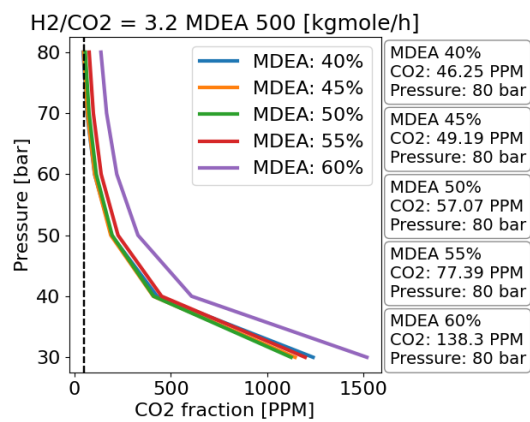
(a) MDEA flowrate 200 kgmole/h



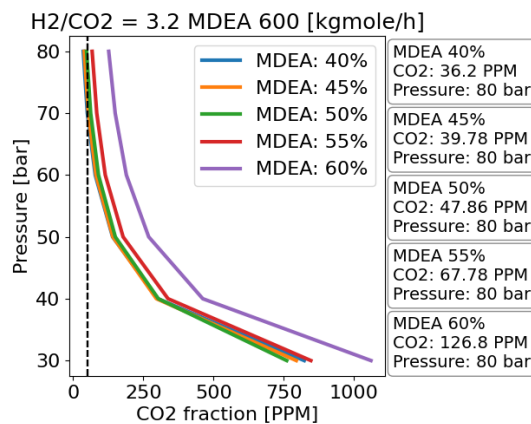
(b) MDEA flow rate 300 kgmole/h



(c) MDEA flow rate 400 kgmole/h



(d) MDEA flow rate 500 kgmole/h



(e) MDEA flow rate 600 kgmole/h

Figure 32: Sensitivity analysis from pressure, MDEA flow rate, and concentration on case 3.2

6.2.3 Sensitivity Analysis on Case: 3.5

The sensitivity results for case 3.5 is shown in Figure 33. Here, the influence from pressure, MDEA/water concentration gave little effect when the MDEA flow rate was set to 100 kgmole/h seen in 33a. Doubling the MDEA molar flow in 33b, the increase in pressure had more impact on the CO₂ content in the product stream. It decreased for all MDEA/water concentration cases between 40-60%, but the best result had a CO₂ content of 1622 PPM at 80 bar and concentration 55%. For 33c, there is a considerable reduction in the CO₂ content, with the best result being 52.59 PPM CO₂ in the product at 80 bar and MDEA/water concentration of 40%. In 33d with an MDEA molar flow rate of 400 kgmole/h CO₂ fraction requirement was met. Here the lowest value at 37.27 PPM CO₂ was achieved with a pressure of 80 bar and an MDEA/water concentration of 40% before the absorber.

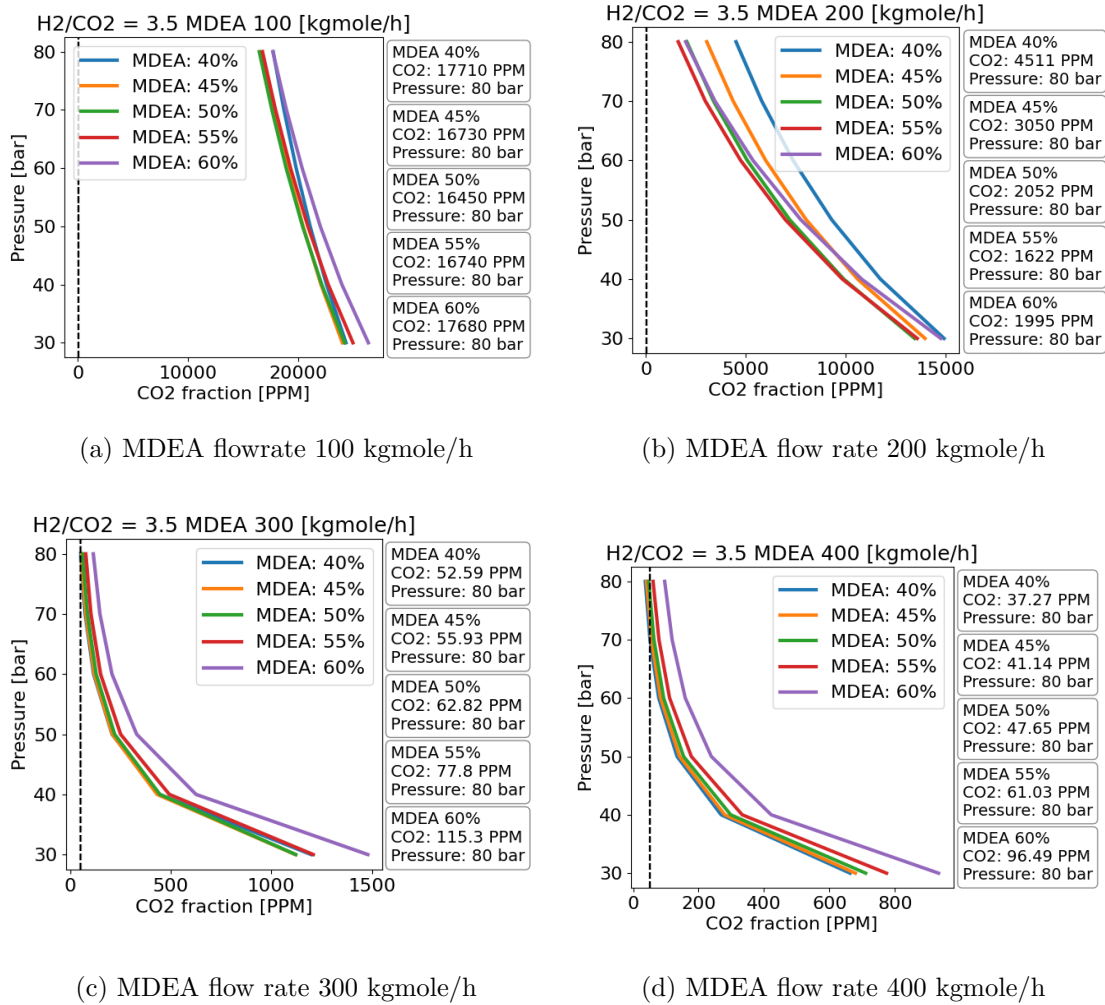
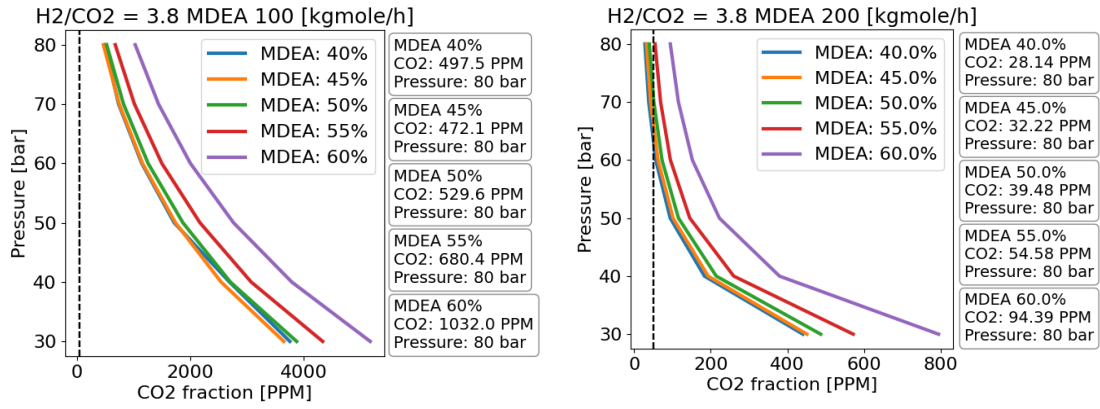


Figure 33: Sensitivity analysis from pressure, MDEA flow rate, and concentration on case 3.5

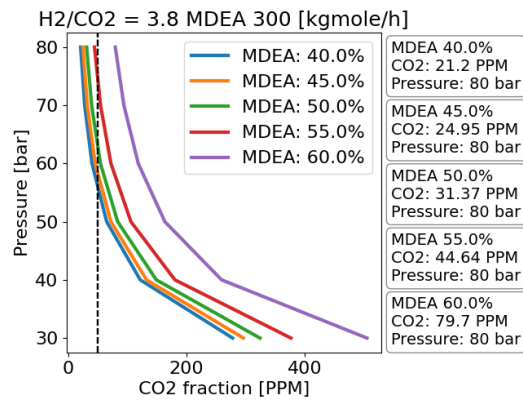
6.2.4 Sensitivity Analysis on Case: 3.8

The sensitivity results for case 3.8 is shown in Figure 34. Here, the increase in pressure has significant effects on decreasing the CO₂ fraction in the product stream for Figure 34a, 34b, and 34c. Most interesting, an MDEA/water concentration of 60% did not meet the required CO₂ fraction requirement for all MDEA molar flow rates. At the earliest MDEA molar flow rate of 200 kgmole/h, the CO₂ fraction requirement was met in Figure 34b. Here, the PPM requirement can be achieved with a pressure of 70 bar with a concentration of 40-45%. With the best result at a pressure of 80 bar and MDEA/water concentration of 40%. The CO₂ fraction in the product stream was 28.14 PPM. The best result for Figure 34a with an MDEA molar flow rate of 100 kgmole/h was achieved with pressure at 80 bar and MDEA/water concentration of 45%. Increasing the flow rate higher to 300 kgmole/h gave more reduction in CO₂ fraction and can reduce the pressure to between 60-70 bar for a concentration between 40-50%. With a pressure of 80 bar, concentration values 40-55% met the product requirement. The best result for an MDEA flow rate of 300 kgmole/h was achieved with pressure at 80 bar, concentration at 40%, and a CO₂ fraction of 21.2 PPM.



(a) MDEA flowrate 100 kgmole/h

(b) MDEA flow rate 200 kgmole/h



(c) MDEA flow rate 300 kgmole/h

Figure 34: Sensitivity analysis from pressure, MDEA flow rate, and concentration on case 3.8

6.2.5 Hyprotech SQP Optimizer Polishing Unit

After the Case study, each case's process was optimized sequentially using the Hyprotech SQP optimizer in Aspen HYSYS V10.1. For this case, the polishing unit is highlighted, and the objective of the polishing unit was to maximize the CO₂ absorption reaction in the absorber to produce product methane that meets the 50 PPM CO₂ fraction requirement.

Case 3.0

Figure 35 shows the Hyprotech optimizer results for case 3.0. Here the optimizer was stopped due to step convergence and gave results satisfying the optimizer constraints. Here, the best solution had a CO₂ content of 29.0819 PPM in the product stream with an amine flow of 800 kgmole/h. The pressure was calculated at 80 bar for all iterations of the optimizer, and the amine concentration was iterated between 40-45%. Iterations 2 to 7 yielded good results with an amine flow rate of 570-800 kgmole/h. To cut down on the cost of the MDEA solution for the process, the independent variables for iteration 3 are chosen to calculate the cost estimate. The independent variables from the optimizer will be rounded to even numbers. The absorber pressure, Stripper pressure, rich temperature into the stripper, Lean amine temperature into the absorber, MDEA flow rate, and MDEA concentration are set to 80 bar, 1,3 bar, 78°C, 49°C, 615 kgmole/h, and 42%, respectively.

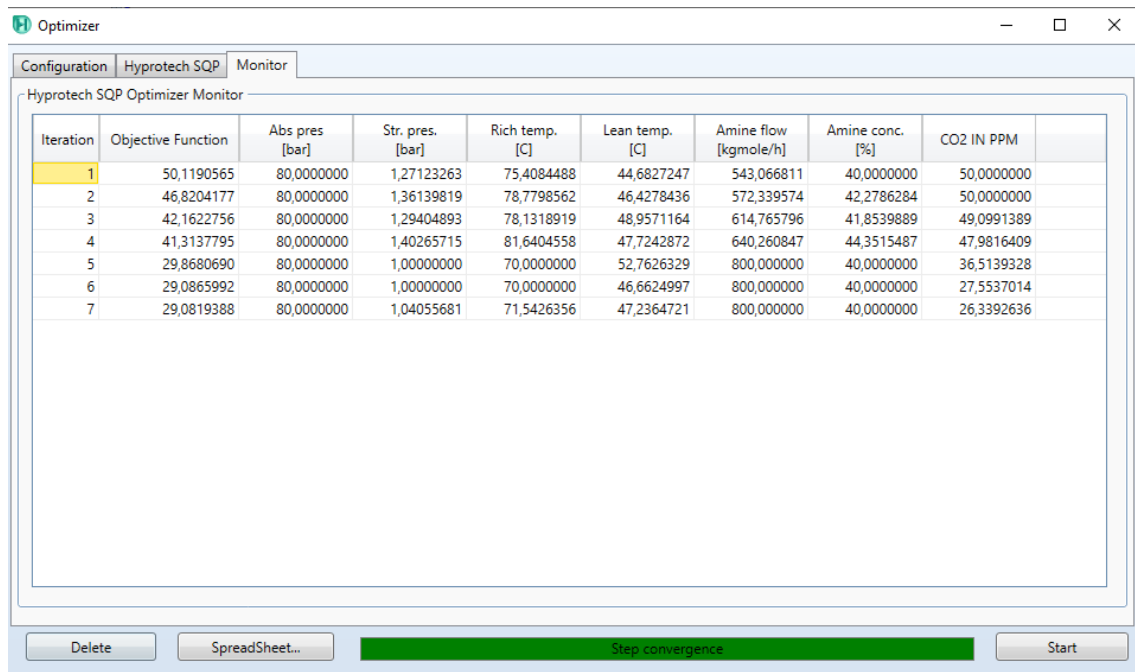


Figure 35: Optimizer results on the polishing process for case 3.0

Case 3.2

Figure 36 shows the Hyprotech optimizer results for case 3.2. The optimizer was stopped due to step convergence in the regeneration stripper but found good results satisfying the optimizer constraints. The best solution from the optimizer gave a CO₂ fraction of 29.082 PPM in the product methane with an amine flow rate, pressure, stripper pressure, Rich temperature, lean temperature, and amine concentration of 800 kgmole/h, 80 bar, 1.0405 bar, 71.54°C, 47.236°C, and 40%. Iterations from 3-11 gave good results satisfying the optimizer constraints. An amine flow rate of 477.63 kgmole/h gave was the lowest flow rate satisfying the constraints. The independent variables in iteration 3 were chosen to proceed with the cost estimation, and the values will be rounded to even numbers. The absorber pressure, stripper pressure, rich temperature into the stripper, lean amine temperature into the absorber, MDEA flow rate, and MDEA concentration are set to 80 bar, 1.06 bar, 78°C, 46°C, 478 kgmole/h, and 41%, respectively.

Iteration	Objective Function	Abs pres [bar]	Str. pres. [bar]	Rich temp. [C]	Lean temp. [C]	Amine flow [kgmole/h]	Amine conc. [%]	CO2 IN PPM
1	67,2176732	80,0000000	1,06243260	77,8093099	46,8866896	400,000000	40,0000000	50,0000000
2	55,3939382	80,0000000	1,05284866	77,6601659	45,6742560	438,126751	40,6179544	50,0000000
3	48,3583352	80,0000000	1,06290581	77,8166740	46,3809652	477,637062	40,5043398	50,0000000
4	43,5627721	80,0000000	1,07175685	77,9544126	48,0213984	515,088373	40,4308501	50,0000000
5	26,3983947	80,0000000	1,07610136	78,0220213	51,0497410	790,723721	40,0000000	50,0000000
6	26,0221806	80,0000000	1,00000000	70,0000000	40,0000000	800,000000	40,0000000	50,0000000
7	25,4696139	80,0000000	1,00000000	70,0000000	44,5948190	800,000000	40,0000000	50,0000000
8	25,4607790	80,0000000	1,06598066	71,1140128	44,8607393	800,000000	40,0000000	50,0000000
9	25,4555740	80,0000000	1,16475178	73,2425921	45,0518310	800,000000	40,0000000	50,0000000
10	25,4517800	80,0000000	1,12497256	72,9484816	45,3181781	800,000000	40,0000000	50,0000000
11	25,4515137	80,0000000	1,18451594	74,5624139	45,8275272	800,000000	40,0000000	50,0000000

Figure 36: Optimizer results on the polishing process for case 3.2

Case 3.5

Figure 37 shows the Hyprotech optimizer results for case 3.5. From the sensitivity analysis, the independent variable MDEA amine flow rate was set to vary between 100 and 500 kgmole/h. This was to cut down on optimization time and narrow the variable scope. Here, the best result from the optimizer gave a CO₂ fraction of 29.845 PPM in the product. The best result had an amine flow rate, pressure, stripper pressure, rich temperature, lean temperature, and amine concentration of 500 kgmole/h, 80 bar, 1.3 bar, 72.35°C, 44.14°C, and 40%. The optimizer stopped because of step convergence in the regeneration stripper after going through 15 iterations. Iterations 8 to 15 gave results satisfying the objective constraints set in the optimizer. Further, the independent variables achieved in iteration 8 are chosen based on reducing the cost of amine flow rate while achieving product specifications. To simplify, the independent variables for absorber pressure, stripper pressure, the rich temperature in the stripper, lean amine temperature into the absorber, MDEA flow rate, and MDEA concentration were set to 80 bar, 1.3 bar, 70°C, 40°C, 431 kgmole/h, and 44%, respectively.

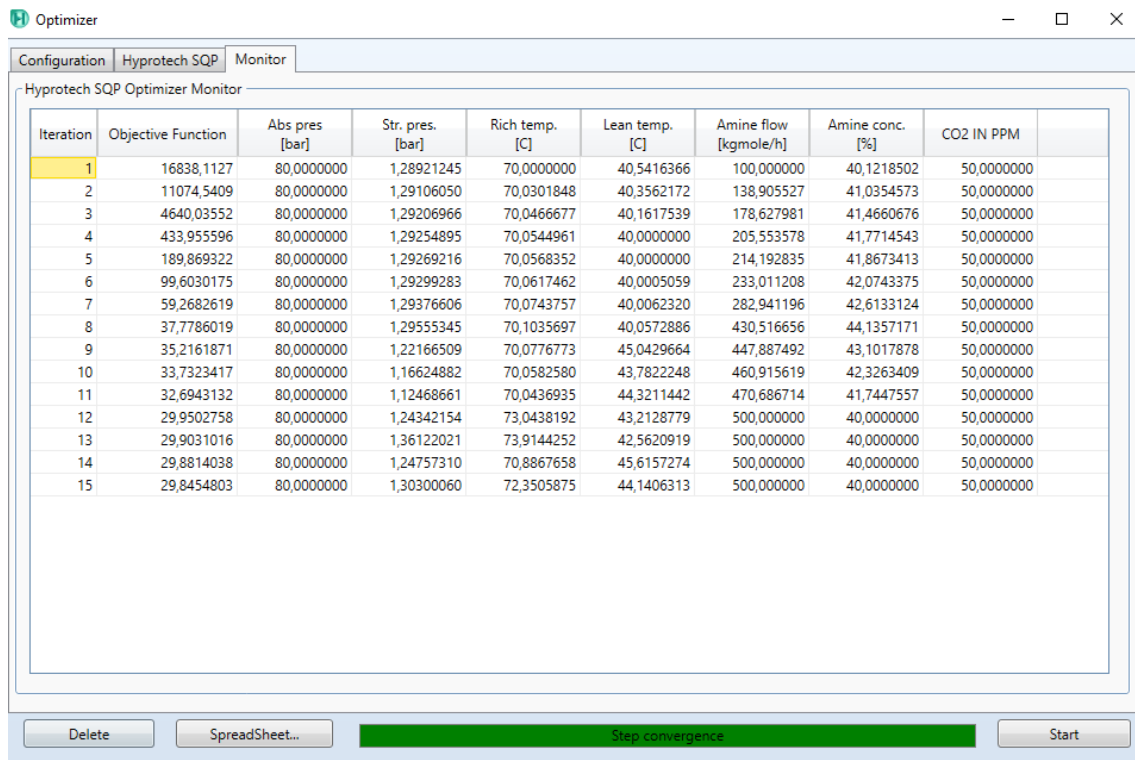


Figure 37: Optimizer results on the polishing process for case 3.5

Case 3.8

The optimizer results for case 3.8 is shown in Figure 38. Here, the optimizer stopped the cause of step convergence trouble in the regeneration stripper. The cause of the convergence trouble this early in the process came from high stripper pressure and an increase in the MDEA flow rate, which made the stripper column not converge for the optimizer. Unfortunately, the iterations stopped before the optimizer could calculate a result satisfying the objective constraint CO₂ fraction of 50 PPM. Proceeding further, the absorber pressure, stripper pressure, Rich temperature, lean temperature, MDEA flow rate, and MDEA concentration is set to 80 bar, 1.04 bar, 79°C, 48°C, 200 kgmole/h, and 40%, respectively. These values were chosen to meet the product specification and avoid convergence problems in the regeneration stripper. Increasing the stripper pressure leads to convergence problems and long optimizer simulation times. The CO₂ fraction was 31.50 PPM in the product methane using the set independent variables.

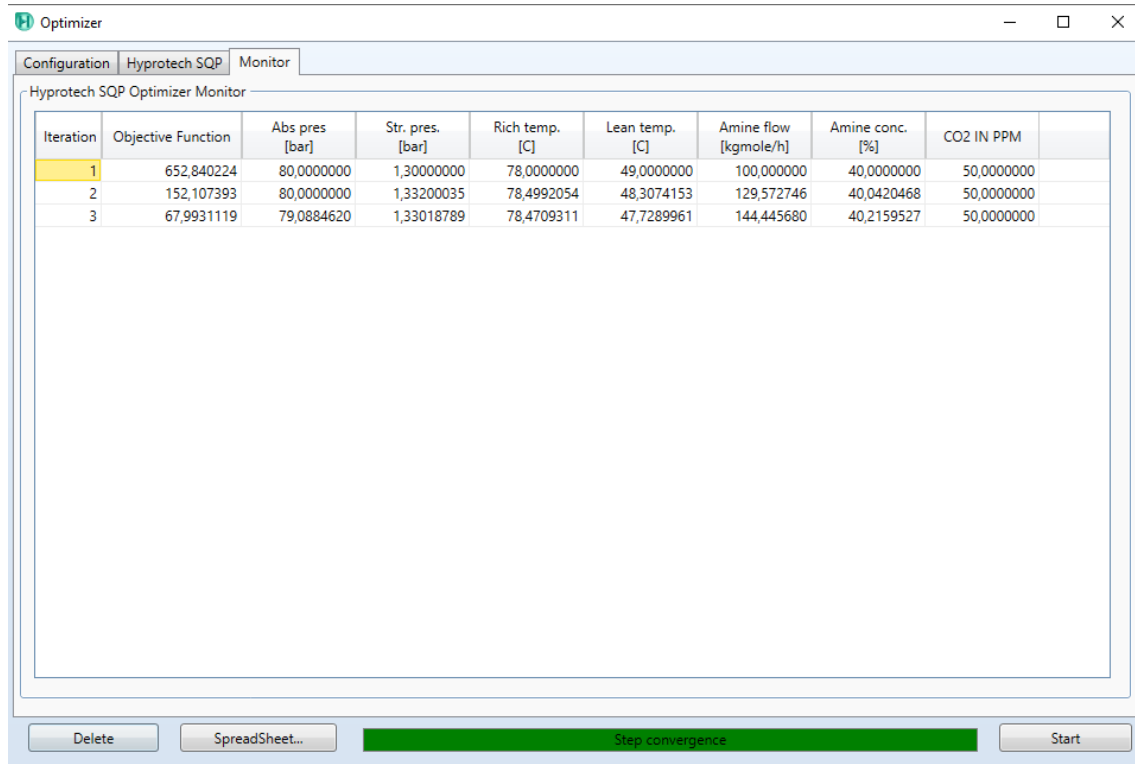


Figure 38: Optimizer results on the polishing process for case 3.8

7 Cost Analysis

This section will perform a cost estimate for the Power-to-Methane plant cases for the different instances [3.0, 3.2, 3.5, 3.8] H₂/CO₂ ratios. A cost study involved in a project can be classified into capital expenditures (CAPEX) and operating expenditures (OPEX). The CAPEX is the cost of maintaining physical assets, in this case, a Power-to-Methane plant. For the case results in Chapter 6, the CAPEX is based on capital cost estimates for process equipment from Sinnott & Towler "Chemical Engineering Design" [28] and Turton et al. "Analysis, synthesis and design of chemical processes"[29]. The OPEX is the operational costs associated with the production, operation of the plant and variable utility costs [28].

7.1 Capital Expenditures CAPEX

To calculate the capital expenditures related to the different cases, the factorial method described in Sinnott & Towler [28] was used. The method gives an approximate estimate of the fixed capital investment needed for a project, and the steps are presented as follows [28]:

1. Prepare material and energy balances, draw preliminary flow sheets, size major equipment items, and select construction material.
2. Estimate the purchased cost of the major equipment items.
3. Calculate the Inside Battery Limit (ISBL) installed capital cost using cost and material factors.
4. Calculate the offsite Outside Battery Limit (OSBL), engineering, and contingency costs using appropriate factors.
5. The sum of ISBL, OSBL, engineering, and contingency costs is the fixed capital investment C_{FC} .
6. Estimate the working capital as a percentage of the fixed capital investment C_{FC} .
7. Add the fixed and working capital to get the total investment required.

7.1.1 Estimating Purchased Equipment Costs

Using the factorial method of cost estimates to estimate the purchased equipment costs requires good estimates. The best source of purchased equipment costs is recent data on prices paid for similar equipment. Usually, Engineering, Procurement, and Construction (EPC) companies have large amounts of data to give a good cost estimate for equipment cost. For the thesis, cost factors based on Sinnott and Towler [28] and Turton et al. [29] are used to calculate an estimate for the different types of equipment.

The correlations to calculate an estimate of the purchased equipment costs is given by equation 30.

$$C_e = a + B \cdot S^n \quad (30)$$

Here, C_e is the estimate of the equipment cost, a and b are the cost constants, S is the size parameter with equipment-specific units, and n is the exponent for that type of equipment. The values for cost constants a and b , exponent n and the size parameter range are given by table 6.6 in literature Sinnott & Towler [28]. The equipment-specific values for S are taken from the simulations. The estimate for purchased cost by [28] is used for the methanation reactors, pumps, compressors, heat exchangers, and knock-out vessels. For the expander, absorber, and stripper columns, the purchased cost estimate provided by Turton et al. is applied. The purchased cost estimate proposed by [29] $C_{p0,j}$ is shown in equation 31.

$$\log(C_{p0,j}) = K_{1,j} + K_{2,j} \cdot \log(A_j) + K_{3,j} \cdot (\log(A_j))^2 \quad (31)$$

where A_j is the capacity of equipment 'j', K_1 , K_2 , and K_3 are constants values specific for equipment 'j'.

The cost-estimating equation uses historical data to forecast the future cost, which is affected by inflation and needs to be updated to relate to the present cost. This is done by using different cost indexes. In this thesis, present cost estimates are calculated using the Chemical Engineering Plant Cost Index (CEPCI), shown in equation 33.

$$\text{Cost in year } A = \text{Cost in year } B \cdot \frac{\text{Cost index year } A}{\text{Cost index year } B} \quad (32)$$

$$C_e \text{ in year } A = C_e \text{ in year } B \cdot \left(\frac{\text{CEPCI year } A}{\text{CEPCI year } B} \right) \quad (33)$$

Here, the CEPCI value for A is for the year 2008 with calculation using Sinnott & Towler [28], and 2001 for calculations using Turton [29], and B is for January 2023. The CEPCI value cost calculation from Turton et al. is based on the value from 2001, which was the earliest value found from [30].

Table 15: CEPCI values for Sinnott & Towler (2009), Turton (1996) and Current day (Jan 2023) [28] [30]

Cost index	CEPCI value	year
Sinnott & Towler	478.6	Jan 2006 [28]
Turton	394.3	2001 [29] [30]
Present day	802,6	Jan 2023 [30]

Table 16 summarises the equipment cost estimate for each case. A detailed overview of the calculation for the individual components in the process model is shown in Appendix E and F.

Table 16: Cost estimation for the equipment

Equipment cost estimate C_e MUSD				
Equipment	3.0	3.2	3.5	3.8
Compressors & pump	2.17	2.16	2.20	2.22
Heat exchangers	0.58	0.60	0.60	0.61
Methanation reactors	0.15	0.17	0.17	0.19
Absorber	0.09	0.09	0.09	0.09
Stripper	0.08	0.08	0.08	0.08
Expander & Valves	0.32	0.44	0.43	0.38
Knock-out vessels	0.17	7.94	3.28	2.51
Total C_e	3.56	11.31	6.68	5.80

7.1.2 Installation Cost

The installation cost is a direct cost incurred in the construction of a plant and relates to equipment erection, piping, instrumentation, electrical power, process buildings, etc., and material. It is often referred to as the ISBL Plant cost. The contribution of each of these items to the capital cost is calculated by multiplying the equipment cost estimate with several appropriate factors as seen in equations 34 and 35.

$$C = \sum_{i=1}^{i=M} C_{e,I,CS}[(1 + f_p)f_m + (f_{er} + f_{el} + f_i + f_c + f_s + f_l)] \quad (34)$$

$$C = \sum_{i=1}^{i=M} C_{e,I,SS}[(1 + f_p) + (f_{er} + f_{el} + f_i + f_c + f_s + f_l)/f_m] \quad (35)$$

here, $C_{e,i,CS}$ is the purchased equipment cost of equipment i in carbon steel (CS), $C_{e,i,SS}$ is the purchased equipment cost of equipment i in stainless steel (SS), and M is the total number of pieces of equipment. The factors f and their values are given in Table 17.

Table 17: Factor for estimation of fluid type process projects [28].

Factor f	Description	Value
f_m	Installation factor for material (CS & 304 SS)	1 & 1.3
f_p	Installation factor for piping	0.8
f_{er}	Installation factor for equipment erection	0.3
f_{el}	Installation factor for electrical work	0.2
f_i	Installation factor for instrumentation and control	0.3
f_c	Installation factor for civil engineering work	0.3
f_s	Installation factor for structures and buildings	0.2
f_l	Installation factor for lagging, insulation, or paint	0.1

Table 18 shows the installation cost of the main process components for the individual cases. A detailed overview of the individual installation cost calculations can be found in Appendix E and F.

Table 18: Installation Cost for the equipment

Installation cost C in MUSD				
Equipment	3.0	3.2	3.5	3.8
Compressors & pump	6.93	6.87	7.03	7.09
Heat exchangers	1.37	1.36	1.36	1.33
Methanation reactors	0.43	0.49	0.49	0.54
Absorber	0.26	0.26	0.26	0.26
Stripper	0.24	0.26	0.26	0.26
Expander & Valves	1.35	1.27	1.24	1.09
Knock-out vessels	0.48	22.84	9.43	7.22
Total installation cost: C	11.06	33.36	20.04	17.76

7.1.3 Total Fixed Capital Cost

After an estimated cost value is found, the total fixed capital cost can be found. The Total Fixed Capital Cost can be found using the equation 36.

$$C_{FC} = C(1 + OSBL)(1 + D\&E + X) \quad (36)$$

here, the C is the installed cost for the equipment (ISBL), OSBL is the offsite battery limit, D&E is the factor for design and engineering, and X is the contingency factor. The values and the Total fixed capital cost results are in Table 19. The offsite cost usually relates to the cost of the additions that must be made to the site infrastructure to accommodate the Power-to-Methane plant or increase the capacity of an existing plant. It is usually between 20% to 50% of the ISBL costs. For this thesis, it is set to 30% of ISBL. The Design and Engineering cost, referred to as contractor charges, include costs of detailed design and engineering services required to carry out the project. It is usually calculated as 30% of the ISBL plus the OSBL cost. The contingency charges are extra costs added to a project budget to allow for variation from the cost estimate. A minimum contingency charge of 10% of ISBL plus OSBL cost should be used on all projects [28]. Table 19 summarize the

total fixed capital cost for each case. A detailed overview of the cost for each parameter is shown in Appendix E and F.

Table 19: Total Fixed capital cost of the PtM plant for the cases.

Fixed capital cost for each Case					
Cost parameter	Value	3.0	3.2	3.5	3.8
Installation cost [C]		11.06	33.36	20.04	17.76
Offsites [OSBL]	0.3 ISBL	3.32	10.01	6.01	5.33
Design and Engineering [D&E]	0.3 ISBL + OSBL	6.63	20.02	12.03	10.65
Contingency [X]	0.1 ISBL + OSBL	4.42	13.35	8.02	7.10
Total Fixed Capital Cost [C_{FC}]		25.43	76.74	46.10	40.84

7.2 OPEX - Operational Expenditures

The operation expenditures generally are associated with day-to-day expenses that a company/project incurs to keep its business running. For a Power-to-methane plant, it can be divided into variable costs of production and fixed costs of production. Further, in this subsection, the operational expenditures for the different cases will be covered. To accommodate for weekends and holidays, it is assumed that the plant is operational for 8000 hours/year.

7.2.1 Variable Costs of Production

The variable cost of production is costs related to the plant output and operation rate. This includes costs for raw material consumed, utilities (cooling water, steam, electricity, Hydrogen), consumables (solvents, catalysts, acids, absorbents, etc.), effluent disposal, and packaging and shipping [28]. For the Power-to-methane case, variable production costs mostly include utilities and consumables. The utility cost factors are listed in table 20. A summary of the variable cost of production for each case is shown in the table 21. A detailed calculation for each individual utility cost can be found in Appendix E and F. The average cost of electricity in USD/MWh for the Trøndelag region was based upon the Nordpool average price for the region in 2022 [31].

Table 20: Utility specific price parameters

Utility	Value	Unit
Cooling water - [29]	0.354	USD/GJ
Steam at 5 bar - [29]	0.0277	USD/kg
Steam at 40 bar - [29]	0.0299	USD/kg
Electricity Nordpol 2022 - [31]	44.45	USD/MWh
MDEA - [29]	2.6	USD/kg
Catalyst - [32]	15539	USD/m ³ Catalyst
Green H ₂ - [33]	4.8	USD/kg H ₂

Table 21: Variable cost for utility

Utility Cost in MUSD				
Utility	3.0	3.2	3.5	3.8
Cooling water at 20°C	0.058	0.055	0.059	0.055
Steam at 5 bar	0.31	0.23	0.25	0.07
Steam at 40 bar	1.18	1.24	1.40	1.53
MDEA	0.00033	0.00018	0.00018	0.00029
Catalyst	0.026	0.03	0.03	0.035
Green H ₂	18.58	19.82	21.68	23.53
Electricity	5.54	5.49	5.65	5.48
Total:	25.7	26.9	29.1	30.7

7.2.2 Fixed cost of Production

The fixed cost of production costs are costs related operation of a plant, regardless of production rate and plant operation rate or output. The fixed costs include eleven different costs. For the power-to-methane plant cases, the fixed costs of production costs include the following:

1. Operating labor
2. Supervision
3. Direct salary overhead
4. Maintenance, materials, and labor.
5. Property tax and insurance
6. General plant overhead - charges to corporate functions such as Human resources, research and development (R&D), finance, etc.

The costs excluded were related to the rent of land, allocated environmental charges, license fees and royalty payments, capital charges, and sales and marketing [28]. To calculate the operation labor costs, it was assumed an annual operator salary of \$50,000 per shift position per year, not including overhead, with the plant operating on a four-shift basis with five operators per shift position. This is to give allowance for weekends, vacations, and holidays and some leeway for overtime. The operation labor cost is calculated by equation 37 [34].

$$LC = \frac{\tau \cdot L_S}{L_{Y,op}} \cdot S_{op} \quad (37)$$

Here, S_{op} is the operator salary, τ is the number of operating shifts per year ($\tau = 1000$ shift/year), $L_{Y,OP}$ is the number of shifts handled by one operator per year ($L_{Y,OP} = 245$ operator shift/year). Labor cost was calculated to be 1.02 MUSD or 9.8 MNOK. The fixed costs can be summarized in Table 22. The conversion from USD to NOK is based on the average currency price for 1 USD to NOK in 2022 by Norges Bank [35]. More detailed calculations for each fixed production cost can be found in Appendix E and F.

Table 22: Fixed cost of production

Fixed cost of Production		
Parameter	Estimate	
1) Operating Labor	5 operator per shift	
2) Supervision	25% of operation labor	
3) Direct salary overhead	60% of operating labor + supervision	
4) Maintenance	5% of ISBL	
5) Property tax & Insurance	2% of ISBL	
6) General plant overhead	65% of [(1) + 2) + 3)] + 4)	
Case	Cost [MUSD]	Cost [MNOK]
3.0	4.64	44.7
3.2	7.31	70.4
3.5	5.71	55.0
3.8	5.43	52.3

7.3 Total Annualized Investment Cost

To analyze the profitability of the process integrations, the revenues of the LBM need to be calculated. The revenues for a project are the incomes earned from sales of main products and byproducts. The byproducts of the methanation process are the steam produced from exothermic heat release and compression used for heat integration[28]. In the revenue calculations, the byproduct will be excluded. The exact value of liquid biomethane is not clear. The International Renewable Energy Agency (IREA) estimates that the cost of production per Sm^3 for producing methane ranges between 0.22 to 0.39 USD/ Sm^3 for manure-based biogas production and 0.11 to 0.50 USD/ Sm^3 for industrial waste-based biogas production [36]. From the U.S. Energy Information Administration (EIA), the average price of liquefied natural gas (LNG) was 3.82 USD/MMBtu for 2022 [37]. Further, this LNG price and the IREA estimate compare the production cost per cubic meter (Sm^3) of LBM and the revenue. The potential revenue can be calculated if liquid biomethane is sold at LNG market prices. The LNG price with conversion equals 1.61 NOK/ Sm^3 or 0.17 USD/ Sm^3 . The LNG market price uses the standard gas flow of natural gas. For this thesis, the standard gas flow for the LBM stream is used to calculate the revenue for each case to give a more accurate production cost comparison. The revenue of the Liquid biomethane produced from the different cases are shown in Table 23.

Table 23: Total revenue of LBM for the different cases

Total revenue of LBM for the different cases			
Case	Std Gas flow [Sm ³ /h]	Value [USD/Sm ³]	Revenue [MUSD/Sm ³]
3.0	4191	0.17	5.7
3.2	4261	0.17	5.8
3.5	4392	0.17	6.0
3.8	4462	0.17	6.1

Table 23 showcases the annual revenue for the different cases if the LBM produced is sold with an LNG market price of 0.17 USD/Sm³. This indicates that the process is not yet profitable since the revenue should cover the annual operational costs, and the fixed capital cost for each case must also be financed.

The production cost per kg and Sm³ are also interesting. The total annualized cost must be determined to calculate the production cost per kg and Sm³. First, the annual capital charge ratio (ACCR) is calculated by taking the interest rate of 6% and the lifetime n (assumed to be 20 years). ACCR is the fraction of interest that must be paid each year to fully repay the principal and all accumulated interest of the life of the investment, and determined by equation 38.

$$ACCR = \frac{[i \cdot (1 + i)^n]}{[(1 + i)^n - 1]} = 0.087 \quad (38)$$

After finding the annual capital charge, the total annualized Cost (TAC) can be found by equation.

$$TAC = \text{operating cost} + ACCR \cdot C_{FC} \quad (39)$$

Table 24 summarizes the cost estimate for the different cases.

The production cost per kg and Sm³ are calculated by taking the total annualized cost and dividing it by the annual production of LBM in kg and Sm³. The results for the production cost based on the plant capacity for one Sm³ LBM is summarized in Table 25.

Table 24: Summary of total cost estimate for each case

Total cost estimate for the PtM facility				
Cost Parameter	3.0	3.2	3.5	3.8
C_{FC}	25.43	76.74	46.10	40.84
Operating cost	30.34	34.31	34.81	36.13
TAC	32.55 MUSD	40.87 MUSD	38.79 MUSD	39.70 MUSD

Table 25: Production cost for each case

Cost Parameter	3.0	3.2	3.5	3.8	Unit
Production LBM in Sm^3	33.53	34.1	35.13	35.7	M Sm^3 /yr
Production cost per unit	0.971	1.20	1.104	1.112	USD/ Sm^3
Production LBM kg	22.7	23.13	23.8	24.41	M kg/yr
Production cost per unit	1.43	1.77	1.63	1.63	USD/kg

8 Discussion

This chapter discusses the findings and assumptions of the sensitivity analysis, optimization, and cost analysis chapters for the different cases 3.0, 3.2, 3.5, and 3.8 for the Power-to-Methane process.

8.1 Methanation Process

In the case ratios, the independent variables chosen for the sensitivity analysis were based on finding the optimal setup for optimization from the influence of pressure, coolant temperature, and the number of tubes in the methanation reactor. However, the independent variables regarding the methanation reactor and catalyst were chosen and kept constant at similar values to the literature to limit the scope of the thesis. It could be interesting to analyze in more detail the influence the length, diameter, and void fraction have on the methanation reaction and the performance of the process. For this thesis, the sensitivity analysis on the influence of pressure, coolant temperature, and the number of tubes gives a good impression of the process modeled.

The independent variables pressure, coolant temperature, and the number of tubes varied in the case ratios' sensitivity analysis. By varying the pressure and coolant temperature in the reactors, changes are seen to the H₂ conversion, CO₂ conversion, and heat flow. It indicated the process highly depended on the independent variables and favored increased pressures into the methanation reactor and coolant temperatures around 240-260°C. Since the methanation reaction favors low temperatures, the inlet temperature was set constant at 200°C. Decreasing the coolant temperature lower than 240°C saw a drastic reduction in CO₂ conversion, and a combination of high pressure and coolant temperature gave good CO₂ and a H₂ ≥ 99.9% for all cases. This can be related to a relatively high coolant temperature, and exothermic heat ensures high conversion. The coolant used for the reactor is high-pressurized steam. For the different cases, a coolant temperature of 240°C was chosen for cases 3.0 and 3.2, and 250°C was chosen for cases 3.5 and 3.8. This was to limit the temperature run away not exceeding 550°C while maintaining sufficient driving forces to initiate the Sabatier reaction in the reactor. Exceeding a temperature run away over 550°C leads to catalyst deactivation. Lowering the coolant temperature can help reduce the methanation runaway temperature, but considering the H₂ and CO₂ conversion reduced drastically with lowered temperatures, it is avoided. Increasing the coolant

temperature above 240-260°C indicated that H₂ and CO₂ conversion was at a maximum, where the reactors had converted 99.9% of the hydrogen in the stream. Increasing the variables further would not increase the methanation but could lead to increased runaway temperatures in the reactors and catalyst deactivation.

Varying the number of tubes in the reactor, there was a significant reduction in CO₂ and H₂, and heat flow with lower numbers. Heat flow increased until a maximum was established by increasing the number of tubes. Increasing the number of tubes decreases the superficial velocity in the tubes, which must stay below 1 m/s. As long as sufficient velocity was maintained, the CO₂ conversion is high if not reached equilibrium. The increase in heat flow by increasing the number of tubes correlates well with how the designed heat transfer is calculated for a cooled wall fixed-bed reactor by equation 19.

The Hyprotech SQP optimizer resulted in step convergence but violated constraints for all cases. This was due to the optimizer reaching a step collapse below the step tolerance during the optimization. The cause for the step collapse could be caused by the small boundaries for minimum conversion of H₂ out of the methanation reactor with maximizing for methane molar flow rate out of the reactor. Using the optimizer tool to optimize for 0.01 digits in the molar flow is too narrow margins for the optimizer. To continue, the results and optimization for the polishing unit were fixed. The fixed independent variables were pressure, coolant temperatures, and the number of tubes for reactors 1 and 2.

8.2 Polishing Process

In the sensitivity analysis of the case studies, the independent variables of inlet pressure to the absorber, MDEA flow rate, and amine concentration were varied. This was to study the impact pressure, MDEA flow rate, and amine concentration had on the CO₂ absorption in the absorber column. The independent variables, stripper pressure, rich temperatures, and amine temperatures, were kept to similar values from the literature. It could be interesting to analyze the regeneration step of lean amine and the impact of stripper pressure and lean temperatures on the regeneration stripper. For this thesis, the sensitivity analysis covered the effect of inlet pressure on the absorber, MDEA flow rate, and amine concentration in the lean amine stream into the absorber.

Pressure significantly impacted the CO₂ absorption for all case ratios. The sensitivity results concluded that increasing the pressure to 80 bar gave all amine flow rates the best

results. From the literature on amine absorption for biogas upgrading, the pressure is usually set between 2-7 bar. Here the pressure had to be elevated to over ten times the values. This is likely due to the low concentration of CO₂ after the methanation unit. For a normal biogas upgrading process, the inlet stream into the absorber contains around 40% CO₂. With the methanation process, there are around 5-10% of the mole fractions for the different cases. So elevating the pressure is needed to absorb for the low CO₂ fractions in the stream.

Increasing the MDEA molar flow rate also increased the absorption of CO₂ in the absorber with a combination of high pressure and increased amine flow rate. For cases 3.0, 3.2, 3.5, and 3.8, an amine flow rate of 600, 400, and 200 kgmole/h was needed to achieve the product specification. The lower H₂/CO₂ ratios needed more amine in the absorber to meet the product specifications. Lowering the H₂/CO₂ ratio increases the CO₂ content in the stream after methanation since less of the CO₂ is converted due to limited H₂ for Sabatier reaction. To meet the product specifications, the polishing unit needed to absorb more of the CO₂ in the stream. Increasing the H₂/CO₂ ratio decreases the CO₂ content because the methanation unit converts more of the CO₂ in the stream. Resulting in higher H₂/CO₂ ratios and requiring less MDEA amine flow rate in their processes.

Increasing the amine concentration gave varying results for some ratios. For cases 3.0 and 3.2, the CO₂ absorption increased with increasing the amine concentration up to 50%. Beyond 50%, the CO₂ fraction increased in the product stream for all amine flow rates tested in the sensitivity analysis. In cases 3.5 and 3.8, the CO₂ fraction decreased with increasing amine concentration up to 50% for the lower amine flow rates. Increasing the MDEA flow rate showed that increasing amine concentration increased the CO₂ fraction. The cause of this might come from correlation with the low mole fraction of CO₂ into the absorber, and with increasing amine flow rate, an increase in amine concentration is not necessary to achieve the product specifications.

The Hyprotech SQP optimizer for the polishing unit gave favorable results for cases 3.0, 3.2, and 3.5. In case 3.8, the optimizer could not calculate an outcome satisfying the objective constraints. The optimizer was stopped for all cases due to step convergence and step collapse below the step tolerance. The cause for the step collapse came from a combination of increased stripper pressure and MDEA molar flow rates resulted in convergence troubles in the regeneration stripper. Especially, an increased inlet stripper pressure increased the optimization time for case 3.8, and the optimizer could not converge the re-

generation stripper with a pressure of 1.3. Lowering the stripper pressure to 1.04 bar avoided convergence troubles in the regeneration stripper for an MDEA flow rate of 200 kgmole/h. Further, some optimization focusing on the regeneration stripper could be analyzed to prevent convergence troubles. For this thesis, optimization for the absorber and reduction in CO₂ fraction in the product methane stream was the focus. Nevertheless, the optimizer was successful for cases 3.0, 3.2, and 3.5, giving optimized variables for absorber pressure, stripper pressure, rich temperatures, lean temperature, MDEA flow rate, and MDEA concentration that produced satisfying product methane with CO₂ fraction less than 50 PPM.

8.3 Cost Analysis

The cost estimation was based on the costing approach by Sinnott & Towler [28], Turton et al. [29], and literature data utility cost and fixed cost of production. The cost estimate factors from Turton et al. may introduce uncertainty regarding the expenses associated with the absorber, stripper, expansion valves, and expander, as the cost estimations rely on assumptions made back in 1998. The CEPCI value for cost estimate using [29] is based upon the CEPCI value of 394.3, the earliest value listed, which will also give inaccurate cost calculations due to inflation [30]. The sensitivity analysis showed that pressure, number of tubes, coolant temperature, MDEA flow rate, and amine concentration affected the production of liquid biomethane. This will give slight variations in the cost estimation for the different cases. Nevertheless, the cost estimation gives a good first impression of the economics of the different cases and process plants.

The equipment cost estimate using equation 30, and 31 heavily relates to the scale of the equipment. Small units will be relatively expensive in capital cost compared to large-scale units [28] [29]. There are some uncertainties regarding the cost of the heat exchangers since the process is not heat integrated with other heat exchangers and other equipment. Optimizing with heat integration could lead to more accurate cost estimation and reduce the cost and energy efficiency of the plant.

Looking at the cost estimate for the different cases, there are little variations for compressors, heat exchangers, methanation reactors, absorbers, strippers, and expanders. Most variations stem from the pressures chosen and the required cooling duty after methanation reactors for the different cases. Large cost variations for the knock-out vessels

take up most of the equipment cost estimate. For all cases, the first knock-out vessel (WR) after the first methanation reactor made up most of the equipment cost. For case 3.0, the knock-out vessel costs are small compared to the other cases because the first knock-out vessel has no liquid water in the stream to separate. This caused the shell mass calculations to be invalid, and the cost for the vessel was not calculated. Case 3.2 had a significant variation in equipment cost for the knock-out vessel. Here, the first vessel after the first reactor took up most of the cost. The high cost came from the vessel having a much larger Liquid volumetric flow rate than the other cases, with small variations between the gas and liquid densities resulting in a large calculated shell mass for the WR vessel. For cases 3.5 and 3.8, the WR vessel also takes most of the equipment cost, making around 95% of the vessel costs. The absorber and stripper equipment cost was the same for all cases since the number of trays, column diameter, and height were set the same.

The operational expenditures saw little variations for the different cases. From the variable cost of utility, the cost on green H₂ was the primary driver being between 73-56% of the utility cost for all cases. This makes the final price for the produced LBM highly dependent on the green H₂ market price. The fixed cost for production has a slight variation, with just case 3.2 having a higher cost than the rest. This is due to the high ISBL cost for this configuration.

Considering methane production, hydrogen conversion, absorption, and cost, Case 3.8 is the most practical choice for implementing direct biogas methanation to produce LBM at lower H₂/CO₂ ratios. This case carries a total estimated cost of 77 million USD and can yield an annual production of 24,408,000 kilograms of LBM. The profits for the different cases must also be considered to find if the direct methanation configuration is profitable. The revenue for the different cases 3.0, 3.2, 3.5, and 3.8 was 5.7, 5.8, 6.0, and 6.1 MUSD/Sm³, respectively. It was calculated with the assumption of being sold with an LNG market price of 0.17 USD/Sm³, indicating that the process is not yet profitable. The revenue should cover the annual operation cost to at least go even annually. From the International Renewable Energy Agency, the production cost per Sm³ for producing methane ranges between 0.22 and 0.39 USD/Sm³ for manure-based biogas production, and 0.11 and 0.5 USD/Sm³ for industrial waste-based biogas production [36]. The production cost for the direct methanation processes was 0.97, 1.2, 1.1, and 1.11 USD/Sm³ for cases 3.0, 3.2, 3.5, and 3.8, respectively. The production cost per Sm³ is higher than for manure and industrial waste-based production. It supports that operating at lower H₂/CO₂ ratios are

not profitable, considering the H₂ cost is covering most of the operational cost. For the direct methanation process plant to be profitable, the H₂ price and the equipment cost related to Knock-out vessels must be reduced.

9 Conclusion

In this master thesis, sensitivity analysis, optimization, and cost analysis were covered for a direct methanation process model with varying H_2/CO_2 case ratios of 3.0, 3.2, 3.5, and 3.8. The objective was to investigate if a direct methanation process could produce product methane at lower H_2/CO_2 ratios and be profitable. The sensitivity analysis and optimization were split into two parts: the methanation unit and the polishing unit, with analyzing how different independent variables affected the CH_4 production, CO_2 conversion and absorption for the direct methanation model. Optimization for each case ratio was covered to maximize the CO_2 and H_2 conversion for the methanation unit. For the polishing unit, the optimization objective was to minimize the CO_2 fraction in the product stream.

The sensitivity analysis and optimization on the methanation and polishing units gave good results for the production of LBM with a lower H_2/CO_2 ratio than 4.0. The sensitivity analysis on the methanation unit indicated the optimal pressure values, coolant temperature, and the number of tubes for reactors 1 and 2 to be around 15-20 bar, 240°C, and tube numbers of 2000-3000 and 1000 for reactors 1 and 2. An Increase in pressure and coolant temperature increased heat flow in the reactors up to 220-240°C but also increased the conversion of H_2 in the reactor. Higher coolant temperature reduced heat flow and minimal change in CO_2 conversion. The number of tubes in the reactor increased the heat flow and reached a maximum for each case. The optimization for the methanation reactor was unsuccessful, and fixed values were set for the cost calculations.

The sensitivity analysis on the polishing unit indicated that CO_2 absorption favored increased pressure and MDEA molar flow rates for all cases. For all cases, an inlet absorption pressure of 80 bar gave the best results with varying MDEA flow rates, dependent on the H_2/CO_2 case ratio. The lower case ratios need higher MDEA flow rates to absorb enough CO_2 to meet the product specifications. The optimizer objective was to minimize CO_2 PPM in the product stream and gave optimized independent variables for cases 3.0, 3.2, and 3.5, which satisfied the optimizer constraints. For case 3.8, the optimizer stopped early due to convergence issues in the regeneration stripper, and fixed independent variables were set for the cost estimations.

Although the sensitivity analysis and optimization indicate that the direct Power-to-Methane process can be operated for lower H_2/CO_2 ratios, the cost analysis showed

revenues for the cases ranging between 5.7-6.1 MUSD annually and had a total annualized cost between 32-41 MUSD. The production cost per Sm^3 for the cases 3.0, 3.2, 3.5, and 3.8 are 0.97, 1.2, 1.1, and 1.11 USD/ Sm^3 , respectively, while the LNG price is 0.17 USD/ Sm^3 . The revenue is much lower than the annualized cost, and the high production cost per Sm^3 indicates that the direct process integration with a lower H_2/CO_2 ratio is not profitable. However, the cost of green H_2 per kg is the major driving factor, accounting for approximately 72-77% of the operational cost. If the price for green H_2 decreases, the direct methanation option could become profitable. The cost estimation and factors for both capital and operation costs were derived from the textbooks authored by Sinnott & Towler, and Turton. However, due to inherent uncertainties, it is crucial to interpret the economic analysis with caution [28] [29].

10 Further Work

Further work on this topic can be done on the following points:

- Continue the optimization of the methanation unit, and polishing unit to avoid the reoccurring step convergence issues in the reactors and the regeneration stripper.
- Analyze the impact of varying different independent variables in the methanation reactor, such as the void fraction, dilution factor, and tube inner diameter, and try to model for other catalyst combinations.
- For the polishing unit, the variation of inlet stripper pressure affected the convergence in the regeneration stripper. Further, the sensitivity and optimization of the regeneration stripper could be analyzed to cut down on iteration time in HYSYS.
- The optimizer could be tested with an objective function based on reducing the cost or maximizing the revenue of the direct methanation configurations. The plant revenue will vary depending on equipment costs and operational costs. Establishing a cost parameter as the objective function with all the necessary restrictions would improve the optimization for the different cases.
- An energy or exergy analysis should be evaluated for analyzing the process efficiency.
- Gather real data for the cost estimation, to make a more accurate cost analysis of the different H_2/CO_2 case ratios.

References

- [1] European Commission: European Union. *REPowerEU: affordable, secure and sustainable energy for Europe*. 2022. URL: https://commission.europa.eu/strategy-and-policy/priorities-2019-2024/european-green-deal/repowerEU-affordable-secure-and-sustainable-energy-europe_en#repowerEU-actions (visited on 28/04/2023).
- [2] International Energy Agency. *Key World Energy Statistics 2021*. 2021. URL: <https://www.iea.org/reports/key-world-energy-statistics-2021> (visited on 28/04/2023).
- [3] K. Ghailb and F.-Z. Ben-Fares. ‘Power-to-Methane: A state-of-the-art review’. In: *Renewable and Sustainable Energy Reviews* 81 (2018), pp. 433–446. DOI: <https://doi.org/10.1016/j.rser.2017.08.004>.
- [4] J. Bremer and K. Sundmacher. ‘Operation range extension via hot-spot control for catalytic CO₂ methanation reactors’. In: *React. Chem. Eng.* 4 (2019), pp. 1019–1037. DOI: <https://doi.org/10.1039/C9RE00147F>.
- [5] M. Götz, J. Lefebvre, F. Mörs, A. M. Koch, F. Graf, S. Bajohr, R. Reimert and T. Kolb. ‘Renewable Power-to-Gas: A technological and economic review’. In: *Renewable Energy* 85 (2016), pp. 1371–1390. DOI: <https://doi.org/10.1016/j.renene.2015.07.066>.
- [6] K. Shanmugam, M. Tysklind and V. K. Upadhyayula. ‘Use of Liquefied Biomethane (LBM) as a Vehicle Fuel for Road Freight Transportation: A Case Study Evaluating Environmental Performance of Using LBM for Operation of Tractor Trailers’. In: *Procedia CIRP* 69 (2018), pp. 517–522. DOI: <https://doi.org/10.1016/j.procir.2017.11.133>.
- [7] Biokraft AS. *Biogas Drivstoff*. 2023. URL: <https://www.biokraft.no/biokraft-biogass/> (visited on 01/05/2023).
- [8] S. Qie, L. Hailong, Y. Jinying, L. Longcheng, Y. Zhixin and Y. Xinhai. ‘Selection of appropriate biogas upgrading technology—a review of biogas cleaning, upgrading and utilisation’. In: *Renewable and Sustainable Energy Reviews* 51 (2015), pp. 521–532. DOI: <https://doi.org/10.1016/j.rser.2015.06.029>.
- [9] S. E. Hashemi. *Development and Optimization of Processes for Liquefied Biomethane Production*. 2022. URL: <https://hdl.handle.net/11250/2989985>.
- [10] M. R. Attanapola. *Power-to-Gas Methanation of Carbon dioxide*. Project work. Internal Report. NTNU, 2022.

-
- [11] A. Mazza, E. Bompard and G. Chicco. ‘Applications of power to gas technologies in emerging electrical systems’. In: *Renewable and Sustainable Energy Reviews* 92 (2018), pp. 794–806. DOI: <https://doi.org/10.1016/j.rser.2018.04.072>.
- [12] J. Gao, Q. Liu, F. Gu, B. Liu, Z. Zhong and F. Su. ‘Recent advances in methanation catalysts for the production of synthetic natural gas’. In: *The Royal Society of Chemistry Adv.* 5 (2015), pp. 22759–22776. DOI: <https://doi.org/10.1039/C4RA16114A>.
- [13] L. Jürgensen, E. A. Ehimen, J. Born and J. B. Holm-Nielsen. ‘Dynamic biogas upgrading based on the Sabatier process: Thermodynamic and dynamic process simulation’. In: *Bioresource Technology* 178 (2015), pp. 323–329. DOI: <https://doi.org/10.1016/j.biortech.2014.10.069>.
- [14] J. Gao, Y. Wang, Y. Ping, D. Hu, G. Xu, F. Gu and F. Su. ‘A thermodynamic analysis of methanation reactions of carbon oxides for the production of synthetic natural gas’. In: *The Royal Society of Chemistry Adv.* 2 (2012), pp. 2358–2368. DOI: <https://doi.org/10.1039/C2RA00632D>.
- [15] C. Mebrahtu, F. Krebs, S. Abate, S. Perathoner, G. Centi and R. Palkovits. ‘Chapter 5 - CO₂ Methanation: Principles and Challenges’. In: *Horizons in Sustainable Industrial Chemistry and Catalysis*. Vol. 178. Elsevier, 2019, pp. 85–103. DOI: <https://doi.org/10.1016/B978-0-444-64127-4.00005-7>.
- [16] S. Rönsch, J. Schneider, S. Matthischke, M. Schlüter, M. Götz, J. Lefebvre, P. Prabhakaran and S. Bajohr. ‘Review on methanation – From fundamentals to current projects’. In: *Fuel* 166 (2016), pp. 276–296. DOI: <https://doi.org/10.1016/j.fuel.2015.10.111>.
- [17] A. Fache, F. Marias, V. Guerré and S. Palmade. ‘Optimization of fixed-bed methanation reactors: Safe and efficient operation under transient and steady-state conditions’. In: *Chemical Engineering Science* 192 (2018), pp. 1124–1137. DOI: <https://doi.org/10.1016/j.ces.2018.08.044>.
- [18] S. G. Pavlostathis and E. Giraldo-Gomez. ‘Kinetics of anaerobic treatment: A critical review’. In: *Critical Reviews in Environmental Control* 21.5-6 (1991), pp. 411–490. DOI: <https://doi.org/10.1080/10643389109388424>.
- [19] I. Angelidaki, L. Treu, P. Tsapekos, G. Luo, S. Campanaro, H. Wenzel and P. G. Kougias. ‘Biogas upgrading and utilization: Current status and perspectives’. In: *Biotechnology Advances* 36.2 (2018), pp. 452–466. DOI: <https://doi.org/10.1016/j.biotechadv.2018.01.011>.
-

-
- [20] L. Yang, X. Ge, C. Wan, F. Yu and Y. Li. ‘Progress and perspectives in converting biogas to transportation fuels’. In: *Renewable and Sustainable Energy Reviews* 40 (2014), pp. 1133–1152. DOI: <https://doi.org/10.1016/j.rser.2014.08.008>.
- [21] S. E. Hashemi, S. Sarker, K. M. Lien, S. K. Schnell and B. Austbø. ‘Cryogenic vs. absorption biogas upgrading in liquefied biomethane production – An energy efficiency analysis’. In: *Fuel* 245 (2019), pp. 294–304. DOI: <https://doi.org/10.1016/j.fuel.2019.01.172>.
- [22] F. Capra, F. Magli and M. Gatti. ‘Biomethane liquefaction: A systematic comparative analysis of refrigeration technologies’. In: *Applied Thermal Engineering* 158 (2019), p. 113815. DOI: <https://doi.org/10.1016/j.applthermaleng.2019.113815>.
- [23] L. Kiewidt and J. Thöming. ‘Predicting optimal temperature profiles in single-stage fixed-bed reactors for CO₂-methanation’. In: *Chemical Engineering Science* 132 (2015), pp. 59–71. DOI: <https://doi.org/10.1016/j.ces.2015.03.068>.
- [24] E. Tsotsas and E.-U. Schlünder. ‘Heat transfer in packed beds with fluid flow: remarks on the meaning and the calculation of a heat transfer coefficient at the wall’. In: *Chemical Engineering Science* 45.4 (1990), pp. 819–837. DOI: [https://doi.org/10.1016/0009-2509\(90\)85005-X](https://doi.org/10.1016/0009-2509(90)85005-X).
- [25] H. Martin and M. Nilles. ‘Radiale Wärmeleitung in durchströmten Schüttungsrohren’. In: *Chemie Ingenieur Technik* 65.12 (1993), pp. 1468–1477. DOI: <https://doi.org/10.1002/cite.330651206>.
- [26] R. J. Kee, M. E. Coltrin, P. Glarborg and H. Zhu. *Chemically reacting flow: theory, modeling, and simulation*. John Wiley & Sons, 2017.
- [27] F. Koschany, D. Schlereth and O. Hinrichsen. ‘On the kinetics of the methanation of carbon dioxide on coprecipitated NiAl(O)_x’. In: *Applied Catalysis B: Environmental* 181 (2016), pp. 504–516. DOI: <https://doi.org/10.1016/j.apcatb.2015.07.026>.
- [28] R. Sinnott and G. Towler. *Chemical Engineering Design: SI edition*. Chemical Engineering Series. Elsevier Science, 2009.
- [29] R. Turton, R. C. Bailie, W. B. Whiting and J. A. Shaeiwitz. *Analysis, synthesis and design of chemical processes*. Pearson Education, 1998.
- [30] Chemical Engineering. *Cost Indices, Chemical Engineering Plant Cost Index (CEPCI)*. 2023. URL: <https://toweringskills.com/financial-analysis/cost-indices/> (visited on 25/05/2023).
-

-
- [31] NordPool. *Day-ahead prices, Market data*. 2023. URL: <https://www.nordpoolgroup.com/en/Market-data1/Dayahead/Area-Prices/NO/Daily1/?dd=NO3&view=chart> (visited on 03/06/2023).
- [32] D. Parigi, E. Giglio, A. Soto and M. Santarelli. ‘Power-to-fuels through carbon dioxide Re-Utilization and high-temperature electrolysis: A technical and economical comparison between synthetic methanol and methane’. In: *Journal of Cleaner Production* 226 (2019), pp. 679–691. DOI: <https://doi.org/10.1016/j.jclepro.2019.04.087>.
- [33] S&P Global Market Intelligence. *Experts explain why green hydrogen costs have fallen and will keep falling*. 2021. URL: <https://www.spglobal.com/marketintelligence/en/news-insights/latest-news-headlines/experts-explain-why-green-hydrogen-costs-have-fallen-and-will-keep-falling-63037203> (visited on 03/06/2023).
- [34] P. Mores, N. Rodríguez, N. Scenna and S. Mussati. ‘CO₂ capture in power plants: Minimization of the investment and operating cost of the post-combustion process using MEA aqueous solution’. In: *International Journal of Greenhouse Gas Control* 10 (2012), pp. 148–163. DOI: <https://doi.org/10.1016/j.ijggc.2012.06.002>.
- [35] Norges Bank. *Valuta Kurser*. 2023. URL: <https://www.norges-bank.no/tema/Statistikk/Valutakurser/?tab=currency&id=USD> (visited on 03/06/2023).
- [36] International Renewable Energy Agency. *Biogas Cost Reductions to Boost Sustainable Transport*. 2017. URL: <https://www.irena.org/news/articles/2017/Mar/Biogas-Cost-Reductions-to-Boost-Sustainable-Transport> (visited on 08/06/2023).
- [37] Global LNG Hub. *Short term tren of Natural gas and LNG Prices*. 2022. URL: <https://globallnghub.com/short-term-trend-of-natural-gas-and-lng-prices.html> (visited on 07/06/2023).
- [38] T. Nejat, A. Movasati, D. A. Wood and H. Ghanbarabadi. ‘Simulated exergy and energy performance comparison of physical–chemical and chemical solvents in a sour gas treatment plant’. In: *Chemical Engineering Research and Design* 133 (2018), pp. 40–54. DOI: <https://doi.org/10.1016/j.cherd.2018.02.040>.
- [39] S. Langè, L. A. Pellegrini, P. Vergani and M. Lo Savio. ‘Energy and Economic Analysis of a New Low-Temperature Distillation Process for the Upgrading of High-CO₂ Content Natural Gas Streams’. In: *Industrial & Engineering Chemistry Research* 54.40 (2015), pp. 9770–9782. DOI: [10.1021/acs.iecr.5b02211](https://doi.org/10.1021/acs.iecr.5b02211).
- [40] H. A. Jakobsen. *Chemical reactor modeling. Multiphase Reactive Flows*. Springer, 2008.
-

-
- [41] A. Ghajar and D. Yunus A. Cengel. *Heat and Mass Transfer: Fundamentals and Applications*. McGraw-Hill Education, 2014.
- [42] A. G. Dixon. ‘An improved equation for the overall heat transfer coefficient in packed beds’. In: *Chemical Engineering and Processing: Process Intensification* 35.5 (1996), pp. 323–331. DOI: [https://doi.org/10.1016/0255-2701\(96\)80012-2](https://doi.org/10.1016/0255-2701(96)80012-2).
- [43] G. Froment, K. Bischoff and J. De Wilde. *Chemical Reactor Analysis and Design, 3rd Edition*. John Wiley & Sons, Incorporated, 2010.
- [44] J. Worstell. ‘Chapter 4 - Scaling Fluid Flow’. In: *Scaling Chemical Processes*. Butterworth-Heinemann, 2016, pp. 77–107. DOI: <https://doi.org/10.1016/B978-0-12-804635-7.00004-0>.
- [45] E. N. Fuller, P. D. Schettler and J. C. Giddings. ‘New method for prediction of binary gas-phase diffusion coefficients’. In: *Industrial & Engineering Chemistry* 58.5 (1966), pp. 18–27.

Appendix

A Conventional Biogas Upgrading

In this section of the appendix, an overview of how a conventional biogas upgrading process model is covered. The polishing unit in the direct methanation model uses the same biogas upgrading technology to polish the product stream. The description of the conventional biogas model is taken from the project thesis from December 2022 [10].

For this model, raw biogas with inlet conditions listed in Table 26 are used as an example. This model was developed by Hashemi [9].

Parameter	Composition	unit
CH ₄	60 %	mol%
CO ₂	40 %	mol%
Temperature	35	°C
Pressure	1,013	Bar
Molar flow	200	kgmol/h

Table 26: Conventional Inlet Biogas specifications

The biogas undergoes a five-stage compression cycle with inter cooling in between each compression cycle. The cooling medium used in the heat exchangers was cooling water with a temperature of 20°C and 1.013 bar. This compresses the biogas to the optimal pressure and temperature for amine-based absorption. The lean amine solvent is injected at the same pressure as the compressed biogas and interacts counter currently. In conventional upgrading shown in Figure 39 below, the inlet (stream 24) temperature and pressure is 30 °C and 48.75 Bar, respectively. The high pressure and temperature in the amine absorption columns are to take advantage of high-pressure biomethane production with less heat requirement in the absorption column and the stripper with MDEA as a solvent [38]. The high purity CH₄ leaves the amine absorber in stream 6 in Figure 39 with a mass methane content of 99.64% missing 0.3% from the product specifications, but satisfying the amine-based upgrading method from [20] of 96-98%. The pure methane leaves then to a liquefaction process with N₂ as a refrigerant to cool the methane down into Liquid biomethane. In Appendix C, the liquefaction process model is added and is a single expander liquefaction process using N₂ as a medium.

The CO₂, H₂S and amine water solution is leaving the bottom of the absorber (stream 27) with a temperature and pressure of 72.92 °C and 48.75 bar. The amine-rich solvent is expanded and heated to a high temperature of 83.23°C to increase the stripper efficiency. The stripping unit regenerates the amine solvent and separates the off-gas that is CO₂ and H₂S rich out the top of the stripper column and amine-rich solvent leaves at the bottom. The amine-rich solvent contains small amounts of CH₄ and is rerouted back with a pump into the amine absorber for recycling. The pumping unit is there to lift the pressure for the amine solvent from 1.430 bar to 48.75 bar, the same as the pressure in the amine absorber. Stream 32 is routed through the heat exchanger before the stripping unit to provide heating. A makeup stream combiner is used to increase the MDEA concentration of the amine solvent before regeneration. This compensates for the loss of MDEA and water in the process. Following the makeup MDEA unit, a heat exchanger CW6 with cooling water is adjusting the temperature of the lean amine solution to the required temperature to the absorber of 46.7°C. There is a temperature difference between the injected lean amine solvent and the inlet compressed biogas of 16.8°C. The difference is placed to facilitate the chemical reaction between the CO₂ and the MDEA [39].

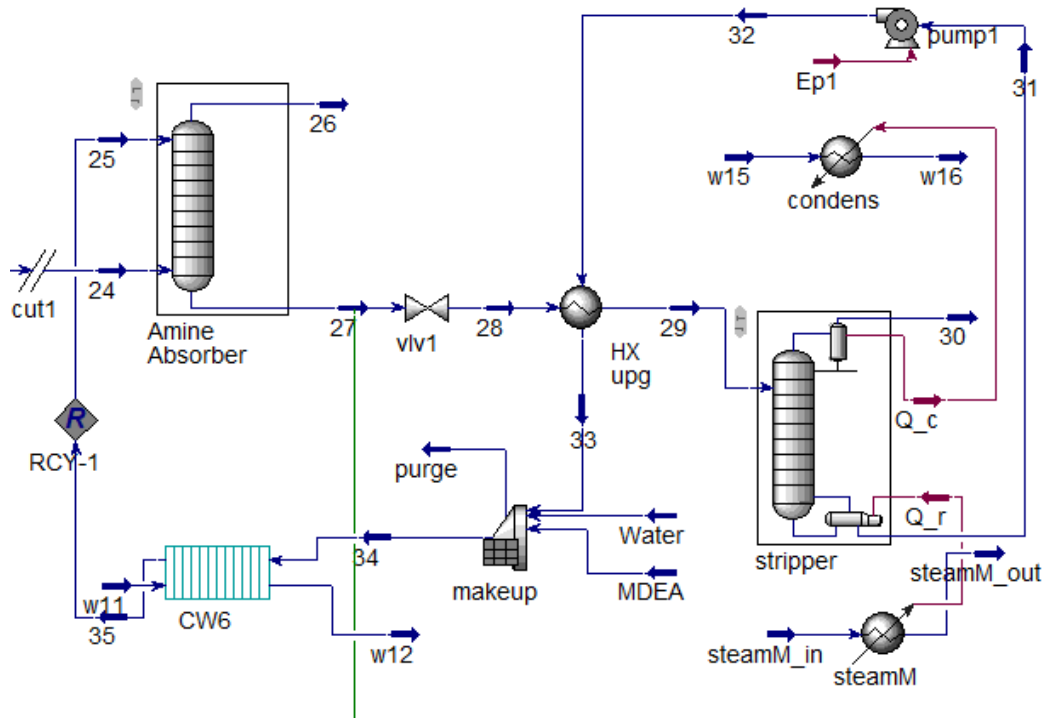
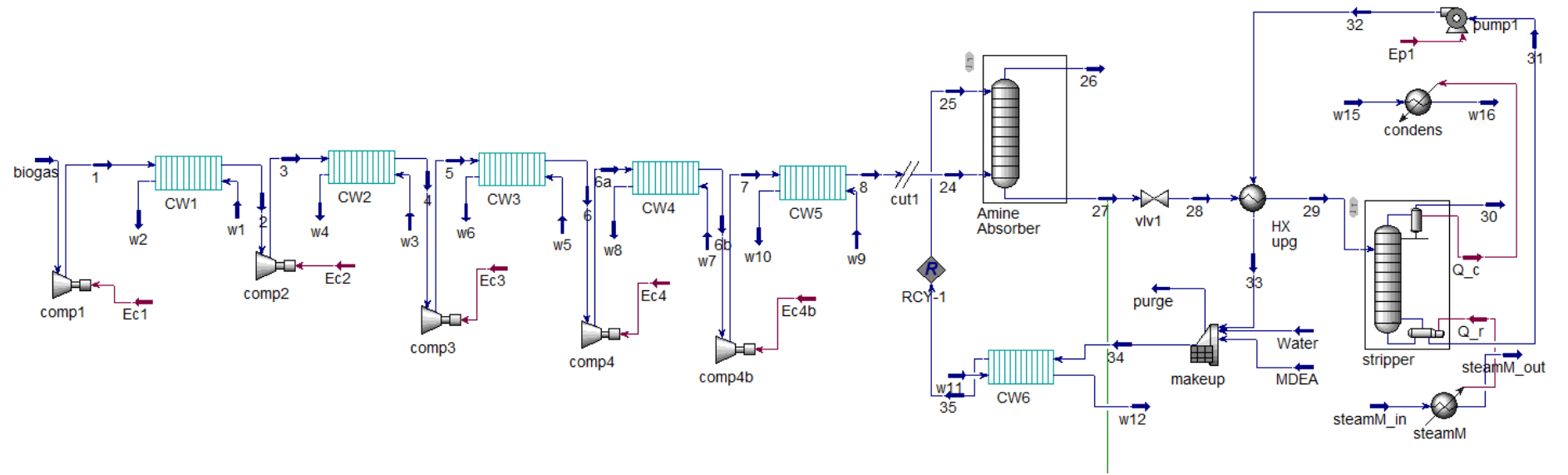


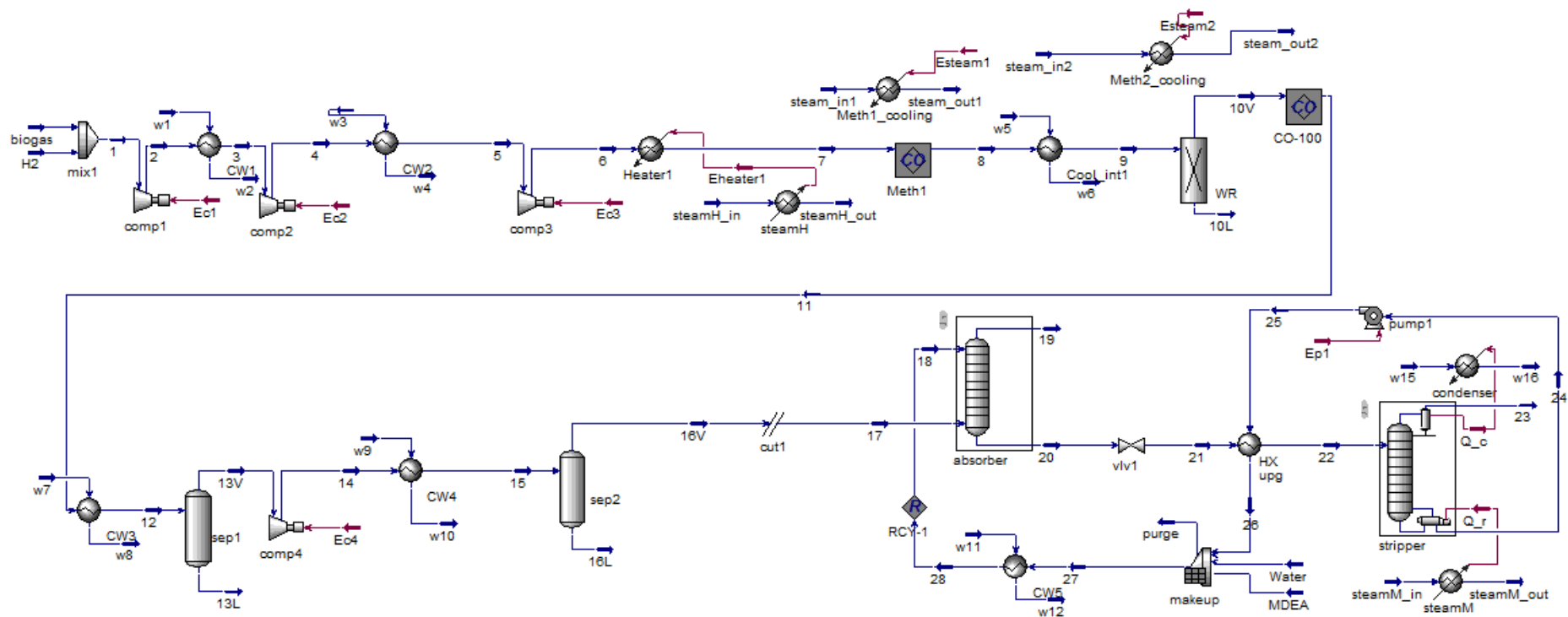
Figure 39: Conventional amine upgrading unit



B Direct Methanation Process Model

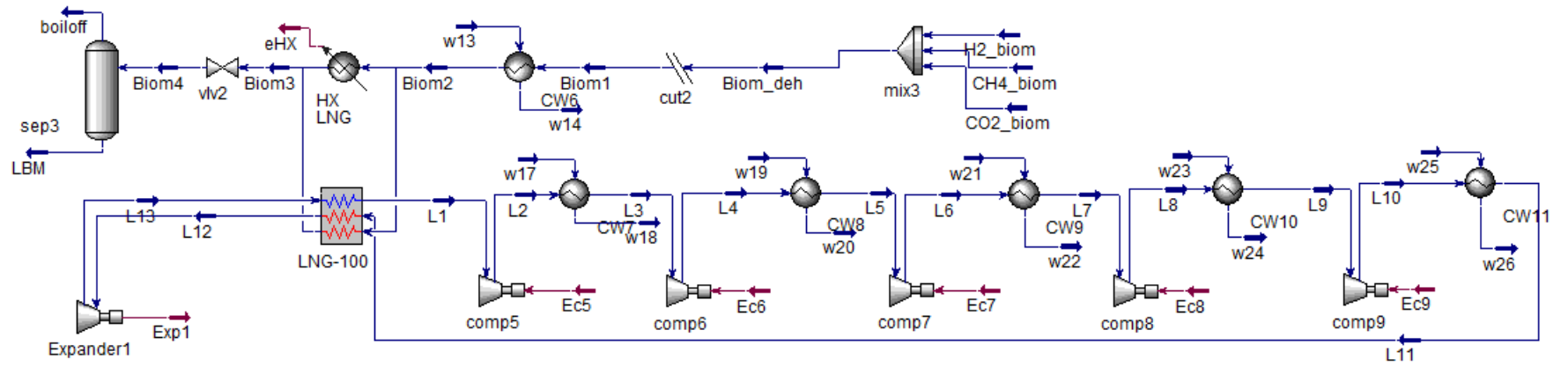
In this appendix section, the direct methanation process model modeled in Aspen HYSYS V10.1 is shown in the figure below.

Λ



C Liquefaction Process Model

In this appendix section, the N_2 liquefaction model used in the direct methanation process is shown in the figure below.



D Modelling of the Methanation Reactors

In this appendix section, the conservation of the equation for mass, energy, and momentum balance used for modeling the methanation reactor is covered.

For the methanation reactors used in this direct methanation process model, a one-dimensional pseudo-homogeneous model was employed in HYSYS. A detailed model of the methanation reactors was modeled in MATLAB instead of available reactor models in Aspen HYSYS. MATLAB was used to account for temperature profiles and avoid potential thermal runaway in the methanation reactors. The detailed description of the MATLAB script will not be documented, but a brief description of the governing equations and employed assumptions and correlations will be described.

The pseudo-homogeneous model was employed to represent a fixed-bed methanation reactor. The reactor was assumed to be a multi-tubular wall-cooled reactor, similar to Bremer et al. [4] and Fache et al. [17].

D.1 Continuity Equation

For the bulk phase inside a cylindrical tube, the continuity balance Equation is given in 40. The continuity equation and the vector derivatives come from "Chemical reactor modeling" by Hugo A. Jakobsen [40].

$$\frac{\partial \rho}{\partial t} + \nabla \cdot (\rho \mathbf{u}) \quad (40)$$

The process is stationary, and the first term is neglected, getting the stationary three-dimensional continuity equation as

$$\nabla \cdot (\rho \mathbf{u}) \quad (41)$$

Further, assuming radial and angular convective terms are neglected, applying the product rule. The equation reduces with further rearrangement.

$$\frac{\partial}{\partial z}(\rho_g u_z) = \rho_g \frac{\partial u_z}{\partial z} + u_z \frac{\partial \rho_g}{\partial z} = 0 \frac{du_z}{dz} = \frac{u_z}{\rho_g} \frac{d\rho_g}{dz} \quad (42)$$

$$\frac{du_z}{dz} = -\frac{u_z}{\rho_g} \frac{d\rho_g}{dz} \quad (43)$$

Replacing the density derivative with assuming ideal gas, the equation is solved too:

$$\frac{du_z}{dz} = -\frac{u_z}{\rho_g} \left(\frac{\rho_g}{M} \frac{dM}{dz} + \frac{\rho_g}{p} \frac{dp}{dz} - \frac{\rho_g}{T} \frac{dT}{dz} \right) \quad (44)$$

Rearranging to obtain the axial velocity profile.

$$\frac{du_z}{dz} = \frac{u_z}{T} \frac{dT}{dz} - \frac{u_z}{p} \frac{dp}{dz} - \frac{u_z}{M} \frac{dM}{dz} \quad (45)$$

The superficial velocity for the plug flow can be calculated based on the total mass balance,

$$u_z = u_{z,in} \cdot \frac{\bar{\rho}_{in}}{\bar{\rho}} \quad (46)$$

D.2 Energy Balance

The energy balance equation is provided in vector form from Hugo's "Chemical reactor design" [40]. This equation is used to find the temperature profile of the bulk phase inside a cylindrical reactor tube.

$$\rho C_p \frac{\partial T}{\partial t} + \rho C_p u \cdot \nabla T = -\nabla \cdot q - \frac{T}{\rho} \left(\frac{\partial \rho}{\partial T} \right) \cdot \frac{Dp}{Dt} - \sigma \cdot \nabla u + \Sigma \frac{h_r}{M_r} \nabla \cdot \mathbf{j}_r + \Sigma \frac{R_r}{M_r} (-\Delta H_{Rr}) \quad (47)$$

Where C_p is the heat capacity of the gas mixture, ρ is the gas density, u is the velocity, T is the temperature, q is heat flux given by Fourier's law $q = -\lambda_{er} \nabla T$, h_r is the convective heat transfer coefficient of a gas, M_r is the molar mass fraction of gas, R_r is the number of chemical reactions, and $-\Delta H_r$ is the heat of the reaction rate, respectively.

An explanation of the individual terms in Equation 47. The first term is the change of heat content with time, for a stationary process is equal to zero. The second term is convective transport. Third, after the equal sign is the heat transport by conduction in the bulk phase, described by Fourier's law. And the last term is the change of heat content with regard to time, and due to compression, is negligible. The fifth and sixth term is the viscous heat dissipation and radiation heat flux in the fluid which is both negligible. The last term is the energy produced/consumed from the chemical reactions in the process. For this case, only CO₂ methanation reaction occurs inside the reactors.

Introducing Fourier's law into the reaction rate Equation 47, and removing negligible terms gives a stationary three-dimensional energy balance.

$$\rho_g C_p u \cdot \nabla T = \nabla \cdot (\lambda_{er} \nabla T) + \sum_{r=1}^R \frac{R_r}{M_r} (-\Delta H_{Rr}) \quad (48)$$

Further, assumptions for radial and angular advective terms are neglected. A constant radial conductivity λ_{er} is constant for the whole cross-section, and negligible angular and axial conduction expresses the axial temperature profile.

$$\frac{\partial T}{\partial z} = \frac{1}{\rho_g C_p u_z} \left(\lambda_{er} \left(\frac{1}{r} \frac{\partial T}{\partial r} + \frac{\partial^2 T}{\partial r^2} \right) \right) + \sum \frac{R_r}{M_r} \cdot (-\Delta H_{Rr}) \quad (49)$$

For this methanation reactor, to account for intraparticle mass limitations of the pseudo-homogenous model, a temperature-dependent effectiveness factor proposed by Kiewit and Thöming was considered. [23].

$$\frac{dT}{dz} = -\frac{4}{D} \cdot k_w \cdot (T - T_c) + \frac{(1 - \varepsilon \cdot \eta \cdot \rho_{cat})}{\bar{\rho} \cdot \bar{c}_p \cdot u_z} \sum \Delta H_R \cdot r \quad (50)$$

Where $k_w, T, T_c, \Delta H_R$, and r refer to the overall heat transfer coefficient, temperature within the reactor, coolant temperature, heat of Sabatier reaction, and reaction rate, respectively.

Heat Balance

In addition, it is necessary to calculate the heat transfer from the gas inside the tubes toward the coolant. With the assumption of a multi-tubular wall-cooled reactor, the heat transfer rate equation can be described as

$$Q = UA\Delta T [W] \quad (51)$$

where U is the overall heat transfer coefficient, A is the tube area, and ΔT is the temperature difference between the wall and coolant. Further integrating over the area of a tube $A = \pi DL$ to find the heat transfer per unit length of a single cylindrical tube

$$Q = \int_0^A (U\Delta T) dA = \int_0^{\pi DL} (U\Delta T) dA \quad (52)$$

Then the heat transfer per unit length of a tube bundle can be calculated for a cooled-wall fixed-bed reactor with coolant temperature T_c , tube diameter D , and N_t number of tubes as

$$\frac{d\dot{Q}}{dz} = \pi \cdot D \cdot N_t \cdot U \cdot (T(z) - T_c) \quad (53)$$

The heat transfer coefficient for conduction k_w in the tube and convection from gas and coolant $h_{gas}, h_{coolant}$ inside and outside of the tube needs to be determined to find an accurate overall heat transfer coefficient U . Three thermal resistances are present to determine the overall heat transfer coefficient U is given below,

$$\frac{1}{U} = \frac{1}{h_{gas}} + \frac{r_1}{k_w} \cdot \ln\left(\frac{r_2}{r_1}\right) + \frac{r_1}{r_2 h_{coolant}} [W^{-1}m^2K^{-1}] \quad (54)$$

The heat transfer coefficient for the gas inside the tube close to the wall is [41],

$$h_{gas} = \frac{Nu\lambda_g}{D_p} [Wm^{-2}K] \quad (55)$$

where Nu is the Nusselt number, λ_g is the gas mixture conductivity, and D_p is the catalyst pore diameter. For our case, the heat transfer at the wall of the reactor is calculated from the overall heat transfer coefficient $k_{w,Dix}$ suggested by Dixon [42]. This equation takes resistance at the inner tube wall, the thermal resistance of the catalyst bed, and resistance at the outer tube wall into consideration.

$$\frac{1}{k_{w,Dix}} = \frac{1}{\alpha_w} + \frac{D}{6 \cdot \lambda_r^{eff}} \cdot \frac{Bi + 3}{Bi + 4} + \frac{1}{\alpha_{coolant}} \quad (56)$$

Here, α_w and λ_r^{eff} refer to the heat transfer coefficient for the inner tube wall and the effective radial thermal conductivity with the assumption a reactor cooled by steam with heat transfer coefficient $\alpha_{coolant}$. Bi refers to the Biot number as defined,

$$Bi = \alpha_w \cdot \frac{D}{2 \cdot \lambda_r^{eff}} \quad (57)$$

The effective radial thermal conductivity can be modeled by considering the presence of two contributions from [43],

$$\lambda_{er} = \lambda_{er}^0 + \lambda_{er}^t \quad (58)$$

The first depends on the flow conditions, and the second is in the absence of flow. λ_{er}^0 is the static term caused by transport through fluid in the void space of the reactor and

the catalyst particles. λ_{er}^t is the dynamic term based on the heat transport in the fluid. For this case, the effective radial thermal conductivity is calculated based on correlations presented by Tsotsas [24],

$$\lambda_r^{eff} = \lambda_{bed} \frac{Pe}{K_r} \cdot \lambda_G \quad (59)$$

Here, λ_{bed} is the thermal conductivity of the fixed-bed reactor without fluid flow, Pe is the particle Peclet number, K_r is a correction factor, and λ_G is the thermal conductivity of the gas mixture. Martin and Nilles suggested an equation based on a correlation for the Nusselt number to calculate the heat transfer coefficient for the inner tube wall α_w [25].

$$Nu_w = \frac{\alpha_w \cdot d}{\lambda_G} = \left(1.3 + \frac{5}{D}\right) \frac{\lambda_{bed}}{\lambda_G} + 0.19 \cdot Re^{0.75} \cdot Pr^{0.33} \quad (60)$$

Here, Re is the Reynolds number, Pr is the Prandtl number calculated for the particle diameter. The following relation can calculate them,

$$Re_p = \frac{\rho_g D_p u_z}{\mu_g} \quad Pr_p = \frac{\mu_g C_{p_g}}{\lambda_g} \quad (61)$$

D.3 Mass Balance Equation

From Hugo A. Jakobsen "Chemical Reactor Modeling" [40] a governing equation using a reduced Eulerian species mass balance,

$$\frac{\partial}{\partial t}(\rho\omega_\alpha) + \frac{\partial}{\partial z}(\rho u_z^\alpha \omega_\alpha) = R_\alpha \quad (62)$$

Equation 62 is valid for a plug flow reactor model for a homogeneous system with dynamic conditions. The first term is mass accumulation for a stationary process and assumed zero. The second term is the transport of heat and mass transfer from convection. The last term is the reaction rate for a gas mixture and can be described by $R_\alpha = R_\alpha M_\alpha \rho_{cat} (1 - \varepsilon) \eta$.

Introducing flux j_α for transport due to molecular diffusion described by Fick's first law $\mathbf{j}_\alpha = -\rho_g D_r \nabla \omega_\alpha$, the governing mass balance equation is,

$$\frac{\partial}{\partial t}(\rho\omega_\alpha) + \frac{\partial}{\partial z}(\rho u_z^\alpha \omega_\alpha) = -\nabla \cdot \mathbf{j}_\alpha + R_\alpha \quad (63)$$

Implementing Fick's first law and reaction terms and removing the mass accumulation term cause of stationary assumption, the mass balance equation becomes,

$$\nabla \cdot (\rho_g u_z \omega_\alpha) = \nabla \cdot (\rho_g D_r \nabla \omega_\alpha) + R_\alpha M_\alpha \rho_{cat} (1 - \varepsilon) \eta \quad (64)$$

Assuming radial and angular convective terms are neglected, the effective dispersion coefficient D_r is constant through the cross-section, angular and axial dispersion is neglected as well, and the above term reduces to,

$$\frac{\partial}{\partial z} (\rho_g u_z \omega_\alpha) = D_r \frac{1}{r} \frac{\partial}{\partial r} \left(r \rho_g \frac{\partial \omega_\alpha}{\partial r} \right) + R_\alpha M_\alpha \rho_{cat} (1 - \varepsilon) \eta \quad (65)$$

The equation can be further reduced for a pseudo-homogeneous reactor model. In the model, the gas and catalyst phases are considered as one pseudo-homogeneous phase neglecting heat and mass transfer resistance between the two phases within the catalyst pellets and taking the catalyst void fraction into account ν . Given these assumptions, the mass and energy balance equations for a one-dimensional methanation reactor along the direction z become:

$$\frac{d\omega_\alpha}{dz} = \frac{M_\alpha \cdot (1 - \varepsilon) \cdot \eta \cdot \rho_{cat}}{\bar{\rho} \cdot u_z} \sum_{\alpha} \nu_\alpha \cdot r \quad (66)$$

D.4 Momentum Balance: Pressure Distribution

For the pseudo-homogeneous reactor used in this thesis, the pressure drop in the methanation reactor was neglected to provide consistent assumptions for the entire process. This was due to considering fine particle size for the catalyst, and early test simulation done by Hashemi [9] showed that the pressure drop in the assumed reactor was between 0.1 kPa and 1 kPa. Further, a brief rundown of the equations on momentum balance to find the pressure profile within a cylindrical reactor. To calculate the pressure change within a fixed-bed reactor, it is assumed that friction is the most dominating factor in the momentum balance. Therefore for plug flow reactor relies on the Ergun equation for flow through porous media to calculate the pressure drop.

$$\frac{dp}{dz} = f \frac{\rho_g u_z^2}{D_p} \quad (67)$$

where f is the friction factor. Sabri Ergun proposed the following pasteurization for the friction factor:

$$f = \frac{1 - \varepsilon}{\varepsilon^3} \left[1.75 + \frac{150(1 - \varepsilon)}{Re_p} \right] \quad (68)$$

The Ergun equation with the friction factor above is often used for the following initial conditions at: $z = 0, \rho_g = \rho_{g,0}, T = T_0, p = p_0$. Inserting the friction factor into the Ergun Equation 68 gives the pressure drop profile over the reactor length.

$$\frac{dp}{dz} = \frac{\rho_g u_z^2}{D_p} \cdot \frac{1 - \varepsilon}{\varepsilon^3} \left[1.75 + \frac{150(1 - \varepsilon)}{Re_p} \right] \quad (69)$$

The purpose of the Ergun equation was to explain the transition zone between laminar flow through a mass of material particles and turbulent flow through the same mass of material particles [44].

D.5 Boundary Conditions

The boundary conditions used for the pseudo-homogeneous reactor model are solved by Neumann and Dirichlet-type boundary conditions. These boundary conditions are provided for the multi-tubular reactor and consist of the inlet ($z = z_0$), center ($r = r_0$), and wall ($r = r_1$) where the parameters for mass fractions ω_α , temperature T , heat flow \dot{Q} , and the superficial velocity u_z are to be solved.

For Mass Fractions ω_α :

$$\omega_\alpha|_{z=z_0} = \omega_{\alpha,in} \quad \text{for } r_0 \leq r \leq r_1$$

For Temperature T :

$$T|_{z=z_0} = T_{in} \quad \text{for } r_0 \leq r \leq r_1$$

For Heat Flow \dot{Q} :

$$\dot{Q}|_{z=z_0} = 0 \quad \text{for } r_0 \leq r \leq r_1$$

For superficial gas velocity u_z :

$$u_z|_{z=z_0} = u_{z,in} \quad \text{for } r_0 \leq r \leq r_1$$

D.6 Reaction Rate

In the multi-tubular methanation model, the reaction rate proposed by Koschany et al. [27] for carbon dioxide methanation was employed.

For this case, a nickel-based catalyst (Ni/Al₂O₃) studied by Koschany et al. [27] is applied. The Langmuir-Hinshelwood-Hougen-Watson (LHHW) describes the reaction kinetics of this catalyst approach for temperatures between 180 °C and 340 °C and pressures between 5 bar and 15 bar. A simple model only considering reactions orders of hydrogen and carbon dioxide is given below:

$$r = k \cdot p_{H_2}^{n_{H_2}} p_{CO_2}^{n_{CO_2}} \left(1 - \frac{p_{CH_4} p_{H_2O}^2}{p_{H_2}^4 p_{CO_2} K_{eq}} \right) \quad (70)$$

Here, k is the reaction rate constant, p refers to the partial pressure of each component, and K_{eq} is the equilibrium constant. For the CO₂ methanation reaction, the reaction rate is described as:

$$r = \frac{k \cdot p_{H_2}^{0.5} \cdot p_{CO_2}^{0.5} \left(1 - \frac{p_{CH_4} p_{H_2O}^2}{p_{H_2}^4 p_{CO_2} K_{eq}} \right)}{\left(1 + K_{OH} \cdot \frac{p_{H_2O}}{p_{H_2}^{0.5}} + K_{H_2} \cdot p_{H_2}^{0.5} + K_{mix} \cdot p_{CO_2}^{0.5} \right)^2} \quad (71)$$

The K_i denote the adsorption constant of the components (i.e $i = H_2, CH_4,$ and CO_2). Using the equation above 71 for operational conditions outside the 180 °C - 340 °temperature range, the rate equation is still valid. Since the reaction rate is limited by chemical equilibrium for tighter temperatures and approaches zero for lower temperatures, the equilibrium constant is calculated based on the species' enthalpies and entropies according to the Shomate equation and data provided by NIST Chemistry WebBook. The values for the reaction rate constant k_i and adsorption constant K_i can be calculated from their parameterized estimation:

$$k = k_{0,ref} \cdot \exp \left(\frac{E_A}{R} \cdot \left(\frac{1}{T_{ref}} - \frac{1}{T} \right) \right) \quad (72)$$

$$K_i = K_{i,0,ref} \cdot \exp \left(\frac{\Delta H_i}{R} \left(\frac{1}{T_{ref}} - \frac{1}{T} \right) \right) \quad (73)$$

Here, E_A is the activation energy, $k_{0,ref}$ and $K_{i,0,ref}$ is the pre-exponential factors, T_{ref} is the reference temperature and ΔH_i is the adsorption enthalpy for component $i = H_2, CO_2, CH_4$ etc.

D.7 Intraparticle Mass Transport Limitations

In the pseudo-homogeneous model, the diffusion and reaction of species are assumed to take place in the bulk phase. In practice, this takes place inside the catalyst. Therefore, the model does not explicitly take the mass transport limitations in the catalyst particles in the calculations. This leads to an unreal representation of the methanation process. The other choice is to model the methanation reactor to a heterogeneous model, but such a model has larger computational efforts and increases the convergence time. To solve this for a pseudo-homogeneous model, the intraparticle mass transport limitations are included. An effectiveness factor η is introduced that associates the pseudo-homogeneous model with a heterogeneous model. The effectiveness factor included in the pseudo-homogeneous model is based on the Thiele modulus ϕ for spherical particles as:

$$\eta = \frac{3}{\phi} \cdot \left[\frac{1}{\tanh\phi} - \frac{1}{\phi} \right], \quad (74)$$

Here, the Thiele modulus ϕ is defined as Equation 75. In the Thiele modulus, it is assumed that the rate of CO₂ is the limiting species because it has the highest overall mass fraction in the gas mixture. Which makes CO₂ the key component in determining the mass diffusion in the catalyst pellets.

$$\phi = \frac{D_p}{2} \sqrt{\frac{r \cdot \rho_{cat} \cdot (1 - \varepsilon) \cdot \bar{R} \cdot T}{D_{CO_2}^{eff} \cdot y_{CO_2} \cdot p \cdot 10^5}}, \quad (75)$$

Here, D_p and y_{CO_2} are the particle diameter and mole fraction of CO₂ in the gas mixture, respectively. $D_{CO_2}^{eff}$ is the effective CO₂ diffusivity and considers gas-gas collisions from the Bosanquet equation $D_{CO_2}^m$ through molecular diffusion, and gas-wall diffusion from Knudsen diffusion $D_{CO_2}^{kn}$. In addition, the effective CO₂ diffusivity takes the characteristics of the particle configurations into account via the particle porosity (ε_p) and particle tortuosity (τ_p) [4].

$$\frac{1}{D_{CO_2}^{eff}} = \frac{\tau_p^2}{\varepsilon} \left(\frac{1}{D_{CO_2}^m} \frac{1}{D_{CO_2}^{kn}} \right) \quad (76)$$

and the Knudsen diffusion independent of the other species is defined as,

$$D_{CO_2}^{kn} = \frac{D_{pore}}{3} \sqrt{\frac{8 \cdot \bar{R} \cdot T}{\pi \cdot M_{CO_2}}} \quad (77)$$

Here, D_{pore} and M_{CO_2} are the average pore diameter and the molar fraction of CO_2 in the gas mixture. The molecular diffusion of CO_2 , which is dependent on the other gas species, is calculated based on the mixed-averaged diffusion coefficient proposed by Maxwell-Stefan [26]:

$$\frac{1}{D_{CO_2}^m} = \sum_i \frac{y_i}{D_{ij}} + \frac{y_j}{1 - w_j} \sum \frac{w_i}{D_{ij}} \quad (78)$$

Here, $i = CH_4, H_2, \text{ and } H_2O$ and $j = CO_2$, respectively. y and w refer to the mole and mass fractions of the components. D_{ij} are the binary diffusion coefficient calculated by the equation from Fuller et al. [45].

$$D_{ij} = \frac{0.00143 \cdot T^{1.75} \cdot \left(\frac{1}{w_i} + \frac{1}{w_j}\right)^{\frac{1}{2}}}{p \cdot \left((\theta_i)^{\frac{1}{3}} + (\theta_j)^{\frac{1}{3}}\right)^2} \quad (79)$$

Here, θ_i and θ_j is the specific diffusion volume of component $i = CH_4, H_2, \text{ and } H_2O$, $j = CO_2$.

θ_i	-
CH ₄	24.42
H ₂	7.07
H ₂ O	12.7
θ_j	-
CO ₂	26.9

Table 27: Diffusion Volumes of simple molecules [45]

E Cost Analysis: Calculations and Sizing

In this section of the appendix, the cost estimate calculation performed for each individual component is covered. The costing and sizing are done for the methanation reactor, Heat exchangers, compressors, knock-out vessels, pumps, absorption column, and stripper column. The variable cost for production will also be covered. A detailed overview of the cost calculations for each individual component in the four cases is presented in Appendix F.

E.1 Heat Exchangers

The estimated equipment cost for the Heat exchangers (HX) is determined from the equation 30 by Sinnott and Towler, using area m^2 as unit size. The area of the individual heat exchangers can be found using Equation 80.

$$A = \frac{Q}{U\Delta T_{LM}} \quad (80)$$

Here, the Q is the heat duty, ΔT_{LM} is the log mean temperature difference, and U is the heat transfer coefficient. The duty Q and the log mean temperature difference was extracted from HYSYS simulations for each heat exchanger, but the log mean temperature difference ΔT_{LM} is calculated by the equation 81.

$$\Delta T_{LM} = \frac{\Delta T_1 - \Delta T_2}{\ln(\Delta T_1/\Delta T_2)} \quad (81)$$

$$\Delta T_1 = T_{hot,out} - T_{cold,in}$$

$$\Delta T_2 = T_{hot,in} - T_{cold,out}$$

The heat transfer coefficient U for the coolers (cooling water), the lean rich-heat exchanger, the condenser, and the reboiler was set to $0.2777 \text{ kW/m}^2 \cdot \text{K}$, $1.005 \text{ kW/m}^2 \cdot \text{K}$, $0.3202 \text{ kW/m}^2 \cdot \text{K}$, and $1.3603 \text{ kW/m}^2 \cdot \text{K}$, respectively [34].

The factors a , b , and n used in the cost Equation 30 are presented in Table 28. It was assumed that the cooling water heat exchangers and condenser were made from carbon steel (CS) and was fixed tube heat exchanger. The Rich lean Heat exchanger was a stainless steel (SS) fixed tube heat exchanger. The reboiler was assumed to be a SS Kettle reboiler. To simplify the methanation reactor's cost estimate, it was considered it could be

calculated floating head shell and tube HX. The cost factors used for the individual units are shown in Table 28. The units used in heat exchanger cost calculation are extracted from the HYSYS simulations.

Table 28: Heat exchanger cost factors and characteristics

Equipment	Characteristic	a	b	n	S [unit]
Cooling water HX	CS Fixed tube HX	10 000	88	1.0	area, m ²
Rich Lean HX	SS Fixed tube HX	10 000	88	1.0	m ²
Condenser HX	CS Fixed tube HX	10 000	88	1.0	m ²
Reboiler HX	SS Kettle Reboiler	14 000	850	1.0	m ²
Liquefaction HX	Plate and frame SS	1 100	850	0.4	m ²
Methanation	Floating head shell tube HX	11 000	115	1.0	m ²

The total cost estimate, installed cost, and Fixed capital cost for all heat exchangers are shown in Table 29. The individual heat exchanger calculation and its values are shown in the Excel spreadsheet in Appendix F.

Table 29: Cost estimate and Installation cost for the heat exchangers in MUSD

Cost results for heat exchangers in MUSD			
Case ratio	Equipment	C_e	C
3.0	Cooling Water HX	0.32	1.02
	Rich Lean HX	0.02	0.06
	Condenser HX	0.021	0.07
	Reboiler HX	0.028	0.08
	Liquefaction HX	0.01	0.03
	Methanation HX	0.151	0.43
	Heater & Cooler	0.035	0.11
3.2	Cooling Water HX	0.31	1.01
	Rich Lean HX	0.022	0.06
	Condenser HX	0.023	0.07
	Reboiler HX	0.027	0.08
	Liquefaction HX	0.011	0.03
	Methanation HX	0.17	0.49
	Heater & Cooler	0.035	0.11
3.5	Cooling Water HX	0.32	1.02
	Rich Lean HX	0.018	0.05
	Condenser HX	0.018	0.06
	Reboiler HX	0.027	0.08
	Liquefaction HX	0.011	0.03
	Methanation HX	0.17	0.49
	Heater & Cooler	0.35	0.11
3.8	Cooling Water HX	0.31	1.00
	Rich Lean HX	0.019	0.05
	Condenser HX	0.018	0.06
	Reboiler HX	0.024	0.07
	Liquefaction HX	0.011	0.04
	Methanation HX	0.19	0.54
	Heater & Cooler	0.035	0.11

E.2 Compressors and Pump

The compressors used in the process model was all modeled to be CS (Carbon Steel) centrifugal compressor. The pump was assumed as a CS centrifugal compressor. The equipment cost estimation for the compressors and the pump is calculated from [28] and is based on the driver power in kW as unit size. The cost factors for the compressors and the pump is shown in Table 30 and are valid for compressors and pumps between 132-29000 kW. The driver power in kW is extracted from the HYSYS simulations.

Table 30: Compressors and Pump cost factors, characteristics, and calculated cost

Equipment	Characteristic	a	b	n	S [unit]
Compressor	CS centrifugal	8400	3100	0.6	driver power, kW
Pump	CS Centrifugal	8400	3100	06.	driver power kW

Calculated cost			
Equipment	Case	Equipment cost C_e	Installation cost C
Compressor	3.0	2.15	6.88
	3.2	2.15	6.87
	3.5	2.19	6.99
	3.8	2.20	7.06
Pump	3.0	0.016	0.05
	3.2	0.014	0.04
	3.5	0.013	0.04
	3.8	0.009	0.03

E.3 Knock-Out Vessel

The knock-out vessels were modeled to remove water, and the cost estimation is based on the shell mass of a pressurized vertical vessel described by [28]. The shell mass can be calculated by Equation 82.

$$m_s = \pi \cdot D_v \cdot H_v \cdot t_w \cdot \rho_s \quad (82)$$

here, m_s , D_v , H_v , t_w , and ρ_s are the vessel's mass, vessel diameter, vessel height, vessel thickness, and density of stainless steel, respectively. Stainless steel has a density of 8000 kg/m³. The minimum vessel diameter can be calculated from equation 83.

$$D_v = \sqrt{\frac{4\dot{V}_g}{\pi u_s}} \quad (83)$$

here, \dot{V}_g is the gas volumetric flow rate, u_s is the settling velocity for the given gas stream. The settling velocity considers the velocity of fluid droplets to be settled out from the gas mixture. To calculate the settling velocity, the settling velocity for a vertical separator without a demister pad (u_t) must be calculated.

$$u_t = 0.07 \cdot \left(\frac{\rho_l - \rho_g}{\rho_g} \right)^{0.5} \quad (84)$$

$$u_s = 0.15 \cdot u_t \quad (85)$$

where ρ_l and ρ_g are the liquid and gas density of the stream. The vessel's height is calculated for the vessel diameter from equation 86.

$$H_v = D_v + \frac{D_v}{2} + H_L + 0.4 \quad (86)$$

where \dot{V}_l is the liquid volumetric flow rate, H_L is the required height of the liquid in the vessel, and should be a minimum of 2 meters. H_L can be calculated by equation.

$$H_L = \frac{4 \cdot D_v}{\pi D_v^2} \cdot t_h \quad (87)$$

Here, t_h is the hold-up time of 10 minutes assumed to provide smooth operation and flow control. Further, the minimum vessel thickness needs to be calculated using the specified equation by ASME code:

$$t_w = \frac{p_d D_v}{2S \cdot E + 1.2 \cdot p_d} \quad (88)$$

here, p_d is the design pressure set 10% above the vessel pressure, S is the maximum allowable stress ($S = 1034$ har for SS 304), and E is the weld efficiency ($E = 1$).

The knock-out vessels were assumed to be modeled as pressurized vertical vessels, and the cost estimate factors are shown in Table 31. The individual calculations for the shell mass, vessel diameter, settling velocity, and vessel height can be seen in the Excel spreadsheet in Appendix F.

Table 31: Knock-out vessel cost factors and characteristics

Equipment	Characteristic	a	b	n	S [unit]
Separator 1	Pressurized vertical vessel	15000	68	0.85	shell mass, kg
Separator 2	Pressurized vertical vessel	15000	68	0.85	shell mass, kg
Separator 3	Pressurized vertical vessel	15000	68	0.85	shell mass, kg
WR	Pressurized vertical vessel	15000	68	0.85	shell mass, kg

Calculated cost			
Equipment	Case	Equipment cost C_e	Installation cost C
Separator 1	3.0	0.049	0.14
	3.2	0.047	0.13
	3.5	0.049	0.14
	3.8	0.048	0.14
Separator 2	3.0	0.066	0.19
	3.2	0.066	0.19
	3.5	0.065	0.19
	3.8	0.064	0.18
Separator 3	3.0	0.026	0.08
	3.2	0.027	0.08
	3.5	0.027	0.08
	3.8	0.027	0.08
WR	3.0	0.025	0.07
	3.2	7.8	22.44
	3.5	3.14	9.03
	3.8	2.4	6.82

E.4 Absorber and Stripper

The absorber and stripper estimated cost is calculated using the cost relation from Turton et al. [29]. The absorber and stripper are assumed to be a Vertical Pressure Vessel from SS, with ceramic packing and valve trays. The cost estimate factors used are shown in Table 32 with the calculated cost estimate for the absorber and stripper. The size unit is extracted from the HYSYS simulations.

Table 32: Absorber and Stripper cost factors and characteristics [9]

Columns						
Equipment	Characteristic	K1	K2	K3	Size [unit]	Range
Absorber	SS Vertical	3.4974	0.4485	0.1074	m^3	0.3-520
Stripper	SS Vertical	3.4974	0.4485	0.1074	m^3	0.3-520
Packing						
Equipment	Characteristic	K1	K2	K3	Size [unit]	Range
Absorber	Ceramic, Valve	3.3322	0.4838	0.3434	m^2	0.7-10.5
Stripper	Ceramic, Valve	3.3322	0.4838	0.3434	m^2	0.7-10.5
Cost estimate MUSD						
Equipment		Case		Ce	C	
Absorber		3.0		0.09	0.26	
		3.2		0.089	0.26	
		3.5		0.089	0.26	
		3.8		0.089	0.26	
Stripper		3.0		0.083	0.24	
		3.2		0.082	0.24	
		3.5		0.082	0.24	
		3.8		0.082	0.24	

E.5 Expander and Expansion Valves

The expander and expansion valve purchased cost estimates used the relation from Turton et al. [29]. It is assumed as a SS 304 Liquid expander, and the cost estimate factors and the calculated cost are shown in Table 33. The size units are extracted from the HYSYS simulations.

Equipment	Characteristic	K_1	K_2	K_3	Size [unit]	range
Expander	SS Liquid expander	2.2476	1.4965	-0.1618	kW	100-1500
Valves	SS Liquid expander	2.2476	1.4965	-0.1618	kW	100-1500

Cost estimate MUSD			
Equipment	Case	Ce	C
Expander	3.0	0.32	0.92
	3.2	0.32	0.92
	3.5	0.32	0.92
	3.8	0.32	0.92
Expansion valves	3.0	0.15	0.43
	3.2	0.12	0.36
	3.5	0.11	0.32
	3.8	0.059	0.17

Table 33: Expander and expansion valve cost factors and characteristics [9]

E.6 Variable Cost of Production

The variable cost of production included costs for the utilities: cooling water, steam, electricity, Hydrogen, catalyst, and absorbent. In this subsection, the calculations for the utilities will be covered.

The required cooling water for each case was calculated by Equation 89.

$$\text{Cooling water cost} = 0.354 \cdot HX \text{ duty} \cdot \text{Operating hours} \quad (89)$$

Operating hours are assumed to be 8000 Hours annually for the processing facility. 0.354 is the Cooling water cost in USD/GJ.

The cost calculations for Steam, MDEA, and H₂ in the process were calculated using the mass flow (kg/s) and calculated by Equation 90.

$$Utility\ Cost = Cost\ factor \cdot mass\ flow \cdot Operating\ hours \cdot sec/h \quad (90)$$

The amount of catalyst needed in the reactors is calculated from the volume inside the tubes. This is calculated by first finding the inner volume of the tubes with Equation 91.

$$V_{tubes,i} = \frac{\pi}{4} D_i^2 \cdot L \cdot N \quad (91)$$

and then using Equation 92 to find the catalyst volume.

$$V_{catalyst,tot} = V_{tubes,i}(1 - \varepsilon) \quad (92)$$

The electricity cost is calculated from the power requirement from the compressors and heat exchangers duty in kW. The variable cost of production for each case is shown in Tables 34,35, 36, 37.

Variable Cost of Production for case 3.0			
Utility	Value [Unit]	Cost MUSD	COST MNOK
Cooling water	0.354 [USD/GJ]	0.058	0.56
Steam 5 Bar	0.0277 [USD/kg]	0.31	2.97
Steam at 40 Bar	0.0299 [USD/kg]	1.18	11.35
Electricity	44.45 USD/MWh	5.53	53.23
MDEA	2.6 [USD/kg]	0.00033	0.0032
Catalyst	15539 [USD/m ³ catalyst]	0.026	0.25
Green H ₂	4.8 [USD/kg H ₂]	18.58	178.8
Total Cost		25.7	247.2

Table 34: Variable cost of production for case 3.0

Variable Cost of Production for case 3.2			
Utility	Value [Unit]	Cost MUSD	COST MNOK
Cooling water	0.354 [USD/GJ]	0.055	0.53
Steam 5 Bar	0.0277 [USD/kg]	0.23	2.22
Steam at 40 Bar	0.0299 [USD/kg]	1.24	11.95
Electricity	44.45 USD/MWh	5.49	52.79
MDEA	2.6 [USD/kg]	0.000018	0.0018
Catalyst	15539 [USD/m ³ catalyst]	0.03	0.29
Green H ₂	4.8 [USD/kg H ₂]	19.82	190.8
Total Cost		26.9	258.6

Table 35: Variable cost of production for case 3.2

Variable Cost of Production for case 3.5			
Utility	Value [Unit]	Cost MUSD	COST MNOK
Cooling water	0.354 [USD/GJ]	0.059	0.57
Steam 5 Bar	0.0277 [USD/kg]	0.25	2.36
Steam at 40 Bar	0.0299 [USD/kg]	1.4	13.45
Electricity	44.45 USD/MWh	5.65	54.36
MDEA	2.6 [USD/kg]	0.00018	0.0017
Catalyst	15539 [USD/m ³ catalyst]	0.03	0.29
Green H ₂	4.8 [USD/kg H ₂]	21.68	208.62
Total Cost		29.1	279.6

Table 36: Variable cost of production for case 3.5

Variable Cost of Production for case 3.8			
Utility	Value [Unit]	Cost MUSD	COST MNOK
Cooling water	0.354 [USD/GJ]	0.055	0.53
Steam 5 Bar	0.0277 [USD/kg]	0.07	0.72
Steam at 40 Bar	0.0299 [USD/kg]	1.53	14.72
Electricity	44.45 USD/MWh	5.48	52.79
MDEA	2.6 [USD/kg]	0.0003	0.0028
Catalyst	15539 [USD/m ³ catalyst]	0.035	0.33
Green H ₂	4.8 [USD/kg H ₂]	23.53	226.45
Total Cost		30.7	295.5

Table 37: Variable cost of production for case 3.8

F Cost analysis calculation Excel sheet

In this section, the cost estimation Excel sheet is presented for the four cases. These Excel sheets were used to calculate the Cost estimation of the equipment, installation cost, Fixed capital cost, variable cost of production, fixed cost of production, and the Revenue and production cost per unit.

Purchased cost estimate Case 3.0

Centrifugal Compressor CS		Cost estimate								Installed Cost Factors		factor	
Comp #	Unit for S duty, kW	Cost C_e USD	a	b	n	Inflation		Installed Cost C USD	MUSD				
Comp 1	438.6	214132	8400	3100	0.6	1.68		685223		Equipment erection	f_er	0.3	
comp 2	464.3	221085	8400	3100	0.6	1.68		707473		Piping	f_P	0.8	
comp 3	435.5	213283	8400	3100	0.6	1.68		682505		Instrumentation	f_i	0.3	
comp4	277.3	166022	8400	3100	0.6	1.68		531269		electrical	f_el	0.2	
comp 5	608.2	257484	8400	3100	0.6	1.68		823949		civil	f_c	0.3	
comp 6	655.4	268648	8400	3100	0.6	1.68		859673		structures	f_s	0.2	
comp 7	656.7	268951	8400	3100	0.6	1.68		860642		lagging and pain	f_l	0.1	
comp 8	659.7	269648	8400	3100	0.6	1.68		862875		Offsite(OS)	OS	0.3	
comp 9	667.1	271365	8400	3100	0.6	1.68		868367		D&E	D&E	0.3	
Total	4862.8	2150617						6881975	6.88	Contingency X	X	0.1	
										Material	f_m	1 1.3	

CS SS

Pump CS Centrifugal	Unit: duty kW	log(C_e)	Cost C_e	K1	K2	K3	Inflation	Installed Cost C USD	MUSD
Pump CS Centrifugal	45.11	3.898760962	16123	3.3892	0.0536	0.1538	2.04	46383.29	0.05

Heat Exchangers	Unit for S , area m^2	Cost C_e	a	b	n	Inflation	duty kW	Installed Cost C USD	MUSD	Heat exchanger duty kj/h
CW1	56.41	25094	10000	88	1	1.68	449.5	80302	0.08	1618000
CW2	57.34	25232	10000	88	1	1.68	467.5	80741	0.08	1683000
CW3	40.07	22683	10000	88	1	1.68	502	72586	0.07	1807000
CW4	37.04	22236	10000	88	1	1.68	339.3	71155	0.07	1211000
CW5	75.61	27928	10000	88	1	1.68	651.9	89369	0.09	2347000
CW6	14.08	18848	10000	88	1	1.68	41.95	60312	0.06	151000
CW7	90.86	30178	10000	88	1	1.68	380.2	96571	0.10	1369000
CW8	127.3	35556	10000	88	1	1.68	679.2	113779	0.11	2445000
CW9	129.9	35940	10000	88	1	1.68	694.4	115007	0.12	2500000
CW10	134.1	36559	10000	88	1	1.68	717.6	116990	0.12	2583000
CW11	140.1	37445	10000	88	1	1.68	749.9	119823	0.12	2700000
Total CW:		317698						1016634	1.02	20414000
Heater1	7.277	17844	10000	88	1	1.68	276.8	57100	0.06	
coolint		16770	10000	88	1	1.68	15.66	53663	0.05	56380
Rich lean HX SS Fixed tube	23.67	20263	10000	88	1	1.68	382.5	58295	0.06	
Condenser CS Fixed tube	29.77	21163	10000	88	1	1.68	143.2	67722	0.07	
Reboiler SS Kettle reboiler	33.24	28104	14000	83	1	1.68	818.9	80854	0.08	
Methanation 1 SS Floating head S&T	394.8	94585	11000	115	1	1.68	2669	272113	0.27	
Methanation 2 SS Floating head S&T	197.5	56535	11000	115	1	1.68	24.18	162647	0.16	
Total Methanation		151120						434760	0.43	
LNG Heat exchanger plate HX	102.3	10921	1100	850	0.4	1.68	670.4	31418	0.03	
Total:		0.58					10674	1365685	1.37	

Columns										
Absorber	unit m^3	log(C_e)	Cost C_e	K1	K2	K3	Inflation	Installed Cost C USD	MUSD	
Pressure Vessel Vertical 304 SS	53.01	4.59	79217	3.4974	0.4485	0.1074	2.04	259111		
Packing Ceramic valve trays	3.89	3.73	10848	3.322	0.4838	0.3434	2.04			
Total:			90065	0.09					0.26	
Stripper										
Pressure Vessel Vertical 304 SS	46.65	4.55	71398	3.4974	0.4485	0.1074	2.04	239426		
Packing Ceramic valve trays	4.28	3.76	11825	3.322	0.4838	0.3434	2.04			
Total:			83223	0.08					0.24	
Expansion Valve + Expander	unit kW	log(C_e)	cost C_e	K1	K2	K3	Inflation	Installed Cost C USD	MUSD	
Expander	696.4	5.19	318396	2.2476	1.4965	-0.1618	2.04	1346831	1.35	
Expansion valve 1	202.7	4.84	140426	2.2476	1.4965	-0.1618	2.04			
Expansion Valve 2	11.69	3.66	9328	2.2476	1.4965	-0.1618	2.04			
Total:			468150	0.47				1346831	1.35	

Knock out vessels (Pressure vessel 304 SS)	Unit S: shell mass, kg,	Cost C_e	a/K1	b/K2	n/K3	Inflation	Installed Cost C USD	MUSD
WR Water	0	25154.6	15000	68	0.85	1.68	72368	
separator 1	544.7	49296.4	15000	68	0.85	1.68	141822	
separator 2	1021	66336.6	15000	68	0.85	1.68	190845	
Separator 3	19.56	26582.5	15000	68	0.85	1.68	76476	
Total:		167370.1	0.17				481511	0.48

Utilities	Unit	Cost factor	Utility	Unit	Annual cost MUSD	Annual cost MNOK			
Cooling water @ 20 C	USD/GJ	0.354	20.47	GJ/h	0.058	0.56	1 USD in 2022 =	9.6245	NOK
Steam @ 5 Bar	USD/KG	0.0277	0.39	kg/s	0.31	2.97	Operating hours	8000	hours annually
Steam @ 40 Bar	USD/KG	0.0299	1.37	kg/s	1.18	11.35		3600	sec/h
MDEA	USD/Kg	2.6	0.000004465	kg/s	0.00033	0.00322	Tube volume 1	2.028	m3
Catalyst	USD/m^3 catalyst	15539			0.026	0.25	Tube volume 2	1.014	m3
Green H2	USD/kg H2	4.8	0.1344	kg/s	18.58	178.82	Catalyst V1	1.115	m3
Electricity Nordpol 2022 MNOK/MWh	NOK/MWh	427.83	15.582	MW		53.33	Catalyst V2	0.5579	m3
Electricity Nordpol 2022 MUSD/MWh	USD/MWh	44.45		MW	5.54		Total catalyst V	1.6729	m3
Total cost:					25.7	247.3			

Shell mass calculations	separator 1	Separator 2	Separator 3	WR				
Gas volumetric flowrate V_g (m3/h)	243.7	54.72	14.68	431		rho SS	8000	
gas density rho_g (kg/m3)	15.15	68.93	1.755	8.785		holdup time	10	
liquid density rho_l (kg/m3)	996.5	999.1	423.1	8.738		S bar allowable	1034	
Liquid volumetric flowrate (m3/h)	0.009318	0.005491	6.72	245.3		E weld efficiency	1	
Pressure seperator P (bar)	20	80	1.013	20				
u_t	0.56	0.2571	1.085					
u_s	0.08450744	0.03857	0.1627					
Vessel Diameter D_V	1.016	0.7083	0.1786					
H_L	0.001916	2.322	44.69					
Vessel Height H_V	1.926	1.465	45.36					
H_V set	2	2	45.36					
P_d bar	22	88	1.115					
t_w	0.01067	0.02867	0.00009619					
shell mass m_s	544.7	1021	19.56					
	Diameter	Column height	tray number	tray space	tray volume	hold up volume	Volume column	Total volume
Absorber	3	7.5	15	0.5	3.534	0.3534	53.01437603	56.90177603
Stripper	3	6.6	12	0.55	3.888	0.3888	46.65265091	50.92945091

Fixed Cost of Production	Estimate	Cost MUSD	Cost MNOK		
1)Operation labor	5 operator per shift	1.02	9.8	Operator labor cost calculation	
2)Supervision	25% of 1	0.26	2.5	S_OP	50000 \$
3)Direct salary overhead	60% of 1 + 2	0.77	7.4	t shift	1000 shift/year
4)Maintenance	5% of ISBL	0.53	5.1	L_s	5 operators/shift
5)Property tax & insurance	2% of ISBL	0.21	2.0	L_Y,OP	245
6)General plant overhead	65% of (1+2+3+4)	1.86	17.9	LC	1020408
Total		4.64	44.7		

Fixed Capital Cost	Value
Installation Cost [C] MUSD	11.06
Offsite OSBL = 0.3 of ISBL	3.32
Design and Engineering 0.3 ISBL + OSBL	6.63
Contingency X = 0.1 ISBL + OSBL	4.42
Total Fixed capital cost: C_FC	25.43

Produced liq biomethane LBM	2843.64	KG/h	Interest rate %	0.06
Produced LBM yearly	22749120.0	kg	lifetime n	20
Std Gas flow	4191	m3/h		
Std Gas flow annualu	33528000	Sm3		
LNG price per Sm3	0.17	USD/Sm3		
Total revenue LBM from gas flow	5.7	MUSD/Sm3		
ACCR	0.087			
Total Annualized cost	32.55	MUSD		
Production cost per unit Sm3	0.971	USD/Sm3		
Production cost per unit kg	1.43	USD/kg		

Purchased cost estimate Case 3.2

Centrifugal Compressor CS		Cost estimate						Installed Cost C USD		MUSD		Installed Cost Factors		factor		
Comp #	Unit for S duty, kW	Cost C_e USD	a	b	n	Inflation										
Comp 1	405.8	205017	8400	3100	0.6	1.68			656055			Equipment erection	f_er	0.3		
comp 2	429.6	211659	8400	3100	0.6	1.68			677309			Piping	f_P	0.8		
comp 3	402.9	204197	8400	3100	0.6	1.68			653431			Instrumentation	f_i	0.3		
comp4	349.4	188621	8400	3100	0.6	1.68			603588			electrical	f_el	0.2		
comp 5	610.7	258084	8400	3100	0.6	1.68			825868			civil	f_c	0.3		
comp 6	655.4	268648	8400	3100	0.6	1.68			859673			structures	f_s	0.2		
comp 7	656.7	268951	8400	3100	0.6	1.68			860642			lagging and pain	f_l	0.1		
comp 8	659.7	269648	8400	3100	0.6	1.68			862875			Offsite(OS)	OS	0.3		
comp 9	667.1	271365	8400	3100	0.6	1.68			868367			D&E	D&E	0.3		
Total	4837.3	2146190							6867808	6.87		Contingency X	X	0.1		
												Material	f_m	1	1.3	

CS SS

Pump CS Centrifugal	Unit: duty kW	log(C_e)	Cost C_e	K1	K2	K3	Inflation	Installed Cost C USD	MUSD
Pump CS Centrifugal	34.56	3.835744317	13945	3.3892	0.0536	0.1538	2.04	40118.52	0.04

Heat Exchangers	Unit for S , area m^2	Cost C_e	a	b	n	Inflation	duty kW	Installed Cost C USD	MUSD	Heat exchanger duty kj/h
CW1	55.97	25029	10000	88	1	1.68	416.5	80094	0.08	1499000
CW2	56.82	25155	10000	88	1	1.68	432	80496	0.08	1555000
CW3	40.76	22785	10000	88	1	1.68	510.7	72912	0.07	1838000
CW4	39.63	22618	10000	88	1	1.68	416.5	72378	0.07	1499000
CW5	50.8	24266	10000	88	1	1.68	365.7	77653	0.08	1317000
CW6	13.09	18701	10000	88	1	1.68	36.25	59845	0.06	130500
CW7	92.58	30432	10000	88	1	1.68	395.7	97383	0.10	1425000
CW8	127.3	35556	10000	88	1	1.68	679.2	113779	0.11	2445000
CW9	129.9	35940	10000	88	1	1.68	694.4	115007	0.12	2500000
CW10	134.1	36559	10000	88	1	1.68	717.6	116990	0.12	2583000
CW11	140.1	37445	10000	88	1	1.68	749.9	119823	0.12	2700000
Total CW:		314487						1006359	1.01	19491500
Heater1	8.23	17984	10000	88	1	1.68	331.6	57550	0.06	
coolint		16770	10000	88	1	1.68	23.51	53663	0.05	84640
Rich lean HX SS Fixed tube	34.09	21801	10000	88	1	1.68	387.2	62718	0.06	
Condenser CS Fixed tube	43.77	23229	10000	88	1	1.68	221.7	74333	0.07	
Reboiler SS Kettle reboiler	21.94	26531	14000	83	1	1.68	612.6	76329	0.08	
Methanation 1 SS Floating head S&T	493.4	113600	11000	115	1	1.68	2830	326818	0.33	
Methanation 2 SS Floating head S&T	197.5	56535	11000	115	1	1.68	47.49	162647	0.16	
Total Methanation		170135						489465	0.49	
LNG Heat exchanger plate HX	103.6	10967	1100	850	0.4	1.68	683.6	31550	0.03	
Total:		0.60					10552	1362502	1.36	

Columns										
Absorber	unit m^3	log(C_e)	Cost C_e	K1	K2	K3	Inflation	Installed Cost C USD	MUSD	
Pressure Vessel Vertical 304 SS	53.01	4.59	79217	3.4974	0.4485	0.1074	2.04	256615		
Packing Ceramic valve trays	3.53	3.69	9980	3.322	0.4838	0.3434	2.04			
Total:			89198	0.09						0.26
Stripper										
Pressure Vessel Vertical 304 SS	46.65	4.55	71398	3.4974	0.4485	0.1074	2.04	236621		
Packing Ceramic valve trays	3.89	3.73	10849	3.322	0.4838	0.3434	2.04			
Total:			82248							0.24
Expansion Valve + Expander	unit kW	log(C_e)	cost C_e	K1	K2	K3	Inflation	Installed Cost C USD	MUSD	
Expander	696.4	5.19	318396	2.2476	1.4965	-0.1618	2.04	1271898	1.27	
Expansion valve 1	154.7	4.75	114077	2.2476	1.4965	-0.1618	2.04			
Expansion Valve 2	12.02	3.67	9631	2.2476	1.4965	-0.1618	2.04			
Total:			442104					1271898	1.27	

Knock out vessels (Pressure vessel 304 SS	Unit S: shell mass, kg,	Cost C_e	a/K1	b/K2	n/K3	Inflation	Installed Cost C USD	MUSD
WR Water	486000	7799721.5	15000	68	0.85	1.68	22439199	
separator 1	475.4	46659.4	15000	68	0.85	1.68	134236	
separator 2	1007	65856.1	15000	68	0.85	1.68	189463	
Separator 3	20.22	26623.4	15000	68	0.85	1.68	76593	
Total:		7938860.4					22839491	22.84

Utilities	Unit	Cost factor	Utility	Unit	Annual cost MUSD	Annual cost MNOK		
Cooling water @ 20 C	USD/GJ	0.354	19.58	GJ/h	0.055	0.53	1 USD in 2022 =	9.6245 NOK
Steam @ 5 Bar	USD/KG	0.0277	0.2896	kg/s	0.23	2.22	Operating hours	8000 h/year
Steam @ 40 Bar	USD/KG	0.0299	1.442	kg/s	1.24	11.95		3600 sec/h
MDEA	USD/kg	2.6	0.00002467	kg/s	0.00018473	0.00178	Tube volume 1	2.535 m3
Catalyst	USD/m^3 catalyst	15539			0.030	0.29	Tube volume 2	1.014 m3
Green H2	USD/kg H2	4.8	0.1434	kg/s	19.82	190.79	Catalyst V1	1.394 m3
Electricity Nordpol 2022 MNOK/MWh	NOK/MWh	427.83	15.42401	MW		52.79	Catalyst V2	0.5579 m3
Electricity Nordpol 2022 MUSD/MWh	USD/MWh	44.45		MW	5.49		Total catalyst V	1.9519 m3
Total cost:					26.9	258.6		

Shell mass calculations	separator 1	Separator 2	Separator 3	WR				
Gas volumetric flowrate V_g (m3/h)	328.4	54.96	26.52	580.5				
gas density rho_g (kg/m3)	11.17	66.6	1.755	6.361		rho SS	8000	
liquid density rho_l (kg/m3)	996.3	999.1	423.1	6.497		holdup time	10	
Liquid volumetric flowrate (m3/h)	0.0242	0.008051	6.832	349.3		S bar allowable	1034	
Pressure separator P (bar)	15	80	1.013	15		E weld efficiency	1	
u_t	0.66	0.2619	1.085	0.01023				
u_s	0.09861	0.039285	0.1627	0.001535				
Vessel Diameter D_V	1.085	0.7034	0.2401	11.56				
H_L	0.004359	0.003453	25.15	0.5543				
Vessel Height H_V	2.032	1.459	25.91	18.3				
H_V set	2.032	2	25.91	18.3				
P_d bar 10% higher than P	16.5	88	1.115	16.5				
t_w	0.008576	0.02847	0.0001293	0.09137				
shell mass m_s	475.4	1007	20.22	486000				
	Diameter	Column height	tray number	tray space	tray volume	hold up volume	Volume column	Total volume
Absorber	3	7.5	15	0.5	3.534	0.3534	53.01437603	56.90177603
Stripper	3	6.6	12	0.55	3.888	0.3888	46.65265091	50.92945091

Fixed Cost of Production	Estimate	Cost MUSD	Cost MNOK		
1)Operation labor	5 operator per shift	1.02	9.8	Operator labor cost calculation	
2)Supervision	25% of 1	0.26	2.5	S_OP	50000 \$
3)Direct salary overhead	60% of 1 + 2	0.77	7.4	t shift	1000 shift/year
4)Maintenance	5% of ISBL	1.64	15.8	L_s	5 operators/shift
5)Property tax & insurance	2% of ISBL	0.66	6.3	L_Y,OP	245
6)General plant overhead	65% of (1+2+3+4)	2.97	28.6	LC	1020408
Total		7.31	70.4		

Fixed Capital Cost	Value
Installation Cost [C] MUSD	33.36
Offsite OSBL = 0.3 of ISBL	10.01
Design and Engineering 0.3 ISBL + OSBL	20.02
Contingency X = 0.1 ISBL + OSBL	13.35
Total Fixed capital cost: C_FC	76.74

Produced liq biomethane LBM	2891.16	KG/h	Interest rate %	0.06
Produced LBM yearly	23129280	kg	lifetime n	20
Std Gas flow	4261	m3/h		
Std Gas flow annualu	34088000	Sm3		
LNG price per Sm3	0.17	USD/Sm3		
Total revenue LBM from gas flow	5.8	MUSD/Sm3		
ACCR	0.087			
Total Annualized cost	40.87	MUSD		
Production cost per unit Sm3	1.20	USD/Sm3		
Production cost per unit kg	1.77	USD/kg		

Purchased cost estimate Case 3.5

Centrifugal Compressor CS		Cost estimate								Installed Cost Factors		
Comp #	Unit for S duty, kW	Cost C_e USD	a	b	n	Inflation	Installed Cost C USD	MUSD	Equipment erection	factor		
Comp 1	478.9	224966	8400	3100	0.6	1.68	719893		f_er	0.3		
comp 2	507.3	232383	8400	3100	0.6	1.68	743626		f_P	0.8		
comp 3	476.1	224226	8400	3100	0.6	1.68	717522		f_i	0.3		
comp4	278.1	166285	8400	3100	0.6	1.68	532110		f_el	0.2		
comp 5	614.9	259089	8400	3100	0.6	1.68	829086		f_c	0.3		
comp 6	655.4	268648	8400	3100	0.6	1.68	859673		f_s	0.2		
comp 7	656.7	268951	8400	3100	0.6	1.68	860642		f_l	0.1		
comp 8	659.7	269648	8400	3100	0.6	1.68	860642		OS	0.3		
comp 9	667.1	271365	8400	3100	0.6	1.68	862875		D&E	0.3		
Total	4994.2	2185560					6993794	6.99	Contingency X	X	0.1	
									Material	f_m	1	
											1.3	

CS SS

Pump CS Centrifugal	Unit: duty kW	log(C_e)	Cost C_e	K1	K2	K3	Inflation	Installed Cost C USD	MUSD
Pump CS Centrifugal	32.44	3.82137552	13491	3.3892	0.0536	0.1538	2.04	38812.90	0.04

Heat Exchangers	Unit for S , area m^2	Cost C_e	a	b	n	Inflation	duty kW	Installed Cost C USD	MUSD	Heat exchanger duty kj/h
CW1	61.06	25781	10000	88	1	1.68	489.7	82498	0.08	1763000
CW2	62.09	25933	10000	88	1	1.68	510.3	82984	0.08	1837000
CW3	41.94	22959	10000	88	1	1.68	525.4	73469	0.07	1892000
CW4	36.78	22198	10000	88	1	1.68	337.2	71032	0.07	1214000
CW5	81.03	28728	10000	88	1	1.68	606.1	91928	0.09	2182000
CW6	10.11	18262	10000	88	1	1.68	23.49	58437	0.06	84570
CW7	95.35	30841	10000	88	1	1.68	421.8	98691	0.10	1518000
CW8	127.3	35556	10000	88	1	1.68	679.2	113779	0.11	2445000
CW9	129.9	35940	10000	88	1	1.68	694.4	115007	0.12	2500000
CW10	134.1	36559	10000	88	1	1.68	717.6	116990	0.12	2583000
CW11	140.1	37445	10000	88	1	1.68	749.9	119823	0.12	2700000
Total CW:		320200						1024639	1.02	20718570
Heater1	7.718	17909	10000	88	1	1.68	291.5	57308	0.06	
coolint	0	16770	10000	88	1	1.68	22.11	53663	0.05	79590
Rich lean HX SS Fixed tube	10.34	18296	10000	88	1	1.68	235.5	52635	0.05	
Condenser CS Fixed tube	9.26	18136	10000	88	1	1.68	38.9	58036	0.06	
Reboiler SS Kettle reboiler	26.31	27140	14000	83	1	1.68	649.7	78079	0.08	
Methanation 1 SS Floating head S&T	493.4	113600	11000	115	1	1.68	3091	326818	0.33	
Methanation 2 SS Floating head S&T	197.5	56535	11000	115	1	1.68	65.29	162647	0.16	
Total Methanation		170135						489465	0.49	
LNG Heat exchanger plate HX	108.7	11144	1100	850	0.4	1.68	705.3	32060	0.03	
Total:		0.60					10854	1356420	1.36	

Columns										
Absorber	unit m^3	log(C_e)	Cost C_e	K1	K2	K3	Inflation	Installed Cost C USD	MUSD	
Pressure Vessel Vertical 304 SS	53.01	4.59	79217	3.4974	0.4485	0.1074	2.04	256615		
Packing Ceramic valve trays	3.53	3.69	9980	3.322	0.4838	0.3434	2.04			0.26
Total:			89198							
Stripper										
Pressure Vessel Vertical 304 SS	46.65	4.55	71398	3.4974	0.4485	0.1074	2.04	236621		
Packing Ceramic valve trays	3.89	3.73	10849	3.322	0.4838	0.3434	2.04			0.24
Total:			82248							
Expansion Valve + Expander	unit kW	log(C_e)	cost C_e	K1	K2	K3	Inflation	Installed Cost C USD	MUSD	
Expander	696.4	5.19	318396	2.2476	1.4965	-0.1618	2.04	1239549	1.24	
Expansion valve 1	135.2	4.70	102455	2.2476	1.4965	-0.1618	2.04			
Expansion Valve 2	12.43	3.69	10008	2.2476	1.4965	-0.1618	2.04			
Total:			430859					1239549	1.24	

Knock out vessels (Pressure vessel 304 SS)	Unit S: shell mass, kg,	Cost C_e	a/K1	b/K2	n/K3	Inflation	Installed Cost C USD	MUSD
WR Water	165600	3138567.1	15000	68	0.85	1.68	9029416	
separator 1	524.5	48533.2	15000	68	0.85	1.68	139626	
separator 2	984.4	65078.4	15000	68	0.85	1.68	187225	
Separator 3	20.94	26667.7	15000	68	0.85	1.68	76721	
Total:		3278846.4					9432989	9.43

Utilities	Unit	Cost factor	Utility	Unit	Annual cost MUSD	Annual cost MNOK		
Cooling water @ 20 C	USD/GJ	0.354	20.80	GJ/h	0.059	0.57	1 USD in 2022 =	9.6245 NOK
Steam @ 5 Bar	USD/KG	0.0277	0.3072	kg/s	0.25	2.36	Operating hours	8000 h/year
Steam @ 40 Bar	USD/KG	0.0299	1.62288	kg/s	1.40	13.45		3600 sec/h
MDEA	USD/Kg	2.6	0.00002385	kg/s	0.00017859	0.00172	Tube volume 1	2.535 m3
Catalyst	USD/m^3 catalyst	15539			0.030	0.29	Tube volume 2	1.014 m3
Green H2	USD/kg H2	4.8	0.1568	kg/s	21.68	208.62	Catalyst V1	1.394 m3
Electricity Nordpol 2022 MNOK/MWh	NOK/MWh	427.83	15.88103	MW		54.36	Catalyst V2	0.5579 m3
Electricity Nordpol 2022 MUSD/MWh	USD/MWh	44.45		MW	5.65		Total catalyst V	1.9519 m3
Total cost:					29.1	279.6		

0.74601962									
Shell mass calculations	separator 1	Separator 2	Separator 3	WR					
Gas volumetric flowrate V_g (m3/h)	244.3	55.28	30.8	438.7					
gas density rho_g (kg/m3)	14.32	63.18	1.755	8.065					
liquid density rho_l (kg/m3)	996.5	999.1	423.1	8.741		rho SS	8000		
Liquid volumetric flowrate (m3/h)	0.00004006	0.00552	7.043	282.8		holdup time	10		
Pressure separator P (bar)	20	80	1.013	20		S bar allowable	1034		
u_t	0.58	0.2694	1.085	0.02027		E weld efficiency	1		
u_s	0.086955	0.04041	0.1627	0.003041					
Vessel Diameter D_V	0.9968	0.6956	0.2588	7.143					
H_L	0.008557	0.002421	22.32	1.176					
Vessel Height H_V	1.904	1.446	23.11	12.29					
H_V set	2	2	23.11	12.29					
P_d bar 10% higher than P	22	88	1.115	22					
t_w	0.01047	0.02815	0.0001393	0.07502					
shell mass m_s	524.5	984.4	20.94	165600					
	Diameter	Column height	tray number	tray space	tray volume	hold up volume	Volume column	Total volume	
Absorber	3	7.5	15	0.5	3.534	0.3534	53.01437603	56.90177603	
Stripper	3	6.6	12	0.55	3.888	0.3888	46.65265091	50.92945091	

Fixed Cost of Production	Estimate	Cost MUSD	Cost MNOK		
1)Operation labor	5 operator per shift	1.02	9.8	Operator labor cost calculation	
2)Supervision	25% of 1	0.26	2.5	S_OP	50000 \$
3)Direct salary overhead	60% of 1 + 2	0.77	7.4	t shift	1000 shift/year
4)Maintenance	5% of ISBL	0.98	9.4	L_s	5 operators/shift
5)Property tax & insurance	2% of ISBL	0.39	3.8	L_Y,OP	245
6)General plant overhead	65% of (1+2+3+4)	2.30	22.2	LC	1020408
Total		5.71	55.0		

Fixed Capital Cost	Value
Installation Cost [C] MUSD	20.04
Offsite OSBL = 0.3 of ISBL	6.01
Design and Engineering 0.3 ISBL + OSBL	12.03
Contingency X = 0.1 ISBL + OSBL	8.02
Total Fixed capital cost: C_FC	46.10

Produced liq biomethane LBM	2980.08	kg/h	Interest rate %	0.06
Produced LBM yearly	23840640	kg	lifetime n	20
Std Gas flow	4392	m3/h		
Std Gas flow annualu	35136000	Sm3		
LNG price per Sm3	0.17	USD/Sm3		
Total revenue LBM from gas flow	6.0	MUSD/Sm3		
ACCR	0.087			
Total Annualized cost	38.79	MUSD		
Production cost per unit Sm3	1.104	USD/Sm3		
Production cost per unit kg	1.63	USD/kg		

Purchased cost estimate Case 3.8

Centrifugal Compressor CS		Cost estimate								Installed Cost Factors		factor	
Comp #	Unit for S duty, kW	Cost C_e USD	a	b	n	Inflation	Installed Cost C USD	MUSD					
Comp 1	503	231271	8400	3100	0.6	1.68	740068		Equipment erection	f_er	0.3		
comp 2	533.1	238978	8400	3100	0.6	1.68	764730		Piping	f_P	0.8		
comp 3	500.4	230597	8400	3100	0.6	1.68	737910		Instrumentation	f_i	0.3		
comp4	278.7	166481	8400	3100	0.6	1.68	532741		electrical	f_el	0.2		
comp 5	618.7	259997	8400	3100	0.6	1.68	831989		civil	f_c	0.3		
comp 6	655.4	268648	8400	3100	0.6	1.68	859673		structures	f_s	0.2		
comp 7	656.7	268951	8400	3100	0.6	1.68	860642		lagging and pain	f_l	0.1		
comp 8	659.7	269648	8400	3100	0.6	1.68	862875		Offsite(OS)	OS	0.3		
comp 9	667.1	271365	8400	3100	0.6	1.68	868367		D&E	D&E	0.3		
Total	5072.8	2205936					7058994	7.06	Contingency X	X	0.1		
									Material	f_m	1	1.3	

Pump CS Centrifugal	Unit: duty kW	log(C_e)	Cost C_e	K1	K2	K3	Inflation	Installed Cost C USD	MUSD
Pump CS Centrifugal	14.27	3.656045571	9220	3.3892	0.0536	0.1538	2.04	26524.44	0.03

Heat Exchangers	Unit for S , area m^2	Cost C_e	a	b	n	Inflation	duty kW	Installed Cost C USD	MUSD	Heat exchanger duty kj/h
CW1	63.85	26192	10000	88	1	1.68	513.8	83815	0.08	1850000
CW2	64.94	26353	10000	88	1	1.68	536	84330	0.08	1930000
CW3	43.56	23198	10000	88	1	1.68	545.7	74234	0.07	1965000
CW4	36.64	22177	10000	88	1	1.68	336.1	70966	0.07	1210000
CW5	16.8	19249	10000	88	1	1.68	119.9	61597	0.06	431700
CW6	14.96	18977	10000	88	1	1.68	43.56	60728	0.06	156800
CW7	97.72	31191	10000	88	1	1.68	445.2	99810	0.10	1603000
CW8	127.3	35556	10000	88	1	1.68	679.2	113779	0.11	2445000
CW9	129.9	35940	10000	88	1	1.68	694.4	115007	0.12	2500000
CW10	134.1	36559	10000	88	1	1.68	717.6	116990	0.12	2583000
CW11	140.1	37445	10000	88	1	1.68	749.9	119823	0.12	2700000
Total CW:		312837						1001079	1.00	19374500
Heater1	7.983	17948	10000	88	1	1.68	300.4	57433	0.06	
coolint	0	16770	10000	88	1	1.68	20.03	53663	0.05	72100
Rich lean HX SS Fixed tube	14.17	18861	10000	88	1	1.68	235.5	54261	0.05	
Condenser CS Fixed tube	8.433	18014	10000	88	1	1.68	40.21	57646	0.06	
Reboiler SS Kettle reboiler	7.028	24456	14000	83	1	1.68	198.6	70358	0.07	
Methanation 1 SS Floating head S&T	592.1	132634	11000	115	1	1.68	3334	381579	0.38	
Methanation 2 SS Floating head S&T	197.5	56535	11000	115	1	1.68	100.6	162647	0.16	
Total Methanation		189169						544226	0.54	
LNG Heat exchanger plate HX	108.7	11144	1100	850	0.4	1.68	725.1	32060	0.03	
Total:		0.61					10336	1326499	1.33	

Columns											
Absorber	unit m^3	log(C_e)	Cost C_e	K1	K2	K3	Inflation	Installed Cost C USD	MUSD		
Pressure Vessel Vertical 304 SS	53.01	4.59	79217	3.4974	0.4485	0.1074	2.04	256615			
Packing Ceramic valve trays	3.53	3.69	9980	3.322	0.4838	0.3434	2.04				
Total:			89198							0.26	
Stripper											
Pressure Vessel Vertical 304 SS	46.65	4.55	71398	3.4974	0.4485	0.1074	2.04	236621			
Packing Ceramic valve trays	3.89	3.73	10849	3.322	0.4838	0.3434	2.04				
Total:			82248							0.24	
Expansion Valve + Expander	unit kW	log(C_e)	cost C_e	K1	K2	K3	Inflation	Installed Cost C USD	MUSD		
Expander	696.4	5.19	318396	2.2476	1.4965	-0.1618	2.04	1085904	1.09		
Expansion valve 1	57.17	4.38	48562	2.2476	1.4965	-0.1618	2.04				
Expansion Valve 2	12.96	3.71	10495	2.2476	1.4965	-0.1618	2.04				
Total:			377453					1085904	1.09		

Knock out vessels (Pressure vessel 304 SS)	Unit S: shell mass, kg,	Cost C_e	a/K1	b/K2	n/K3	Inflation	Installed Cost C USD	MUSD
WR Water	118700	2371103.2	15000	68	0.85	1.68	6821481	
separator 1	512	48058.8	15000	68	0.85	1.68	138261	
separator 2	961.6	64291.0	15000	68	0.85	1.68	184960	
Separator 3	22.01	26733.2	15000	68	0.85	1.68	76909	
Total:		2510186.2					7221612	7.22

Utilities	Unit	Cost factor	Utility	Unit	Annual cost MUSD	Annual cost MNOK		
Cooling water @ 20 C	USD/GJ	0.354	19.45	GJ/h	0.055	0.53	1 USD in 2022 =	9.6245 NOK
Steam @ 5 Bar	USD/KG	0.0277	0.09389	kg/s	0.07	0.72	Operating hours	8000 h/year
Steam @ 40 Bar	USD/KG	0.0299	1.77579	kg/s	1.53	14.72		3600 sec/h
MDEA	USD/Kg	2.6	0.000003909	kg/s	0.00029271	0.00282	Tube volume 1	3.041 m3
Catalyst	USD/m^3 catalyst	15539			0.035	0.33	Tube volume 2	1.014 m3
Green H2	USD/kg H2	4.8	0.1702	kg/s	23.53	226.45	Catalyst V1	1.673 m3
Electricity Nordpol 2022 MNOK/MWh	NOK/MWh	427.83	15.42287	MW		52.79	Catalyst V2	0.5579 m3
Electricity Nordpol 2022 MUSD/MWh	USD/MWh	44.45		MW		5.48	Total catalyst V	2.2309 m3
Total cost:					30.7	295.5		

0.766219

Shell mass calculations	separator 1	Separator 2	Separator 3	WR				
Gas volumetric flowrate V_g (m3/h)	244.7	55.61	49.54	445.3				
gas density rho_g (kg/m3)	13.62	59.81	1.755	7.629		rho SS	8000	
liquid density rho_l (kg/m3)	996.5	999.1	423.1	8.741		holdup time	10	
Liquid volumetric flowrate (m3/h)	0.06644	0.005538	7.211	304.5		S bar allowable	1034	
Pressure separator P (bar)	20	80	1.013	20		E weld efficiency	1	
u_t	0.59	0.2774	1.085	0.02673				
u_s	0.089205	0.04161	0.1627	0.004009				
Vessel Diameter D_V	0.9849	0.6875	0.3282	6.268				
H_L	0.01453	0.002486	14.21	1.645				
Vessel Height H_V	1.892	1.434	15.1	11.45				
H_V set	2	2	15.1	11.45				
P_d bar 10% higher than P	22	88	1.115	22				
t_w	0.01034	0.02783	0.0001768	0.06583				
shell mass m_s	512	961.6	22.01	118700				
	Diameter	Column height	tray number	tray space	tray volume	hold up volume	Volume column	Total volume
Absorber	3	7.5	15	0.5	3.534	0.3534	53.01437603	56.90177603
Stripper	3	6.6	12	0.55	3.888	0.3888	46.65265091	50.92945091

Fixed Cost of Production	Estimate	Cost MUSD	Cost MNOK		
1)Operation labor	5 operator per shift	1.02	9.8		Operator labor cost calculation
2)Supervision	25% of 1	0.26	2.5	S_OP	50000 \$
3)Direct salary overhead	60% of 1 + 2	0.77	7.4	t shift	1000 shift/year
4)Maintenance	5% of ISBL	0.86	8.3	L_s	5 operators/shift
5)Property tax & insurance	2% of ISBL	0.34	3.3	L_Y,OP	245
6)General plant overhead	65%*(1+2+3) + 4)	2.19	21.1	LC	1020408
Total		5.43	52.3		


Fixed Capital Cost	Value
Installation Cost [C] MUSD	17.76
Offsite OSBL = 0.3 of ISBL	5.33
Design and Engineering 0.3 ISBL + OSBL	10.65
Contingency X = 0.1 ISBL + OSBL	7.10
Total Fixed capital cost: C_FC	40.84

Produced liq biomethane LBM	3051	KG/h	Interest rate %	0.06
Produced LBM yearly	24408000	kg	lifetime n	20
Std Gas flow	4462	m3/h		
Std Gas flow annualu	35696000	Sm3		
LNG price per Sm3	0.17	USD/Sm3		
Total revenue LBM from gas flow	6.1	MUSD/Sm3		
ACCR	0.087			
Total Annualized cost	39.70	MUSD		
Production cost per unit Sm3	1.112	USD/Sm3		
Production cost per unit kg	1.63	USD/kg		

G HYSYS Workbooks


The PDFs specified in this Appendix are for cases 3.0, 3.2, 3.5, and 3.8. The PDF included is for the material streams from the direct process model and extracted from HYSYS directly.

G.1 Case 3.0

1	 NORWEGIAN UNIVERSITY OF Bedford, MA USA	Case Name: Masteroppgave 3.0.hsc
2		Unit Set: NewUser3e-1
3		Date/Time: Sat Jun 10 19:37:18 2023
4		
5		


Workbook: Case (Main)

Material Streams							Fluid Pkg:	All
11	Name	biogas	H2	1	6	17		
12	Vapour Fraction	1.0000	1.0000	1.0000	1.0000	1.0000	1.0000	1.0000
13	Temperature (C)	35.00 *	30.00 *	32.46	136.7	30.00		
14	Pressure (bar)	1.013 *	1.013	1.013	20.00 *	80.00		
15	Molar Flow (kgmole/h)	200.0 *	240.0	440.0	440.0	200.3		
16	Mass Flow (kg/s)	1.513	0.1344	1.647	1.647	1.048		
17	Liquid Volume Flow (m3/h)	10.71	12.85	23.57	23.57	10.72		
18	Heat Flow (kJ/h)	-4.035e+007	3.484e+004	-4.032e+007	-3.880e+007	-2.161e+007		
19	Name	18	19	20	21	22		
20	Vapour Fraction	0.0000	1.0000	0.0000	0.0052	0.0199		
21	Temperature (C)	49.00 *	49.01	63.55	63.10	78.00 *		
22	Pressure (bar)	80.00 *	80.00	80.00	1.300 *	1.300		
23	Molar Flow (kgmole/h)	615.0 *	179.4	635.8	635.8	635.8		
24	Mass Flow (kg/s)	4.789	0.7996	5.038	5.038	5.038		
25	Liquid Volume Flow (m3/h)	17.01	9.591	18.14	18.14	18.14		
26	Heat Flow (kJ/h)	-1.856e+008	-1.352e+007	-1.937e+008	-1.937e+008	-1.923e+008		
27	Name	23	24	25	26	Water		
28	Vapour Fraction	1.0000	0.0000	0.0000	0.0000	0.0000		
29	Temperature (C)	30.00	108.9	109.9	88.14	88.14		
30	Pressure (bar)	1.300	1.300	80.00	80.00	80.00		
31	Molar Flow (kgmole/h)	21.90	613.9	613.9	613.9	1.052		
32	Mass Flow (kg/s)	0.2534	4.784	4.784	4.784	5.264e-003		
33	Liquid Volume Flow (m3/h)	1.147	16.99	16.99	16.99	1.899e-002		
34	Heat Flow (kJ/h)	-8.134e+006	-1.817e+008	-1.815e+008	-1.829e+008	-2.956e+005		
35	Name	MDEA	purge	27	28	CH4_biom		
36	Vapour Fraction	0.0000	0.0000	0.0000	0.0000	1.0000		
37	Temperature (C)	88.14	88.15	88.15	49.00 *	49.01		
38	Pressure (bar)	80.00	80.00	80.00	80.00	80.00		
39	Molar Flow (kgmole/h)	1.349e-004	0.0000	615.0	615.0	178.8		
40	Mass Flow (kg/s)	4.465e-006	0.0000	4.789	4.789	0.7969		
41	Liquid Volume Flow (m3/h)	1.551e-005	0.0000	17.01	17.01	9.577		
42	Heat Flow (kJ/h)	-59.06	0.0000	-1.832e+008	-1.856e+008	-1.339e+007		
43	Name	CO2_biom	H2_biom	H2O_biom	MDEA_biom	H2S_biom		
44	Vapour Fraction	1.0000	1.0000	0.0000	0.0000	0.0000		
45	Temperature (C)	49.01	49.01	49.01	49.01	49.01		
46	Pressure (bar)	80.00	80.00	80.00	80.00	80.00		
47	Molar Flow (kgmole/h)	7.552e-003	7.493e-002	0.5040	1.261e-004	0.0000		
48	Mass Flow (kg/s)	9.232e-005	4.196e-005	2.522e-003	4.174e-006	0.0000		
49	Liquid Volume Flow (m3/h)	4.045e-004	4.013e-003	9.097e-003	1.450e-005	0.0000		
50	Heat Flow (kJ/h)	-2997	56.46	-1.431e+005	-56.68	0.0000		
51	Name	Biom_deh	Biom1	Biom3	Biom4	boiloff		
52	Vapour Fraction	1.0000	1.0000	0.0000	0.0093	1.0000		
53	Temperature (C)	49.00	49.00	-164.1	-162.0 *	-162.0		
54	Pressure (bar)	80.00	80.00	80.00	1.013 *	1.013		
55	Molar Flow (kgmole/h)	178.9	178.9	178.9	178.9	1.665		
56	Mass Flow (kg/s)	0.7970	0.7970	0.7970	0.7970	7.157e-003		
57	Liquid Volume Flow (m3/h)	9.582	9.582	9.582	9.582	8.917e-002		
58	Heat Flow (kJ/h)	-1.339e+007	-1.337e+007	-1.593e+007	-1.593e+007	-1.297e+005		
59	Name	LBM	12	13V	13L	15		
60	Vapour Fraction	0.0000	0.9974	1.0000	0.0000	0.9985		
61	Temperature (C)	-162.0	30.00	30.00	30.00	30.00		
62	Pressure (bar)	1.013	20.00	20.00	20.00	80.00		
63	Molar Flow (kgmole/h)	177.2	201.1	200.6	0.5154	200.6		
64	Mass Flow (kg/s)	0.7899	1.052	1.049	2.579e-003	1.049		
65	Liquid Volume Flow (m3/h)	9.493	10.73	10.72	9.303e-003	10.72		
66	Heat Flow (kJ/h)	-1.581e+007	-2.159e+007	-2.144e+007	-1.471e+005	-2.166e+007		

1	 NORWEGIAN UNIVERSITY OF Bedford, MA USA	Case Name: Masteroppgave 3.0.hsc
2		Unit Set: NewUser3e-1
3		Date/Time: Sat Jun 10 19:37:18 2023
4		
5		


Workbook: Case (Main) (continued)

Material Streams (continued)							Fluid Pkg:	All
9								
10								
11	Name	16V	16L	14	9	10L		
12	Vapour Fraction	1.0000	0.0000	1.0000	1.0000	1.0000	1.0000	1.0000
13	Temperature (C)	30.00	30.00	164.5	240.0 *	260.1		
14	Pressure (bar)	80.00	80.00	80.00 *	20.00	20.00		
15	Molar Flow (kgmole/h)	200.3	0.3045	200.6	321.0	119.0		
16	Mass Flow (kg/s)	1.048	1.524e-003	1.049	1.647	0.5953		
17	Liquid Volume Flow (m3/h)	10.72	5.497e-003	10.72	12.97	2.147		
18	Heat Flow (kJ/h)	-2.157e+007	-8.688e+004	-2.044e+007	-4.764e+007	-2.795e+007		
19	Name	steamH_in	steamH_out	steamM_in	steamM_out	7		
20	Vapour Fraction	1.0000 *	0.0000 *	1.0000 *	0.0000 *	1.0000		
21	Temperature (C)	240.0	240.0	151.9	151.9	200.0 *		
22	Pressure (bar)	33.47	33.47	5.000 *	5.000	20.00		
23	Molar Flow (kgmole/h)	31.33	31.33	77.36	77.36	440.0		
24	Mass Flow (kg/s)	0.1568	0.1568	0.3872	0.3872	1.647		
25	Liquid Volume Flow (m3/h)	0.5655	0.5655	1.396	1.396	23.57		
26	Heat Flow (kJ/h)	-7.433e+006	-8.429e+006	-1.840e+007	-2.134e+007	-3.781e+007		
27	Name	8	Biom2	10V	11	2		
28	Vapour Fraction	1.0000	1.0000	1.0000	1.0000	1.0000	1.0000	1.0000
29	Temperature (C)	244.0	30.00	240.0	240.0	139.4		
30	Pressure (bar)	20.00	80.00	20.00	20.00	2.738		
31	Molar Flow (kgmole/h)	321.0	178.9	202.1	201.1	440.0		
32	Mass Flow (kg/s)	1.647	0.7970	1.052	1.052	1.647		
33	Liquid Volume Flow (m3/h)	12.97	9.582	10.82	10.73	23.57		
34	Heat Flow (kJ/h)	-4.759e+007	-1.352e+007	-1.969e+007	-1.978e+007	-3.874e+007		
35	Name	3	4	5	w1	w2		
36	Vapour Fraction	1.0000	1.0000	1.0000	0.0000	0.0000		
37	Temperature (C)	30.00 *	143.2	30.00	20.00 *	25.00 *		
38	Pressure (bar)	2.738	7.400	7.400	1.013 *	1.013		
39	Molar Flow (kgmole/h)	440.0	440.0	440.0	4296	4296		
40	Mass Flow (kg/s)	1.647	1.647	1.647	21.50	21.50		
41	Liquid Volume Flow (m3/h)	23.57	23.57	23.57	77.53	77.53		
42	Heat Flow (kJ/h)	-4.036e+007	-3.869e+007	-4.037e+007	-1.229e+009	-1.228e+009		
43	Name	w3	w4	w5	w6	w7		
44	Vapour Fraction	0.0000	0.0000	0.0000	0.0000	0.0000		
45	Temperature (C)	20.00 *	25.00 *	20.00 *	25.00 *	20.00 *		
46	Pressure (bar)	1.013 *	1.013	1.013 *	1.013	1.013 *		
47	Molar Flow (kgmole/h)	4467	4467	149.7	149.7	4797		
48	Mass Flow (kg/s)	22.35	22.35	0.7489	0.7489	24.00		
49	Liquid Volume Flow (m3/h)	80.62	80.62	2.701	2.701	86.58		
50	Heat Flow (kJ/h)	-1.278e+009	-1.277e+009	-4.283e+007	-4.278e+007	-1.373e+009		
51	Name	w8	w9	w10	w11	w12		
52	Vapour Fraction	0.0000	0.0000	0.0000	0.0000	0.0000		
53	Temperature (C)	25.00 *	20.00 *	25.00 *	20.00 *	25.00 *		
54	Pressure (bar)	1.013	1.013 *	1.013	1.013 *	1.013		
55	Molar Flow (kgmole/h)	4797	3242	3242	6229	6229		
56	Mass Flow (kg/s)	24.00	16.22	16.22	31.17	31.17		
57	Liquid Volume Flow (m3/h)	86.58	58.52	58.52	112.4	112.4		
58	Heat Flow (kJ/h)	-1.371e+009	-9.279e+008	-9.267e+008	-1.783e+009	-1.780e+009		
59	Name	w13	w14	w15	w16	steam_in1		
60	Vapour Fraction	0.0000	0.0000	0.0000	0.0000	0.0000 *		
61	Temperature (C)	20.00 *	25.00 *	20.00 *	25.00 *	240.0		
62	Pressure (bar)	1.013 *	1.013	1.013 *	1.013	33.47		
63	Molar Flow (kgmole/h)	400.9	400.9	1368	1368	302.2		
64	Mass Flow (kg/s)	2.006	2.006	6.846	6.846	1.512		
65	Liquid Volume Flow (m3/h)	7.236	7.236	24.69	24.69	5.454		
66	Heat Flow (kJ/h)	-1.147e+008	-1.146e+008	-3.915e+008	-3.910e+008	-8.129e+007		

1	 NORWEGIAN UNIVERSITY OF Bedford, MA USA	Case Name: Masteroppgave 3.0.hsc
2		Unit Set: NewUser3e-1
3		Date/Time: Sat Jun 10 19:37:18 2023
4		
5		

Workbook: Case (Main) (continued)

Material Streams (continued)				Fluid Pkg: All		
9						
10						
11	Name	steam_out1	steam_in2	steam_out2	L1	L2
12	Vapour Fraction	1.0000 *	0.0000 *	1.0000 *	1.0000	1.0000
13	Temperature (C)	240.0	240.0	240.0	8.917	62.83
14	Pressure (bar)	33.47	33.47	33.47	10.00 *	16.44
15	Molar Flow (kgmole/h)	302.2	2.736	2.736	1400 *	1400
16	Mass Flow (kg/s)	1.512	1.369e-002	1.369e-002	10.89	10.89
17	Liquid Volume Flow (m3/h)	5.454	4.939e-002	4.939e-002	74.98	74.98
18	Heat Flow (kJ/h)	-7.168e+007	-7.362e+005	-6.491e+005	-7.539e+005	1.436e+006
19	Name	L3	w17	w18	L4	L5
20	Vapour Fraction	1.0000	0.0000	0.0000	1.0000	1.0000
21	Temperature (C)	30.00	20.00 *	25.00 *	87.99	30.00
22	Pressure (bar)	16.44	1.013 *	1.013	27.02	27.02
23	Molar Flow (kgmole/h)	1400	3633	3633	1400	1400
24	Mass Flow (kg/s)	10.89	18.18	18.18	10.89	10.89
25	Liquid Volume Flow (m3/h)	74.98	65.57	65.57	74.98	74.98
26	Heat Flow (kJ/h)	6.688e+004	-1.040e+009	-1.038e+009	2.426e+006	-1.870e+004
27	Name	w19	w20	L6	L7	w21
28	Vapour Fraction	0.0000	0.0000	1.0000	1.0000	0.0000
29	Temperature (C)	20.00 *	25.00 *	88.12	30.00	20.00 *
30	Pressure (bar)	1.013 *	1.013	44.41	44.41	1.013 *
31	Molar Flow (kgmole/h)	6490	6490	1400	1400	6635
32	Mass Flow (kg/s)	32.48	32.48	10.89	10.89	33.20
33	Liquid Volume Flow (m3/h)	117.1	117.1	74.98	74.98	119.8
34	Heat Flow (kJ/h)	-1.857e+009	-1.855e+009	2.345e+006	-1.545e+005	-1.899e+009
35	Name	w22	L8	L9	w23	w24
36	Vapour Fraction	0.0000	1.0000	1.0000	0.0000	0.0000
37	Temperature (C)	25.00 *	88.26	30.00	20.00 *	25.00 *
38	Pressure (bar)	1.013	73.00	73.00	1.013 *	1.013
39	Molar Flow (kgmole/h)	6635	1400	1400	6857	6857
40	Mass Flow (kg/s)	33.20	10.89	10.89	34.32	34.32
41	Liquid Volume Flow (m3/h)	119.8	74.98	74.98	123.8	123.8
42	Heat Flow (kJ/h)	-1.897e+009	2.220e+006	-3.630e+005	-1.963e+009	-1.960e+009
43	Name	L10	L11	w25	w26	L12
44	Vapour Fraction	1.0000	1.0000	0.0000	0.0000	1.0000
45	Temperature (C)	88.28	30.00	20.00 *	25.00 *	-70.00 *
46	Pressure (bar)	120.0 *	120.0	1.013 *	1.013	120.0
47	Molar Flow (kgmole/h)	1400	1400	7166	7166	1400
48	Mass Flow (kg/s)	10.89	10.89	35.86	35.86	10.89
49	Liquid Volume Flow (m3/h)	74.98	74.98	129.3	129.3	74.98
50	Heat Flow (kJ/h)	2.039e+006	-6.611e+005	-2.051e+009	-2.048e+009	-6.034e+006
51	Name	L13	biom3_dummy	biom4_dummy	20dummy	21dummy
52	Vapour Fraction	1.0000	0.0000	0.0007	0.0000	0.0029
53	Temperature (C)	-166.9	-164.1	-165.0	63.55	52.05
54	Pressure (bar)	10.00	80.00	1.013	80.00	1.300
55	Molar Flow (kgmole/h)	1400	178.9	178.9	635.8	635.8
56	Mass Flow (kg/s)	10.89	0.7970	0.7970	5.038	5.038
57	Liquid Volume Flow (m3/h)	74.98	9.582	9.582	18.14	18.14
58	Heat Flow (kJ/h)	-8.541e+006	-1.593e+007	-1.598e+007	-1.937e+008	-1.944e+008
59	Name	d1	d2	w15_duplicate	w16_duplicate	CO2
60	Vapour Fraction	1.0000	0.6761	0.0000	0.0000	---
61	Temperature (C)	78.56	30.00	20.00 *	25.00 *	---
62	Pressure (bar)	1.300	1.300	1.013 *	1.013 *	---
63	Molar Flow (kgmole/h)	32.39	32.39	1368	1368	20.02
64	Mass Flow (kg/s)	0.3060	0.3060	6.846	6.846	0.2447
65	Liquid Volume Flow (m3/h)	1.337	1.337	24.69	24.69	1.072
66	Heat Flow (kJ/h)	-1.061e+007	-1.113e+007	-3.915e+008	-3.910e+008	---

1	 NORWEGIAN UNIVERSITY OF Bedford, MA USA	Case Name: Masteroppgave 3.0.hsc
2		Unit Set: NewUser3e-1
3		Date/Time: Sat Jun 10 19:37:18 2023
4		
5		

Workbook: Case (Main) (continued)

Material Streams (continued)						Fluid Pkg:	All
Name	H2O	H2S	MDEA_cond	CH4	H2_cond		
Vapour Fraction	---	---	---	---	---		
Temperature (C)	---	---	---	---	---		
Pressure (bar)	---	---	---	---	---		
Molar Flow (kgmole/h)	11.21	0.0000	0.0000	1.159	3.565e-004		
Mass Flow (kg/s)	5.610e-002	0.0000	0.0000	5.165e-003	1.996e-007		
Liquid Volume Flow (m3/h)	0.2024	0.0000	0.0000	6.207e-002	1.910e-005		
Heat Flow (kJ/h)	---	---	---	---	---		
Name	steamH_out_duplicate						
Vapour Fraction	0.0000						
Temperature (C)	240.0						
Pressure (bar)	33.47						
Molar Flow (kgmole/h)	31.33						
Mass Flow (kg/s)	0.1568						
Liquid Volume Flow (m3/h)	0.5655						
Heat Flow (kJ/h)	-8.429e+006						

27
28
29
30
31
32
33
34
35
36
37
38
39
40
41
42
43
44
45
46
47
48
49
50
51
52
53
54
55
56
57
58
59
60
61
62
63
64
65
66
67
68

G.2 Case 3.2

Workbook: Case (Main)

Material Streams Fluid Pkg: All

Name	biogas	H2	1	6	17
Vapour Fraction	1.0000	1.0000	1.0000	1.0000	1.0000
Temperature (C)	35.00 *	30.00 *	32.38	125.9	30.00
Pressure (bar)	1.013 *	1.013	1.013	15.00 *	80.00
Molar Flow (kgmole/h)	200.0 *	256.0	456.0	456.0	200.3
Mass Flow (kg/s)	1.513	0.1434	1.656	1.656	1.017
Liquid Volume Flow (m3/h)	10.71	13.71	24.42	24.42	10.72
Heat Flow (kJ/h)	-4.035e+007	3.716e+004	-4.032e+007	-3.891e+007	-2.033e+007
Name	18	19	20	21	22
Vapour Fraction	0.0000	1.0000	0.0000	0.0060	0.0288
Temperature (C)	46.00 *	46.03	61.02	60.09	78.00 *
Pressure (bar)	80.00 *	80.00	80.00	1.060 *	1.060
Molar Flow (kgmole/h)	478.0 *	183.7	494.6	494.6	494.6
Mass Flow (kg/s)	3.674	0.8183	3.872	3.872	3.872
Liquid Volume Flow (m3/h)	13.06	9.821	13.96	13.96	13.96
Heat Flow (kJ/h)	-1.441e+008	-1.385e+007	-1.505e+008	-1.505e+008	-1.491e+008
Name	23	24	25	26	Water
Vapour Fraction	1.0000	0.0000	0.0000	0.0000	0.0000
Temperature (C)	30.00	103.1	104.1	74.93	74.93
Pressure (bar)	1.060	1.060	80.00	80.00	80.00
Molar Flow (kgmole/h)	17.63	477.0	477.0	477.0	0.9929
Mass Flow (kg/s)	0.2035	3.669	3.669	3.669	4.969e-003
Liquid Volume Flow (m3/h)	0.9191	13.04	13.04	13.04	1.792e-002
Heat Flow (kJ/h)	-6.543e+006	-1.412e+008	-1.411e+008	-1.425e+008	-2.800e+005
Name	MDEA	purge	27	28	CH4_biom
Vapour Fraction	0.0000	0.0000	0.0000	0.0000	1.0000
Temperature (C)	74.93	74.94	74.94	46.00 *	46.03
Pressure (bar)	80.00	80.00	80.00	80.00	80.00
Molar Flow (kgmole/h)	7.468e-005	0.0000	478.0	478.0	183.1
Mass Flow (kg/s)	2.472e-006	0.0000	3.674	3.674	0.8158
Liquid Volume Flow (m3/h)	8.588e-006	0.0000	13.06	13.06	9.805
Heat Flow (kJ/h)	-33.00	0.0000	-1.427e+008	-1.441e+008	-1.373e+007
Name	CO2_biom	H2_biom	H2O_biom	MDEA_biom	H2S_biom
Vapour Fraction	1.0000	1.0000	0.0000	0.0000	0.0000
Temperature (C)	46.03	46.03	46.03	46.03	46.03
Pressure (bar)	80.00	80.00	80.00	80.00	80.00
Molar Flow (kgmole/h)	8.876e-003	0.1294	0.4540	9.868e-005	0.0000
Mass Flow (kg/s)	1.085e-004	7.247e-005	2.272e-003	3.266e-006	0.0000
Liquid Volume Flow (m3/h)	4.754e-004	6.931e-003	8.195e-003	1.135e-005	0.0000
Heat Flow (kJ/h)	-3525	86.19	-1.290e+005	-44.44	0.0000
Name	Biom_deh	Biom1	Biom3	Biom4	boiloff
Vapour Fraction	1.0000	1.0000	0.0000	0.0164	1.0000
Temperature (C)	46.00	46.00	-163.1	-162.0 *	-162.0
Pressure (bar)	80.00	80.00	80.00	1.013 *	1.013
Molar Flow (kgmole/h)	183.2	183.2	183.2	183.2	3.008
Mass Flow (kg/s)	0.8160	0.8160	0.8160	0.8160	1.293e-002
Liquid Volume Flow (m3/h)	9.812	9.812	9.812	9.812	0.1611
Heat Flow (kJ/h)	-1.374e+007	-1.371e+007	-1.630e+007	-1.630e+007	-2.342e+005

Workbook: Case (Main) (continued)

Material Streams (continued)						Fluid Pkg:	All
12	Name	LBM	12	13V	13L	15	
12	Vapour Fraction	0.0000	0.9934	1.0000	0.0000	0.9978	
13	Temperature (C)	-162.0	30.00	30.00	30.00	30.00	
14	Pressure (bar)	1.013	15.00	15.00	15.00	80.00	
15	Molar Flow (kgmole/h)	180.2	202.1	200.8	1.338	200.8	
16	Mass Flow (kg/s)	0.8031	1.026	1.019	6.696e-003	1.019	
17	Liquid Volume Flow (m3/h)	9.651	10.75	10.73	2.415e-002	10.73	
18	Heat Flow (kJ/h)	-1.607e+007	-2.056e+007	-2.018e+007	-3.819e+005	-2.042e+007	
19	Name	16V	16L	14	9	10L	
20	Vapour Fraction	1.0000	0.0000	1.0000	1.0000	1.0000	
21	Temperature (C)	30.00	30.00	194.0	240.0 *	255.2	
22	Pressure (bar)	80.00	80.00	80.00 *	15.00	15.00	
23	Molar Flow (kgmole/h)	200.3	0.4465	200.8	330.0	126.0	
24	Mass Flow (kg/s)	1.017	2.234e-003	1.019	1.656	0.6304	
25	Liquid Volume Flow (m3/h)	10.72	8.060e-003	10.73	13.20	2.274	
26	Heat Flow (kJ/h)	-2.030e+007	-1.274e+005	-1.892e+007	-4.814e+007	-2.958e+007	
27	Name	steamH_in	steamH_out	steamM_in	steamM_out	7	
28	Vapour Fraction	1.0000 *	0.0000 *	1.0000 *	0.0000 *	1.0000	
29	Temperature (C)	240.0	240.0	151.9	151.9	200.0 *	
30	Pressure (bar)	33.47	33.47	5.000 *	5.000	15.00	
31	Molar Flow (kgmole/h)	37.54	37.54	57.88	57.88	456.0	
32	Mass Flow (kg/s)	0.1879	0.1879	0.2896	0.2896	1.656	
33	Liquid Volume Flow (m3/h)	0.6776	0.6776	1.045	1.045	24.42	
34	Heat Flow (kJ/h)	-8.905e+006	-1.010e+007	-1.376e+007	-1.597e+007	-3.772e+007	
35	Name	8	Biom2	10V	11	2	
36	Vapour Fraction	1.0000	1.0000	1.0000	1.0000	1.0000	
37	Temperature (C)	245.9	30.00	240.0	240.0	128.6	
38	Pressure (bar)	15.00	80.00	15.00	15.00	2.488	
39	Molar Flow (kgmole/h)	330.0	183.2	204.1	202.1	456.0	
40	Mass Flow (kg/s)	1.656	0.8160	1.026	1.026	1.656	
41	Liquid Volume Flow (m3/h)	13.20	9.812	10.93	10.75	24.42	
42	Heat Flow (kJ/h)	-4.805e+007	-1.384e+007	-1.855e+007	-1.873e+007	-3.886e+007	
43	Name	3	4	5	w1	w2	
44	Vapour Fraction	1.0000	1.0000	1.0000	0.0000	0.0000	
45	Temperature (C)	30.00 *	131.9	30.00	20.00 *	25.00 *	
46	Pressure (bar)	2.488	6.109	6.109	1.013 *	1.013	
47	Molar Flow (kgmole/h)	456.0	456.0	456.0	3980	3980	
48	Mass Flow (kg/s)	1.656	1.656	1.656	19.92	19.92	
49	Liquid Volume Flow (m3/h)	24.42	24.42	24.42	71.84	71.84	
50	Heat Flow (kJ/h)	-4.036e+007	-3.881e+007	-4.036e+007	-1.139e+009	-1.138e+009	
51	Name	w3	w4	w5	w6	w7	
52	Vapour Fraction	0.0000	0.0000	0.0000	0.0000	0.0000	
53	Temperature (C)	20.00 *	25.00 *	20.00 *	25.00 *	20.00 *	
54	Pressure (bar)	1.013 *	1.013	1.013 *	1.013	1.013 *	
55	Molar Flow (kgmole/h)	4128	4128	224.6	224.6	4880	
56	Mass Flow (kg/s)	20.66	20.66	1.124	1.124	24.42	
57	Liquid Volume Flow (m3/h)	74.51	74.51	4.055	4.055	88.08	
58	Heat Flow (kJ/h)	-1.181e+009	-1.180e+009	-6.430e+007	-6.421e+007	-1.397e+009	

Workbook: Case (Main) (continued)

Material Streams (continued)							Fluid Pkg:	All
11	Name	w8	w9	w10	w11	w12		
12	Vapour Fraction	0.0000	0.0000	0.0000	0.0000	0.0000		
13	Temperature (C)	25.00 *	20.00 *	25.00 *	20.00 *	25.00 *		
14	Pressure (bar)	1.013	1.013 *	1.013	1.013 *	1.013		
15	Molar Flow (kgmole/h)	4880	3980	3980	3495	3495		
16	Mass Flow (kg/s)	24.42	19.92	19.92	17.49	17.49		
17	Liquid Volume Flow (m3/h)	88.08	71.84	71.84	63.08	63.08		
18	Heat Flow (kJ/h)	-1.395e+009	-1.139e+009	-1.138e+009	-1.000e+009	-9.989e+008		
19	Name	w13	w14	w15	w16	steam_in1		
20	Vapour Fraction	0.0000	0.0000	0.0000	0.0000	0.0000 *		
21	Temperature (C)	20.00 *	25.00 *	20.00 *	25.00 *	240.0		
22	Pressure (bar)	1.013 *	1.013	1.013 *	1.013	33.47		
23	Molar Flow (kgmole/h)	346.4	346.4	2119	2119	320.3		
24	Mass Flow (kg/s)	1.733	1.733	10.60	10.60	1.603		
25	Liquid Volume Flow (m3/h)	6.252	6.252	38.24	38.24	5.781		
26	Heat Flow (kJ/h)	-9.913e+007	-9.900e+007	-6.064e+008	-6.056e+008	-8.616e+007		
27	Name	steam_out1	steam_in2	steam_out2	L1	L2		
28	Vapour Fraction	1.0000 *	0.0000 *	1.0000 *	1.0000	1.0000		
29	Temperature (C)	240.0	240.0	240.0	10.05	64.17		
30	Pressure (bar)	33.47	33.47	33.47	10.00 *	16.44		
31	Molar Flow (kgmole/h)	320.3	5.376	5.376	1400 *	1400		
32	Mass Flow (kg/s)	1.603	2.690e-002	2.690e-002	10.89	10.89		
33	Liquid Volume Flow (m3/h)	5.781	9.703e-002	9.703e-002	74.98	74.98		
34	Heat Flow (kJ/h)	-7.598e+007	-1.446e+006	-1.275e+006	-7.070e+005	1.491e+006		
35	Name	L3	w17	w18	L4	L5		
36	Vapour Fraction	1.0000	0.0000	0.0000	1.0000	1.0000		
37	Temperature (C)	30.00	20.00 *	25.00 *	87.99	30.00		
38	Pressure (bar)	16.44	1.013 *	1.013	27.02	27.02		
39	Molar Flow (kgmole/h)	1400	3781	3781	1400	1400		
40	Mass Flow (kg/s)	10.89	18.92	18.92	10.89	10.89		
41	Liquid Volume Flow (m3/h)	74.98	68.25	68.25	74.98	74.98		
42	Heat Flow (kJ/h)	6.688e+004	-1.082e+009	-1.081e+009	2.426e+006	-1.870e+004		
43	Name	w19	w20	L6	L7	w21		
44	Vapour Fraction	0.0000	0.0000	1.0000	1.0000	0.0000		
45	Temperature (C)	20.00 *	25.00 *	88.12	30.00	20.00 *		
46	Pressure (bar)	1.013 *	1.013	44.41	44.41	1.013 *		
47	Molar Flow (kgmole/h)	6490	6490	1400	1400	6635		
48	Mass Flow (kg/s)	32.48	32.48	10.89	10.89	33.20		
49	Liquid Volume Flow (m3/h)	117.1	117.1	74.98	74.98	119.8		
50	Heat Flow (kJ/h)	-1.857e+009	-1.855e+009	2.345e+006	-1.545e+005	-1.899e+009		
51	Name	w22	L8	L9	w23	w24		
52	Vapour Fraction	0.0000	1.0000	1.0000	0.0000	0.0000		
53	Temperature (C)	25.00 *	88.26	30.00	20.00 *	25.00 *		
54	Pressure (bar)	1.013	73.00	73.00	1.013 *	1.013		
55	Molar Flow (kgmole/h)	6635	1400	1400	6857	6857		
56	Mass Flow (kg/s)	33.20	10.89	10.89	34.32	34.32		
57	Liquid Volume Flow (m3/h)	119.8	74.98	74.98	123.8	123.8		
58	Heat Flow (kJ/h)	-1.897e+009	2.220e+006	-3.630e+005	-1.963e+009	-1.960e+009		

Workbook: Case (Main) (continued)

Material Streams (continued)						Fluid Pkg:	All	
11	Name	L10	L11	w25	w26	L12		
12	Vapour Fraction	1.0000	1.0000	0.0000	0.0000	1.0000		
13	Temperature (C)	88.28	30.00	20.00 *	25.00 *	-70.00 *		
14	Pressure (bar)	120.0 *	120.0	1.013 *	1.013	120.0		
15	Molar Flow (kgmole/h)	1400	1400	7166	7166	1400		
16	Mass Flow (kg/s)	10.89	10.89	35.86	35.86	10.89		
17	Liquid Volume Flow (m3/h)	74.98	74.98	129.3	129.3	74.98		
18	Heat Flow (kJ/h)	2.039e+006	-6.611e+005	-2.051e+009	-2.048e+009	-6.034e+006		
19	Name	L13	biom3_dummy	biom4_dummy	20dummy	21dummy		
20	Vapour Fraction	1.0000	0.0000	0.0025	0.0000	0.0031		
21	Temperature (C)	-166.9	-163.1	-164.2	61.02	49.44		
22	Pressure (bar)	10.00	80.00	1.013	80.00	1.060		
23	Molar Flow (kgmole/h)	1400	183.2	183.2	494.6	494.6		
24	Mass Flow (kg/s)	10.89	0.8160	0.8160	3.872	3.872		
25	Liquid Volume Flow (m3/h)	74.98	9.812	9.812	13.96	13.96		
26	Heat Flow (kJ/h)	-8.541e+006	-1.630e+007	-1.635e+007	-1.505e+008	-1.511e+008		
27	Name	d1	d2	w15_duplicate	w16_duplicate	CO2		
28	Vapour Fraction	1.0000	0.5123	0.0000	0.0000	---		
29	Temperature (C)	83.10	30.00	20.00 *	25.00 *	---		
30	Pressure (bar)	1.060	1.060	1.013 *	1.013 *	---		
31	Molar Flow (kgmole/h)	34.42	34.42	2119	2119	16.03		
32	Mass Flow (kg/s)	0.2875	0.2875	10.60	10.60	0.1960		
33	Liquid Volume Flow (m3/h)	1.222	1.222	38.24	38.24	0.8587		
34	Heat Flow (kJ/h)	-1.054e+007	-1.133e+007	-6.064e+008	-6.056e+008	---		
35	Name	H2O	H2S	MDEA_cond	CH4	H2_cond		
36	Vapour Fraction	---	---	---	---	---		
37	Temperature (C)	---	---	---	---	---		
38	Pressure (bar)	---	---	---	---	---		
39	Molar Flow (kgmole/h)	17.50	0.0000	0.0000	0.8945	4.673e-004		
40	Mass Flow (kg/s)	8.755e-002	0.0000	0.0000	3.986e-003	2.617e-007		
41	Liquid Volume Flow (m3/h)	0.3158	0.0000	0.0000	4.791e-002	2.503e-005		
42	Heat Flow (kJ/h)	---	---	---	---	---		
43	Name	steamH_out_duplicate						
44	Vapour Fraction	0.0000						
45	Temperature (C)	240.0						
46	Pressure (bar)	33.47						
47	Molar Flow (kgmole/h)	37.54						
48	Mass Flow (kg/s)	0.1879						
49	Liquid Volume Flow (m3/h)	0.6776						
50	Heat Flow (kJ/h)	-1.010e+007						

51	
52	
53	
54	
55	
56	
57	
58	
59	
60	
61	
62	

G.3 Case 3.5

Workbook: Case (Main)

Material Streams Fluid Pkg: All

Name	biogas	H2	1	6	17
Vapour Fraction	1.0000	1.0000	1.0000	1.0000	1.0000
Temperature (C)	35.00 *	30.00 *	32.27	137.9	30.00
Pressure (bar)	1.013 *	1.013	1.013	20.00 *	80.00
Molar Flow (kgmole/h)	200.0 *	280.0	480.0	480.0	200.3
Mass Flow (kg/s)	1.513	0.1568	1.670	1.670	0.9702
Liquid Volume Flow (m3/h)	10.71	15.00	25.71	25.71	10.72
Heat Flow (kJ/h)	-4.035e+007	4.065e+004	-4.031e+007	-3.865e+007	-1.841e+007
Name	18	19	20	21	22
Vapour Fraction	0.0000	1.0000	0.0000	0.0025	0.0052
Temperature (C)	40.00 *	40.03	50.08	51.34	70.00 *
Pressure (bar)	80.00 *	80.00	80.00	1.300 *	1.300
Molar Flow (kgmole/h)	431.0 *	189.6	441.7	441.7	441.7
Mass Flow (kg/s)	3.448	0.8446	3.573	3.573	3.573
Liquid Volume Flow (m3/h)	12.24	10.14	12.82	12.82	12.82
Heat Flow (kJ/h)	-1.310e+008	-1.433e+007	-1.351e+008	-1.351e+008	-1.342e+008
Name	23	24	25	26	Water
Vapour Fraction	1.0000	0.0000	0.0000	0.0000	0.0000
Temperature (C)	30.00	109.0	110.0	91.24	91.24
Pressure (bar)	1.300	1.300	80.00	80.00	80.00
Molar Flow (kgmole/h)	11.27	430.4	430.4	430.4	0.5514
Mass Flow (kg/s)	0.1283	3.445	3.445	3.445	2.760e-003
Liquid Volume Flow (m3/h)	0.5903	12.23	12.23	12.23	9.954e-003
Heat Flow (kJ/h)	-4.100e+006	-1.279e+008	-1.278e+008	-1.286e+008	-1.548e+005
Name	MDEA	purge	27	28	CH4_biom
Vapour Fraction	0.0000	0.0000	0.0000	0.0000	1.0000
Temperature (C)	91.24	91.25	91.25	40.00 *	40.03
Pressure (bar)	80.00	80.00	80.00	80.00	80.00
Molar Flow (kgmole/h)	7.205e-005	0.0000	431.0	431.0	189.1
Mass Flow (kg/s)	2.385e-006	0.0000	3.448	3.448	0.8427
Liquid Volume Flow (m3/h)	8.286e-006	0.0000	12.24	12.24	10.13
Heat Flow (kJ/h)	-31.48	0.0000	-1.288e+008	-1.310e+008	-1.424e+007
Name	CO2_biom	H2_biom	H2O_biom	MDEA_biom	H2S_biom
Vapour Fraction	1.0000	1.0000	0.0000	0.0000	0.0000
Temperature (C)	40.03	40.03	40.03	40.03	40.03
Pressure (bar)	80.00	80.00	80.00	80.00	80.00
Molar Flow (kgmole/h)	7.125e-003	0.1493	0.3518	7.188e-005	0.0000
Mass Flow (kg/s)	8.711e-005	8.359e-005	1.761e-003	2.379e-006	0.0000
Liquid Volume Flow (m3/h)	3.816e-004	7.995e-003	6.350e-003	8.266e-006	0.0000
Heat Flow (kJ/h)	-2836	73.18	-1.001e+005	-32.49	0.0000
Name	Biom_deh	Biom1	Biom3	Biom4	boiloff
Vapour Fraction	1.0000	1.0000	0.0000	0.0185	1.0000
Temperature (C)	40.00	40.00	-162.8	-162.0 *	-162.0
Pressure (bar)	80.00	80.00	80.00	1.013 *	1.013
Molar Flow (kgmole/h)	189.3	189.3	189.3	189.3	3.494
Mass Flow (kg/s)	0.8429	0.8429	0.8429	0.8429	1.502e-002
Liquid Volume Flow (m3/h)	10.14	10.14	10.14	10.14	0.1871
Heat Flow (kJ/h)	-1.424e+007	-1.421e+007	-1.684e+007	-1.684e+007	-2.721e+005

Workbook: Case (Main) (continued)

Material Streams (continued)							Fluid Pkg:	All
12	Name	LBM	12	13V	13L	15		
12	Vapour Fraction	0.0000	0.9891	1.0000	0.0000	0.9985		
13	Temperature (C)	-162.0	30.00	30.00	30.00	30.00		
14	Pressure (bar)	1.013	20.00	20.00	20.00	80.00		
15	Molar Flow (kgmole/h)	185.8	202.8	200.6	2.216	200.6		
16	Mass Flow (kg/s)	0.8278	0.9828	0.9717	1.109e-002	0.9717		
17	Liquid Volume Flow (m3/h)	9.949	10.77	10.73	4.000e-002	10.73		
18	Heat Flow (kJ/h)	-1.656e+007	-1.888e+007	-1.825e+007	-6.325e+005	-1.846e+007		
19	Name	16V	16L	14	9	10L		
20	Vapour Fraction	1.0000	0.0000	1.0000	1.0000	1.0000		
21	Temperature (C)	30.00	30.00	164.6	240.0 *	260.0		
22	Pressure (bar)	80.00	80.00	80.00 *	20.00	20.00		
23	Molar Flow (kgmole/h)	200.3	0.3061	200.6	342.8	137.2		
24	Mass Flow (kg/s)	0.9702	1.532e-003	0.9717	1.670	0.6867		
25	Liquid Volume Flow (m3/h)	10.72	5.526e-003	10.73	13.49	2.477		
26	Heat Flow (kJ/h)	-1.838e+007	-8.735e+004	-1.725e+007	-4.900e+007	-3.224e+007		
27	Name	steamH_in	steamH_out	steamM_in	steamM_out	7		
28	Vapour Fraction	1.0000 *	0.0000 *	1.0000 *	0.0000 *	1.0000		
29	Temperature (C)	240.0	240.0	151.9	151.9	200.0 *		
30	Pressure (bar)	33.47	33.47	5.000 *	5.000	20.00		
31	Molar Flow (kgmole/h)	33.00	33.00	61.38	61.38	480.0		
32	Mass Flow (kg/s)	0.1651	0.1651	0.3072	0.3072	1.670		
33	Liquid Volume Flow (m3/h)	0.5957	0.5957	1.108	1.108	25.71		
34	Heat Flow (kJ/h)	-7.829e+006	-8.878e+006	-1.460e+007	-1.693e+007	-3.760e+007		
35	Name	8	Biom2	10V	11	2		
36	Vapour Fraction	1.0000	1.0000	1.0000	1.0000	1.0000		
37	Temperature (C)	245.3	30.00	240.0	240.0	140.4		
38	Pressure (bar)	20.00	80.00	20.00	20.00	2.738		
39	Molar Flow (kgmole/h)	342.8	189.3	205.5	202.8	480.0		
40	Mass Flow (kg/s)	1.670	0.8429	0.9828	0.9828	1.670		
41	Liquid Volume Flow (m3/h)	13.49	10.14	11.01	10.77	25.71		
42	Heat Flow (kJ/h)	-4.892e+007	-1.430e+007	-1.675e+007	-1.699e+007	-3.859e+007		
43	Name	3	4	5	w1	w2		
44	Vapour Fraction	1.0000	1.0000	1.0000	0.0000	0.0000		
45	Temperature (C)	30.00 *	144.5	30.00	20.00 *	25.00 *		
46	Pressure (bar)	2.738	7.400	7.400	1.013 *	1.013		
47	Molar Flow (kgmole/h)	480.0	480.0	480.0	4679	4679		
48	Mass Flow (kg/s)	1.670	1.670	1.670	23.42	23.42		
49	Liquid Volume Flow (m3/h)	25.71	25.71	25.71	84.46	84.46		
50	Heat Flow (kJ/h)	-4.035e+007	-3.853e+007	-4.036e+007	-1.339e+009	-1.338e+009		
51	Name	w3	w4	w5	w6	w7		
52	Vapour Fraction	0.0000	0.0000	0.0000	0.0000	0.0000		
53	Temperature (C)	20.00 *	25.00 *	20.00 *	25.00 *	20.00 *		
54	Pressure (bar)	1.013 *	1.013	1.013 *	1.013	1.013 *		
55	Molar Flow (kgmole/h)	4876	4876	211.2	211.2	5021		
56	Mass Flow (kg/s)	24.40	24.40	1.057	1.057	25.12		
57	Liquid Volume Flow (m3/h)	88.01	88.01	3.813	3.813	90.62		
58	Heat Flow (kJ/h)	-1.396e+009	-1.394e+009	-6.046e+007	-6.038e+007	-1.437e+009		

Workbook: Case (Main) (continued)

Material Streams (continued)							Fluid Pkg:	All
11	Name	w8	w9	w10	w11	w12		
12	Vapour Fraction	0.0000	0.0000	0.0000	0.0000	0.0000		0.0000
13	Temperature (C)	25.00 *	20.00 *	25.00 *	20.00 *	25.00 *		25.00 *
14	Pressure (bar)	1.013	1.013 *	1.013	1.013 *	1.013		1.013
15	Molar Flow (kgmole/h)	5021	3222	3222	5791	5791		5791
16	Mass Flow (kg/s)	25.12	16.12	16.12	28.98	28.98		28.98
17	Liquid Volume Flow (m3/h)	90.62	58.15	58.15	104.5	104.5		104.5
18	Heat Flow (kJ/h)	-1.435e+009	-9.221e+008	-9.208e+008	-1.657e+009	-1.655e+009		-1.655e+009
19	Name	w13	w14	w15	w16	steam_in1		
20	Vapour Fraction	0.0000	0.0000	0.0000	0.0000	0.0000 *		0.0000 *
21	Temperature (C)	20.00 *	25.00 *	20.00 *	25.00 *	240.0		240.0
22	Pressure (bar)	1.013 *	1.013	1.013 *	1.013	33.47		33.47
23	Molar Flow (kgmole/h)	224.5	224.5	371.7	371.7	349.9		349.9
24	Mass Flow (kg/s)	1.123	1.123	1.860	1.860	1.751		1.751
25	Liquid Volume Flow (m3/h)	4.052	4.052	6.709	6.709	6.315		6.315
26	Heat Flow (kJ/h)	-6.425e+007	-6.416e+007	-1.064e+008	-1.062e+008	-9.413e+007		-9.413e+007
27	Name	steam_out1	steam_in2	steam_out2	L1	L2		
28	Vapour Fraction	1.0000 *	0.0000 *	1.0000 *	1.0000	1.0000		1.0000
29	Temperature (C)	240.0	240.0	240.0	11.94	66.43		66.43
30	Pressure (bar)	33.47	33.47	33.47	10.00 *	16.44		16.44
31	Molar Flow (kgmole/h)	349.9	7.390	7.390	1400 *	1400		1400
32	Mass Flow (kg/s)	1.751	3.698e-002	3.698e-002	10.89	10.89		10.89
33	Liquid Volume Flow (m3/h)	6.315	0.1334	0.1334	74.98	74.98		74.98
34	Heat Flow (kJ/h)	-8.300e+007	-1.988e+006	-1.753e+006	-6.283e+005	1.585e+006		1.585e+006
35	Name	L3	w17	w18	L4	L5		
36	Vapour Fraction	1.0000	0.0000	0.0000	1.0000	1.0000		1.0000
37	Temperature (C)	30.00	20.00 *	25.00 *	87.99	30.00		30.00
38	Pressure (bar)	16.44	1.013 *	1.013	27.02	27.02		27.02
39	Molar Flow (kgmole/h)	1400	4030	4030	1400	1400		1400
40	Mass Flow (kg/s)	10.89	20.17	20.17	10.89	10.89		10.89
41	Liquid Volume Flow (m3/h)	74.98	72.75	72.75	74.98	74.98		74.98
42	Heat Flow (kJ/h)	6.688e+004	-1.154e+009	-1.152e+009	2.426e+006	-1.870e+004		-1.870e+004
43	Name	w19	w20	L6	L7	w21		
44	Vapour Fraction	0.0000	0.0000	1.0000	1.0000	0.0000		0.0000
45	Temperature (C)	20.00 *	25.00 *	88.12	30.00	20.00 *		20.00 *
46	Pressure (bar)	1.013 *	1.013	44.41	44.41	1.013 *		1.013 *
47	Molar Flow (kgmole/h)	6490	6490	1400	1400	6635		6635
48	Mass Flow (kg/s)	32.48	32.48	10.89	10.89	33.20		33.20
49	Liquid Volume Flow (m3/h)	117.1	117.1	74.98	74.98	119.8		119.8
50	Heat Flow (kJ/h)	-1.857e+009	-1.855e+009	2.345e+006	-1.545e+005	-1.899e+009		-1.899e+009
51	Name	w22	L8	L9	w23	w24		
52	Vapour Fraction	0.0000	1.0000	1.0000	0.0000	0.0000		0.0000
53	Temperature (C)	25.00 *	88.26	30.00	20.00 *	25.00 *		25.00 *
54	Pressure (bar)	1.013	73.00	73.00	1.013 *	1.013		1.013
55	Molar Flow (kgmole/h)	6635	1400	1400	6857	6857		6857
56	Mass Flow (kg/s)	33.20	10.89	10.89	34.32	34.32		34.32
57	Liquid Volume Flow (m3/h)	119.8	74.98	74.98	123.8	123.8		123.8
58	Heat Flow (kJ/h)	-1.897e+009	2.220e+006	-3.630e+005	-1.963e+009	-1.960e+009		-1.960e+009

Workbook: Case (Main) (continued)

Material Streams (continued)							Fluid Pkg:	All
11	Name	L10	L11	w25	w26	L12		
12	Vapour Fraction	1.0000	1.0000	0.0000	0.0000	1.0000		
13	Temperature (C)	88.28	30.00	20.00 *	25.00 *	-70.00 *		
14	Pressure (bar)	120.0 *	120.0	1.013 *	1.013	120.0		
15	Molar Flow (kgmole/h)	1400	1400	7166	7166	1400		
16	Mass Flow (kg/s)	10.89	10.89	35.86	35.86	10.89		
17	Liquid Volume Flow (m3/h)	74.98	74.98	129.3	129.3	74.98		
18	Heat Flow (kJ/h)	2.039e+006	-6.611e+005	-2.051e+009	-2.048e+009	-6.034e+006		
19	Name	L13	biom3_dummy	biom4_dummy	20dummy	21dummy		
20	Vapour Fraction	1.0000	0.0000	0.0032	0.0000	0.0022		
21	Temperature (C)	-166.9	-162.8	-164.0	50.08	39.61		
22	Pressure (bar)	10.00	80.00	1.013	80.00	1.300		
23	Molar Flow (kgmole/h)	1400	189.3	189.3	441.7	441.7		
24	Mass Flow (kg/s)	10.89	0.8429	0.8429	3.573	3.573		
25	Liquid Volume Flow (m3/h)	74.98	10.14	10.14	12.82	12.82		
26	Heat Flow (kJ/h)	-8.541e+006	-1.684e+007	-1.688e+007	-1.351e+008	-1.356e+008		
27	Name	d1	d2	w15_duplicate	w16_duplicate	CO2		
28	Vapour Fraction	1.0000	0.8035	0.0000	0.0000	---		
29	Temperature (C)	68.12	30.00	20.00 *	25.00 *	---		
30	Pressure (bar)	1.300	1.300	1.013 *	1.013 *	---		
31	Molar Flow (kgmole/h)	14.02	14.02	371.7	371.7	10.03		
32	Mass Flow (kg/s)	0.1421	0.1421	1.860	1.860	0.1227		
33	Liquid Volume Flow (m3/h)	0.6400	0.6400	6.709	6.709	0.5373		
34	Heat Flow (kJ/h)	-4.747e+006	-4.887e+006	-1.064e+008	-1.062e+008	---		
35	Name	H2O	H2S	MDEA_cond	CH4	H2_cond		
36	Vapour Fraction	---	---	---	---	---		
37	Temperature (C)	---	---	---	---	---		
38	Pressure (bar)	---	---	---	---	---		
39	Molar Flow (kgmole/h)	3.127	0.0000	0.0000	0.8635	4.775e-004		
40	Mass Flow (kg/s)	1.565e-002	0.0000	0.0000	3.848e-003	2.674e-007		
41	Liquid Volume Flow (m3/h)	5.644e-002	0.0000	0.0000	4.625e-002	2.557e-005		
42	Heat Flow (kJ/h)	---	---	---	---	---		
43	Name	steamH_out_duplicate						
44	Vapour Fraction	0.0000						
45	Temperature (C)	240.0						
46	Pressure (bar)	33.47						
47	Molar Flow (kgmole/h)	33.00						
48	Mass Flow (kg/s)	0.1651						
49	Liquid Volume Flow (m3/h)	0.5957						
50	Heat Flow (kJ/h)	-8.878e+006						

Licensed to: NORWEGIAN UNIVERSITY OF * Specified by user.

G.4 Case 3.8

Workbook: Case (Main)

Material Streams Fluid Pkg: All

Name	biogas	H2	1	6	17
Vapour Fraction	1.0000	1.0000	1.0000	1.0000	1.0000
Temperature (C)	35.00 *	30.00 *	32.17	138.6	30.00
Pressure (bar)	1.013 *	1.013	1.013	20.00 *	80.00
Molar Flow (kgmole/h)	200.0 *	304.0	504.0	504.0	200.4
Mass Flow (kg/s)	1.513	0.1702	1.683	1.683	0.9238
Liquid Volume Flow (m3/h)	10.71	16.28	26.99	26.99	10.73
Heat Flow (kJ/h)	-4.035e+007	4.413e+004	-4.031e+007	-3.856e+007	-1.649e+007
Name	18	19	20	21	22
Vapour Fraction	0.0000	1.0000	0.0000	0.0025	0.0136
Temperature (C)	48.00 *	48.06	49.75	50.97	79.00 *
Pressure (bar)	80.00 *	80.00	80.00	1.040 *	1.040
Molar Flow (kgmole/h)	200.0 *	196.3	204.1	204.1	204.1
Mass Flow (kg/s)	1.517	0.8743	1.567	1.567	1.567
Liquid Volume Flow (m3/h)	5.394	10.50	5.625	5.625	5.625
Heat Flow (kJ/h)	-6.011e+007	-1.479e+007	-6.182e+007	-6.182e+007	-6.117e+007
Name	23	24	25	26	Water
Vapour Fraction	1.0000	0.0000	0.0000	0.0000	0.0000
Temperature (C)	30.00	102.5	103.5	70.91	70.91
Pressure (bar)	1.040	1.040	80.00	80.00	80.00
Molar Flow (kgmole/h)	4.630	199.4	199.4	199.4	0.5527
Mass Flow (kg/s)	5.223e-002	1.515	1.515	1.515	2.766e-003
Liquid Volume Flow (m3/h)	0.2412	5.384	5.384	5.384	9.976e-003
Heat Flow (kJ/h)	-1.669e+006	-5.893e+007	-5.888e+007	-5.952e+007	-1.560e+005
Name	MDEA	purge	27	28	CH4_biom
Vapour Fraction	0.0000	0.0000	0.0000	0.0000	1.0000
Temperature (C)	70.91	70.92	70.92	48.00 *	48.06
Pressure (bar)	80.00	80.00	80.00	80.00	80.00
Molar Flow (kgmole/h)	1.181e-004	0.0000	200.0	200.0	195.6
Mass Flow (kg/s)	3.909e-006	0.0000	1.517	1.517	0.8715
Liquid Volume Flow (m3/h)	1.358e-005	0.0000	5.394	5.394	10.47
Heat Flow (kJ/h)	-52.33	0.0000	-5.968e+007	-6.011e+007	-1.465e+007
Name	CO2_biom	H2_biom	H2O_biom	MDEA_biom	H2S_biom
Vapour Fraction	1.0000	1.0000	0.0000	0.0000	0.0000
Temperature (C)	48.06	48.06	48.06	48.06	48.06
Pressure (bar)	80.00	80.00	80.00	80.00	80.00
Molar Flow (kgmole/h)	6.167e-003	0.2355	0.5331	1.184e-004	0.0000
Mass Flow (kg/s)	7.539e-005	1.319e-004	2.668e-003	3.919e-006	0.0000
Liquid Volume Flow (m3/h)	3.303e-004	1.261e-002	9.622e-003	1.361e-005	0.0000
Heat Flow (kJ/h)	-2448	170.8	-1.514e+005	-53.24	0.0000
Name	Biom_deh	Biom1	Biom3	Biom4	boiloff
Vapour Fraction	1.0000	1.0000	0.0000	0.0287	1.0000
Temperature (C)	48.02	48.02	-161.3	-162.0 *	-162.0
Pressure (bar)	80.00	80.00	80.00	1.013 *	1.013
Molar Flow (kgmole/h)	195.8	195.8	195.8	195.8	5.620
Mass Flow (kg/s)	0.8717	0.8717	0.8717	0.8717	2.416e-002
Liquid Volume Flow (m3/h)	10.49	10.49	10.49	10.49	0.3010
Heat Flow (kJ/h)	-1.466e+007	-1.463e+007	-1.740e+007	-1.740e+007	-4.377e+005

Workbook: Case (Main) (continued)

Material Streams (continued)						Fluid Pkg:	All
11	Name	LBM	12	13V	13L	15	
12	Vapour Fraction	0.0000	0.9820	1.0000	0.0000	0.9985	
13	Temperature (C)	-162.0	30.00	30.00	30.00	30.00	
14	Pressure (bar)	1.013	20.00	20.00	20.00	80.00	
15	Molar Flow (kgmole/h)	190.2	204.4	200.7	3.675	200.7	
16	Mass Flow (kg/s)	0.8475	0.9437	0.9253	1.839e-002	0.9253	
17	Liquid Volume Flow (m3/h)	10.19	10.80	10.73	6.633e-002	10.73	
18	Heat Flow (kJ/h)	-1.696e+007	-1.739e+007	-1.634e+007	-1.049e+006	-1.655e+007	
19	Name	16V	16L	14	9	10L	
20	Vapour Fraction	1.0000	0.0000	1.0000	1.0000	1.0000	
21	Temperature (C)	30.00	30.00	164.7	240.0 *	260.0	
22	Pressure (bar)	80.00	80.00	80.00 *	20.00	20.00	
23	Molar Flow (kgmole/h)	200.4	0.3071	200.7	356.3	147.7	
24	Mass Flow (kg/s)	0.9238	1.537e-003	0.9253	1.683	0.7393	
25	Liquid Volume Flow (m3/h)	10.73	5.543e-003	10.73	13.84	2.667	
26	Heat Flow (kJ/h)	-1.646e+007	-8.762e+004	-1.534e+007	-4.977e+007	-3.471e+007	
27	Name	steamH_in	steamH_out	steamM_in	steamM_out	7	
28	Vapour Fraction	1.0000 *	0.0000 *	1.0000 *	0.0000 *	1.0000	
29	Temperature (C)	240.0	240.0	151.9	151.9	200.0 *	
30	Pressure (bar)	33.47	33.47	5.000 *	5.000	20.00	
31	Molar Flow (kgmole/h)	34.00	34.00	18.76	18.76	504.0	
32	Mass Flow (kg/s)	0.1702	0.1702	9.389e-002	9.389e-002	1.683	
33	Liquid Volume Flow (m3/h)	0.6137	0.6137	0.3387	0.3387	26.99	
34	Heat Flow (kJ/h)	-8.066e+006	-9.148e+006	-4.462e+006	-5.176e+006	-3.748e+007	
35	Name	8	Biom2	10V	11	2	
36	Vapour Fraction	1.0000	1.0000	1.0000	1.0000	1.0000	
37	Temperature (C)	244.7	30.00	240.0	240.0	141.0	
38	Pressure (bar)	20.00	80.00	20.00	20.00	2.738	
39	Molar Flow (kgmole/h)	356.3	195.8	208.5	204.4	504.0	
40	Mass Flow (kg/s)	1.683	0.8717	0.9437	0.9437	1.683	
41	Liquid Volume Flow (m3/h)	13.84	10.49	11.17	10.80	26.99	
42	Heat Flow (kJ/h)	-4.970e+007	-1.479e+007	-1.506e+007	-1.543e+007	-3.850e+007	
43	Name	3	4	5	w1	w2	
44	Vapour Fraction	1.0000	1.0000	1.0000	0.0000	0.0000	
45	Temperature (C)	30.00 *	145.3	30.00	20.00 *	25.00 *	
46	Pressure (bar)	2.738	7.400	7.400	1.013 *	1.013	
47	Molar Flow (kgmole/h)	504.0	504.0	504.0	4910	4910	
48	Mass Flow (kg/s)	1.683	1.683	1.683	24.57	24.57	
49	Liquid Volume Flow (m3/h)	26.99	26.99	26.99	88.62	88.62	
50	Heat Flow (kJ/h)	-4.035e+007	-3.843e+007	-4.036e+007	-1.405e+009	-1.403e+009	
51	Name	w3	w4	w5	w6	w7	
52	Vapour Fraction	0.0000	0.0000	0.0000	0.0000	0.0000	
53	Temperature (C)	20.00 *	25.00 *	20.00 *	25.00 *	20.00 *	
54	Pressure (bar)	1.013 *	1.013	1.013 *	1.013	1.013 *	
55	Molar Flow (kgmole/h)	5122	5122	191.4	191.4	5215	
56	Mass Flow (kg/s)	25.63	25.63	0.9577	0.9577	26.10	
57	Liquid Volume Flow (m3/h)	92.45	92.45	3.454	3.454	94.13	
58	Heat Flow (kJ/h)	-1.466e+009	-1.464e+009	-5.477e+007	-5.470e+007	-1.493e+009	

Workbook: Case (Main) (continued)

Material Streams (continued)							Fluid Pkg:	All
11	Name	w8	w9	w10	w11	w12		
12	Vapour Fraction	0.0000	0.0000	0.0000	0.0000	0.0000		
13	Temperature (C)	25.00 *	20.00 *	25.00 *	20.00 *	25.00 *		
14	Pressure (bar)	1.013	1.013 *	1.013	1.013 *	1.013		
15	Molar Flow (kgmole/h)	5215	3211	3211	1146	1146		
16	Mass Flow (kg/s)	26.10	16.07	16.07	5.734	5.734		
17	Liquid Volume Flow (m3/h)	94.13	57.96	57.96	20.68	20.68		
18	Heat Flow (kJ/h)	-1.491e+009	-9.191e+008	-9.178e+008	-3.280e+008	-3.275e+008		
19	Name	w13	w14	w15	w16	steam_in1		
20	Vapour Fraction	0.0000	0.0000	0.0000	0.0000	0.0000 *		
21	Temperature (C)	20.00 *	25.00 *	20.00 *	25.00 *	240.0		
22	Pressure (bar)	1.013 *	1.013	1.013 *	1.013	33.47		
23	Molar Flow (kgmole/h)	416.2	416.2	384.2	384.2	377.4		
24	Mass Flow (kg/s)	2.083	2.083	1.923	1.923	1.889		
25	Liquid Volume Flow (m3/h)	7.512	7.512	6.935	6.935	6.812		
26	Heat Flow (kJ/h)	-1.191e+008	-1.190e+008	-1.100e+008	-1.098e+008	-1.015e+008		
27	Name	steam_out1	steam_in2	steam_out2	L1	L2		
28	Vapour Fraction	1.0000 *	0.0000 *	1.0000 *	1.0000	1.0000		
29	Temperature (C)	240.0	240.0	240.0	13.65	68.46		
30	Pressure (bar)	33.47	33.47	33.47	10.00 *	16.44		
31	Molar Flow (kgmole/h)	377.4	11.39	11.39	1400 *	1400		
32	Mass Flow (kg/s)	1.889	5.699e-002	5.699e-002	10.89	10.89		
33	Liquid Volume Flow (m3/h)	6.812	0.2056	0.2056	74.98	74.98		
34	Heat Flow (kJ/h)	-8.953e+007	-3.064e+006	-2.702e+006	-5.576e+005	1.670e+006		
35	Name	L3	w17	w18	L4	L5		
36	Vapour Fraction	1.0000	0.0000	0.0000	1.0000	1.0000		
37	Temperature (C)	30.00	20.00 *	25.00 *	87.99	30.00		
38	Pressure (bar)	16.44	1.013 *	1.013	27.02	27.02		
39	Molar Flow (kgmole/h)	1400	4254	4254	1400	1400		
40	Mass Flow (kg/s)	10.89	21.29	21.29	10.89	10.89		
41	Liquid Volume Flow (m3/h)	74.98	76.79	76.79	74.98	74.98		
42	Heat Flow (kJ/h)	6.688e+004	-1.218e+009	-1.216e+009	2.426e+006	-1.870e+004		
43	Name	w19	w20	L6	L7	w21		
44	Vapour Fraction	0.0000	0.0000	1.0000	1.0000	0.0000		
45	Temperature (C)	20.00 *	25.00 *	88.12	30.00	20.00 *		
46	Pressure (bar)	1.013 *	1.013	44.41	44.41	1.013 *		
47	Molar Flow (kgmole/h)	6490	6490	1400	1400	6635		
48	Mass Flow (kg/s)	32.48	32.48	10.89	10.89	33.20		
49	Liquid Volume Flow (m3/h)	117.1	117.1	74.98	74.98	119.8		
50	Heat Flow (kJ/h)	-1.857e+009	-1.855e+009	2.345e+006	-1.545e+005	-1.899e+009		
51	Name	w22	L8	L9	w23	w24		
52	Vapour Fraction	0.0000	1.0000	1.0000	0.0000	0.0000		
53	Temperature (C)	25.00 *	88.26	30.00	20.00 *	25.00 *		
54	Pressure (bar)	1.013	73.00	73.00	1.013 *	1.013		
55	Molar Flow (kgmole/h)	6635	1400	1400	6857	6857		
56	Mass Flow (kg/s)	33.20	10.89	10.89	34.32	34.32		
57	Liquid Volume Flow (m3/h)	119.8	74.98	74.98	123.8	123.8		
58	Heat Flow (kJ/h)	-1.897e+009	2.220e+006	-3.630e+005	-1.963e+009	-1.960e+009		

Workbook: Case (Main) (continued)

Material Streams (continued)							Fluid Pkg:	All
11	Name	L10	L11	w25	w26	L12		
12	Vapour Fraction	1.0000	1.0000	0.0000	0.0000	1.0000		
13	Temperature (C)	88.28	30.00	20.00 *	25.00 *	-70.00 *		
14	Pressure (bar)	120.0 *	120.0	1.013 *	1.013	120.0		
15	Molar Flow (kgmole/h)	1400	1400	7166	7166	1400		
16	Mass Flow (kg/s)	10.89	10.89	35.86	35.86	10.89		
17	Liquid Volume Flow (m3/h)	74.98	74.98	129.3	129.3	74.98		
18	Heat Flow (kJ/h)	2.039e+006	-6.611e+005	-2.051e+009	-2.048e+009	-6.034e+006		
19	Name	L13	biom3_dummy	biom4_dummy	20dummy	21dummy		
20	Vapour Fraction	1.0000	0.0000	0.0080	0.0000	0.0022		
21	Temperature (C)	-166.9	-161.3	-163.2	49.75	39.92		
22	Pressure (bar)	10.00	80.00	1.013	80.00	1.040		
23	Molar Flow (kgmole/h)	1400	195.8	195.8	204.1	204.1		
24	Mass Flow (kg/s)	10.89	0.8717	0.8717	1.567	1.567		
25	Liquid Volume Flow (m3/h)	74.98	10.49	10.49	5.625	5.625		
26	Heat Flow (kJ/h)	-8.541e+006	-1.740e+007	-1.744e+007	-6.182e+007	-6.202e+007		
27	Name	d1	d2	w15_duplicate	w16_duplicate	CO2		
28	Vapour Fraction	1.0000	0.6058	0.0000	0.0000	---		
29	Temperature (C)	77.83	30.00	20.00 *	25.00 *	---		
30	Pressure (bar)	1.040	1.040	1.013 *	1.013 *	---		
31	Molar Flow (kgmole/h)	7.644	7.644	384.2	384.2	4.055		
32	Mass Flow (kg/s)	6.732e-002	6.732e-002	1.923	1.923	4.957e-002		
33	Liquid Volume Flow (m3/h)	0.2956	0.2956	6.935	6.935	0.2172		
34	Heat Flow (kJ/h)	-2.385e+006	-2.529e+006	-1.100e+008	-1.098e+008	---		
35	Name	H2O	H2S	MDEA_cond	CH4	H2_cond		
36	Vapour Fraction	---	---	---	---	---		
37	Temperature (C)	---	---	---	---	---		
38	Pressure (bar)	---	---	---	---	---		
39	Molar Flow (kgmole/h)	3.203	0.0000	0.0000	0.3849	3.380e-004		
40	Mass Flow (kg/s)	1.603e-002	0.0000	0.0000	1.715e-003	1.893e-007		
41	Liquid Volume Flow (m3/h)	5.782e-002	0.0000	0.0000	2.061e-002	1.810e-005		
42	Heat Flow (kJ/h)	---	---	---	---	---		
43	Name	steamH_out_duplicate						
44	Vapour Fraction	0.0000						
45	Temperature (C)	240.0						
46	Pressure (bar)	33.47						
47	Molar Flow (kgmole/h)	34.00						
48	Mass Flow (kg/s)	0.1702						
49	Liquid Volume Flow (m3/h)	0.6137						
50	Heat Flow (kJ/h)	-9.148e+006						

Licensed to: NORWEGIAN UNIVERSITY OF * Specified by user.



 **NTNU**

Norwegian University of
Science and Technology